

**Functional Elucidation and Targeting of the Bcl-2 Pro-Survival Proteins
in Various Cancers**

by

Karson J. Kump

A dissertation submitted in partial fulfillment
of the requirements for the degree of
Doctor of Philosophy
(Chemical Biology)
in the University of Michigan
2020

Doctoral Committee:

Associate Professor Zaneta Nikolovska-Coleska, Chair
Professor Thomas E. Carey
Professor Duxin Sun
Professor Shaomeng Wang

Karson J. Kump

kjkump@umich.edu

ORCID iD: 0000-0001-5013-8743

© Karson J. Kump 2020

Dedication

This body of work is dedicated to my wife, **Jenessa Kump**, the real MVP, and our two little girls, **Lyla** and **Cali**. I would be remiss to not include my parents, **Kary** and **Terri Kump**, who were the first to teach me the value of hard work, perseverance, and integrity.

Acknowledgements

I wouldn't be who I am without my four older brothers, Kasey, Kyle, Kris (RIP), and Kolby, who are my heroes and best friends. My competitive nature and tenacity came from trying to keep up with them and I'm grateful they always looked out for me. I owe the world to my mom and dad who never gave up on me and taught me how to harness my stubbornness for good causes, they deserve all the credit for my successes in life. I learned many life lessons on the football field growing up and had incredible coaches and mentors, especially Coaches Tony and Hazelton, who always reminded me of my potential and to never let my foot off the gas. I was able to funnel those lessons learned on the football field into my academic and career pursuits.

My academic endeavors would've never commenced if it wasn't for Santa Barbara City College, I owe more gratitude to Drs. Carroll, Young, Doohan, and Miner than they will ever know, they lit a fire inside of me and motivated me to study science. The most important degree in my educational journey will always be my A.A. from SBCC. A big thank you to Dr. Mike Rogers who gave me my first research experience in his lab at Harvard Medical School, because before that, I had no idea what research was. Dr. Dave at BYU taught me that research can be both intellectually stimulating and fun, I thoroughly enjoyed his mentorship and the two years I spent in his lab.

I owe a vast amount of gratitude to my PhD mentor, Dr. Zaneta Nikolovska-Coleska. There is always talk about finding the right mentor in graduate school and I am

confident that I had the right mentor for me, I wouldn't have finished my PhD without her. She always pushed me to look at problems from all angles and to pay close attention to details. She always supported me in pursuing my goals in and (most importantly) out of the lab by providing me with countless opportunities to help reach them. One of the highlights of my PhD was us being selected as Science2Startup finalists and working together on proposals and pitch decks, which helped me explore my interest in the business side of drug development.

The research community at the University of Michigan is parallel to none, certainly full of the "leaders and best." I was lucky to have a committee composed of outstanding scientists, Drs. Carey, Sun, and Wang, who I look up to and hope to accomplish a fraction of the things they have in their careers. I have nothing but praise for the Program in Chemical Biology, especially those who kept the well-oiled machine running, Traci, Laura, and Anna Mapp. I am grateful for the funding and everyone I was able to work with through the NIH T32 Training Program in Translational Research, including Laura L. and Dr. Lieberman who co-directed the program with Dr. Nikolovska-Coleska. The TPTR enabled me to work with amazing physician-scientists, including my clinical co-mentor, Dr. Bixby, along with Drs. Phillips, Wilcox, Talpaz, and Malek, who each taught me important lessons on how to make my research more clinically relevant. I also need to thank Malathi at the Cancer Center for helping coordinate the countless patient samples I took back to the lab to test. It was a pleasure working together with Dr. Charlie Foucar gathering data in support of an AML clinical trial design.

When I think of my time at UofM I will always be reminded of my lab mates, especially Ahmed Mady and Sierrah Grigsby, who were like brother and sister to me. I

worked with them for 3.5 years and they were the first to help me adjust to grad school and we always had a good time in the lab, working hard and enjoying life. Dr. Mady set me on the right course for my dissertation work as I picked up where he left off and I owe a lot to him for his patience and kindness. I was grateful for the friendship of Dr. Andrej Perdih who would come from Slovenia every summer to work in our lab, we always had a good time swapping cultural insights and he was always there to help talk me through my research struggles. Thank you to all the organic chemists I worked with, Lei, Mohan, Nurul, Bing, and Uttar for keeping me busy testing all your compounds, you were all great friends and I wish the best for you. To my other fellow lab mates, Ejaz and Yuting, thank you for your examples. Thank you to all the rotation students and undergrads who helped me with my project, especially Eli, Matt, and Ayza.

The most important person to thank is my wife Jenessa, who worked just as hard as (if not harder than) me throughout my doctoral studies to take care of our family. I wouldn't have survived my PhD mentally, physically, or even hygienically without her... She always put up with me working long hours and my infamous late-night line, "I just have to run into my lab for 20 mins," even though I wouldn't be back for 2-3 hours. We started our family during my PhD with two little girls, Lyla and Cali, who were always there to cheer me up after a long day. I always tried to spend as much time with them as I could, even if coming home for dinner meant I'd have to go back to lab after they were asleep until 3 AM. I love these three girls more than anything and I'm excited to continue this journey of life with them.

Preface

The data, text, figures, and tables presented in Chapter 4 have been previously published and are being reused and adapted with permission from:

Kump KJ, et al. Discovery and characterization of 2,5-substituted benzoic acid dual inhibitors of the anti-apoptotic Mcl-1 and Bfl-1 proteins. *Journal of Medicinal Chemistry*. 2020; 63(5):2489-2510. Copyright © 2020, American Chemical Society.

This publication was a follow-up to:

Mady ASA, Liao C, Bajwa N, **Kump KJ**, et al. Discovery of Mcl-1 inhibitors from integrated high throughput and virtual screening. *Scientific Reports*. 2018; 8(1):10210.

Table of Contents

Dedication	ii
Acknowledgements	iii
Preface	vi
List of Figures	x
List of Tables	xii
List of Abbreviations	xiii
Abstract	xv
Chapter 1	
The Bcl-2 Protein Family and BH3 Mimetics in Cancer	1
1.1 Precision medicine in oncology	1
1.2 The Bcl-2 protein family regulates intrinsic apoptosis	2
1.3 Bcl-2 proteins are therapeutic targets in cancer	6
1.4 Drugging the Bcl-2 proteins with BH3 mimetics	7
1.5 Development of pan and Bcl-2/Bcl-xL dual and selective inhibitors	8
1.6 Acquired resistance to Bcl-2/Bcl-xL inhibitors	11
1.7 Development of selective Mcl-1 inhibitors	12
1.8 Unmet need for Bfl-1 inhibitors	17
1.9 BH3 profiling: a functional assay to determine survival dependence	18
1.10 Conclusions and research aims	20
1.11 References	21

Chapter 2

Functional Elucidation and Inhibition of the Bcl-2 Pro-Survival Proteins Unveils

Precision Medicine Strategies in a Wide Spectrum of Cancers	31
2.1 Abstract	31
2.2 Introduction	32
2.3 <i>In vitro</i> binding and functional validation of chemical tools	33
2.4 Parsing anti-apoptotic dependence in hematologic malignancies	38
2.5 Targeting the Bcl-2 proteins in ovarian cancer	43
2.6 Characterizing survival dependence in diverse solid tumors	47
2.7 Dynamic BH3 profiling in solid tumors to target resistance	50
2.8 Conclusions	52
2.9 Materials and methods	54
2.10 Contributions	60
2.11 References	60

Chapter 3

Targeting the Bcl-2 Proteins to Overcome Resistance in Melanoma	66
3.1 Abstract	66
3.2 Introduction	67
3.3 Functional evaluation of Bcl-2 family proteins in melanoma cell lines	68
3.4 Genetic and pharmacological targeting of Bcl-xL and Mcl-1	71
3.5 Functional analysis and targeting of Bfl-1	74
3.6 Vemurafenib resistance selectively increases Mcl-1 dependence	75
3.7 Short term BRAF/MEK inhibitor treatment primes for Mcl-1 dependence	78
3.8 Conclusions	80
3.9 Materials and methods	82
3.10 References	85

Chapter 4

Discovery and Characterization of Mcl-1 and Bfl-1 Dual Inhibitors	88
4.1 Abstract	88
4.2 Introduction	88
4.3 Design of a 2,5-substituted benzoic acid scaffold that inhibits Mcl-1/Bfl-1	90
4.4 SAR of novel Mcl-1/Bfl-1 dual inhibitors	94
4.5 Co-crystallography and structure-based design of optimized inhibitors	102
4.6 Elucidation of dual inhibitors binding to Bfl-1 by HSQC-NMR and docking	108
4.7 Binding selectivity to anti-apoptotic Bcl-2 family proteins	112
4.8 Biological evaluation of dual inhibitors	113
4.9 Conclusions	117
4.10 Materials and methods	118
4.11 Contributions	127
4.12 References	128

Chapter 5

Conclusions and Future Directions	133
5.1 Impact and translational relevance	133
5.2 Optimizing BH3 profiling for solid tumor patient samples	135
5.3 Using BH3 profiling in clinical trials	135
5.4 Further development of Mcl-1/Bfl-1 dual and Bfl-1 selective inhibitors	138
5.5 Concluding remarks	139
5.6 References	140

List of Figures

Figure 1.1 Cancer precision medicine strategy	2
Figure 1.2 The Bcl-2 protein family.....	3
Figure 1.3 BH3 binding site of anti-apoptotic proteins	8
Figure 1.4 Bcl-2 family pan and Bcl-2/Bcl-xL dual and selective inhibitors	9
Figure 1.5 Structures of reported Mcl-1 selective inhibitors.....	14
Figure 1.6 BH3 profiling workflow.....	19
Figure 2.1 Binding affinity and selectivity of anti-apoptotic protein inhibitors	35
Figure 2.2 Apoptotic priming in E μ -Myc cell lines and example of Bcl-2 dependence..	37
Figure 2.3 Functional assessment of chemical tools in E μ -Myc Lymphoma cell lines..	38
Figure 2.4 Targeting Mcl-1 and Bcl-2 dual dependence in AML.....	40
Figure 2.5 Survival dependence trends in B-cell and T-cell lymphoma subtypes.....	42
Figure 2.6 mRNA expression of Bcl-2 family anti-apoptotic proteins in lymphomas.....	43
Figure 2.7 Targeting pro-survival proteins in ovarian cancer.....	46
Figure 2.8 Gene expression of Bcl-2 proteins in ovarian cancer patients.....	47
Figure 2.9 Targeting Bcl-2 anti-apoptotic proteins in solid tumor cell lines	49
Figure 2.10 Dynamic BH3 profiling in melanoma and colon cancer	51
Figure 2.11 siRNA knockdown confirmation in ovarian cancer PDX lines.....	59
Figure 3.1 BH3 profiling of melanoma cell line panel.....	70
Figure 3.2 siRNA and BH3 mimetic targeting dual Bcl-xL/Mcl-1 dependent cell lines..	72

Figure 3.3 Targeting Bcl-xL and Mcl-1 in sole dependent cell lines..	73
Figure 3.4 Targeting Bfl-1 in the M14 cell line	75
Figure 3.5 Vemurafenib acquired resistance increases Mcl-1 dependence	78
Figure 3.6 MAPK inhibitors selectively prime for Mcl-1 dependence	80
Figure 3.7 siRNA knockdown validation in melanoma.....	83
Figure 4.1 Compound 1 design and HSQC-NMR guided binding mode to Mcl-1/Bfl-1	94
Figure 4.2 Physicochemical evaluation of dual inhibitors	100
Figure 4.3 Co-crystal structures of compounds 20 and 22 with Mcl-1	103
Figure 4.4 Binding affinity determination by BLI	106
Figure 4.5 Co-crystal structures of compounds 24 and 27 bound to Mcl-1.....	108
Figure 4.6 Bfl-1 protein alignments and minimization	111
Figure 4.7 HSQC-NMR and docking of optimized compounds with Bfl-1	112
Figure 4.8 Biological evaluation of dual inhibitors.....	116
Figure 5.1 Future clinical trial designs for BH3 mimetics	138

List of Tables

Table 1.1 Mcl-1 inhibitors in phase I clinical trials	15
Table 2.1 BH3-only peptide sequences	55
Table 2.2 Primary patient sample information.....	56
Table 2.3 Antibodies used for western blotting	58
Table 3.1 Melanoma cell line panel	68
Table 4.1 SAR of 2-,5-substituents of benzoic acid core	96
Table 4.2 SAR of 5-(phenethylthio)-2-(arylsulfonamido) benzoic acid compounds.....	98
Table 4.3 Mcl-1 and Bfl-1 binding of methyl ester analogues	101
Table 4.4 Optimized dual inhibitors with terminal R ² <i>tert</i> -butyl moiety	104
Table 4.5 Binding selectivity to anti-apoptotic proteins	113
Table 4.6 Crystallography data collection and refinement statistics.....	123

List of Abbreviations

- ALCL** – Anaplastic large cell lymphoma
- AML** – Acute myeloid leukemia
- APAF-1** – Apoptotic protease activating factor 1
- Bad** – Bcl-2 agonist of cell death
- Bak** – Bcl-2 homologous antagonist killer
- Bax** – Bcl-2 associated X protein
- Bcl-2** – B-cell lymphoma 2
- Bcl-xL** – B-cell lymphoma-extra large
- Bfl-1** - Bcl-2-related gene expressed in fetal liver
- BH3** – Bcl-2 homology domain 3
- Bid** – BH3 interacting domain death agonist
- BLI** – Bio-layer interferometry
- CLL** – Chronic lymphocytic leukemia
- FP** – Fluorescence polarization
- Hrk** – Activator of apoptosis harakiri
- HSQC** – Heteronuclear single quantum coherence spectroscopy
- HTS** – High throughput screening
- ITC** – Isothermal titration calorimetry
- K_D** – Dissociation constant

K_i – Inhibition constant

MAPK – Mitogen-activated protein kinase

MCL – Mantle cell lymphoma

Mcl-1 – Myeloid cell leukemia 1

MOMP – Mitochondrial outer membrane permeabilization

NMR – Nuclear magnetic resonance

NSCLC – Non-small cell lung cancer

PDX – Patient derived xenograft

PK – Pharmacokinetic

PPI – Protein-protein interaction

Puma – p53 upregulated modulator of apoptosis

SAR – Structure activity relationship

Smac – Second mitochondria-derived activator of caspases

SPR – Surface plasmon resonance

TR-FRET – Time-resolved fluorescence energy transfer

Abstract

Cancer is a heterogeneous group of diseases defined by distinct capabilities, including resistance to programmed cell death, or apoptosis. The Bcl-2 protein family governs the integrity of the mitochondria, which acts as a central nexus of the apoptotic cascade and is commonly dysregulated in cancers. The Bcl-2 protein family consists of a delicate balance of pro- and anti- apoptotic members that interact with one another via a selective network of protein-protein interactions. In many cancers, the anti-apoptotic proteins (Bcl-2, Bcl-xL, Mcl-1, and Bfl-1) are overexpressed and contribute to aggressive malignancy and therapeutic resistance. Selective small molecule inhibitors of these proteins (BH3 mimetics) are therapeutic modalities with promise in diverse cancers. Potent inhibitors of Bcl-2, Bcl-xL, and Mcl-1 are being clinically evaluated, but small molecule Bfl-1 inhibitors have remained elusive.

In this body of work, we utilized and developed selective chemical tools to probe the Bcl-2 proteins in a wide spectrum of cancers. Using BH3 profiling we revealed distinct functional pro-survival trends in various hematologic malignancies. These findings were highlighted by the preferential survival dependence in lymphoma based on cell of origin, where B-cell and T-cell lymphomas predominantly display sole dependence on Bcl-2 and Mcl-1, respectively. These functional discoveries were accompanied by selective sensitivities to the respective BH3 mimetics. The translational relevance of these findings was substantiated by testing primary patient samples. In a

genetically diverse panel of solid tumor cell lines we discovered profound sensitivity to a combination of Bcl-xL and Mcl-1 inhibitors, with some responding to single agent BH3 mimetic treatment. Functional analysis of Bcl-2 family proteins in ovarian cancer identified a highly Mcl-1 dependent patient derived xenograft cell line. In melanoma we discovered that BRAF/MEK inhibitors selectively prime cells for Mcl-1 dependence and led to increased sensitivity to Mcl-1 inhibitors, especially in the context of acquired resistance. Additionally, we explored the role of Bfl-1 in melanoma, which is the cancer where it is most abundantly expressed and highlight an unmet need to develop Bfl-1 inhibitors.

We undertook medicinal chemistry efforts to discover first-in-class small molecule dual inhibitors of the Mcl-1 and Bfl-1 proteins. Building from our previous work on Mcl-1 inhibitors, we designed and developed a class of 2,5-substituted benzoic acid compounds selective for both Mcl-1 and Bfl-1. The most potent inhibitor in this series, compound **24**, displayed equipotent binding ($K_i = 100$ nM) to both Mcl-1 and Bfl-1, with 200-fold selectivity over Bcl-2 and Bcl-xL. Compound **24** selectively disrupts protein-protein interactions between endogenous Mcl-1/Bfl-1 and pro-apoptotic peptides and selectively kills model E μ -Myc lymphoma cell lines that depend on Mcl-1 and Bfl-1 for survival.

From optimizing functional diagnostic strategies, to the development of novel small molecule inhibitors, we have outlined a body of work that contributes to the therapeutic targeting of the Bcl-2 protein family. These findings highlight the use of chemical biology to interrogate various cancers with the translational goal of improving patient outcomes in a precision manner.

Chapter 1

The Bcl-2 Protein Family and BH3 Mimetics in Cancer

1.1 Precision medicine in oncology

Cancer is defined by the uncontrolled growth and invasion of abnormal cells and opposed to being classified as a single disease, cancer is a broad description of over 100 different neoplastic diseases that originate from various cell types from different organs in the body.¹ Cancer cells are genetically modified normal cells that possess aberrant protein machinery in the form of oncogenes and tumor suppressors.² Even cancers that arise from the same originator cell type can be genetically distinct from patient to patient and therefore respond differently to the same therapeutics.³ Traditional therapeutic approaches in oncology consisted of treating patients of the same cancer type with the same drug, but the high heterogeneity within cancer subtypes requires a personalized or precision medicine approach to effectively treat an individual patient.⁴⁻⁶ In order to determine the appropriate therapeutic, a physician must first understand the genetic drivers of a specific patient's tumor cells, which requires intricate diagnostic methods.⁷ What is becoming more important in precision medicine practice is the use of functional diagnostics to better identify actionable biomarkers.^{8,9} Genomic, functional, and real world¹⁰ data need to be analyzed before the appropriate drug can be administered (Figure 1.1). The foundation of this precision strategy comes from basic science discoveries, including those summarized into several well defined hallmarks of

cancer that work together to promote malignancy.¹¹ One prominent hallmark of cancer is resistance to cell death or apoptosis, which has been a hot area for therapeutic discovery over the past two decades.¹²

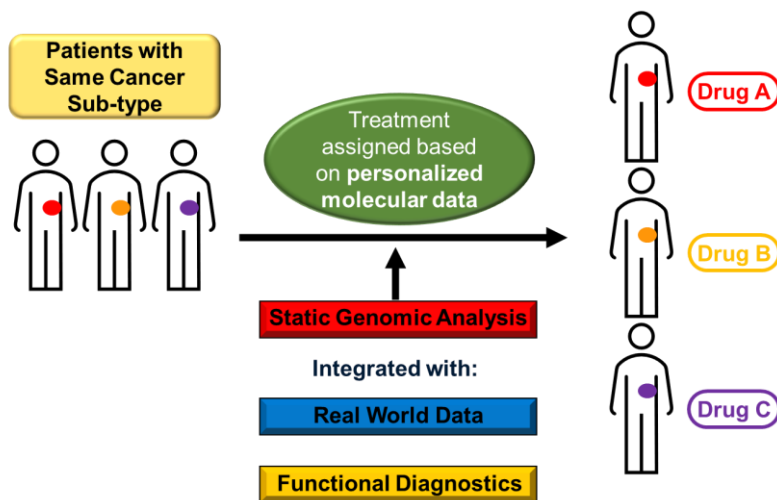


Figure 1.1 Cancer precision medicine strategy

1.2 The Bcl-2 protein family regulates intrinsic apoptosis

Apoptosis is one form of programmed, or genetically determined, cell death and is a tightly regulated physiological process that involves the self-destruction of cells which are no longer needed by an organism.¹³ An important feature of apoptosis is that it is a non-inflammatory process, meaning apoptotic cells do not release their cellular contents, they are quickly phagocytosed, and anti-inflammatory cytokines are not produced by engulfing cells.¹⁴ Apoptosis can either be initiated by cell surface receptors and external ligands (extrinsic) or by mitochondrial sensed signals (intrinsic). The mitochondria acts as a central nexus of intrinsic apoptotic signaling and the fate of a cell relies the constitution of its membrane, which is governed by the B-cell lymphoma-2

(Bcl-2) protein family (Figure 1.2).^{15,16} Control of intrinsic apoptosis by the Bcl-2 protein family plays a vital role in cellular development and homeostasis, specifically in early embryogenesis, nervous system development, and hematopoiesis.¹⁷ In addition to the various physiological roles Bcl-2 proteins play by regulating apoptosis, they also have many non-apoptotic functions. Briefly, these functions range from regulating the morphology and metabolism of the mitochondria, endoplasmic reticulum related processes such as the unfolded protein response and calcium regulation, cell cycle and DNA damage responses within the nucleus, and whole-cell metabolism.¹⁸

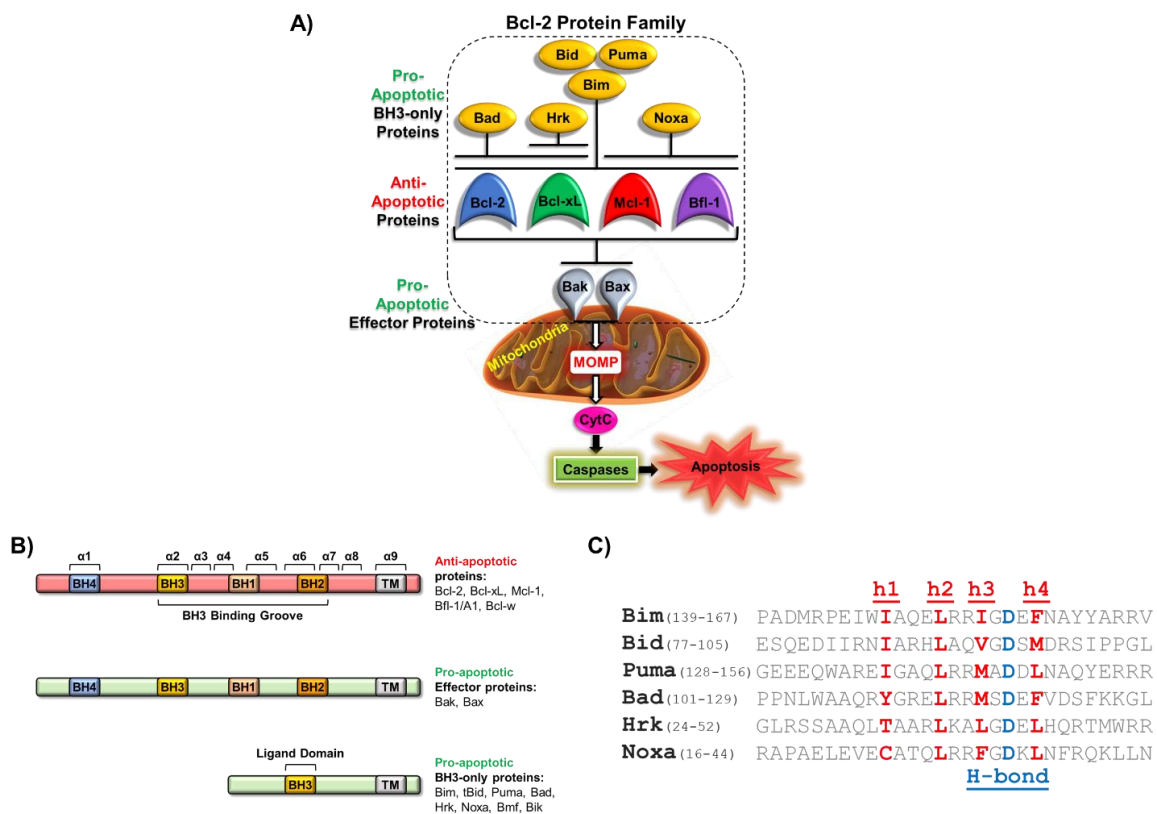


Figure 1.2 The Bcl-2 protein family

A) Intrinsic apoptosis pathway and binding selectivity of pro- and anti- apoptotic family members. **B)** Structural homology of Bcl-2 proteins. **C)** Sequence homology of the BH3-only proteins, indicating the conserved hydrophobic (h1-4) and the hydrogen bond forming Asp residues.

The Bcl-2 protein family consists of two main groups, the anti- and pro- apoptotic proteins, which coexist in a delicate balance and interact with one another via a network of protein-protein interactions (PPIs) (Figure 1.2A). The anti-apoptotic proteins include Bcl-2, Bcl-xL, Mcl-1, Bfl-1/A1, and Bcl-w. The pro-apoptotic proteins are grouped by their structure and function into the BH3-only proteins (Bim, tBid, Puma, Bad, Hrk, and Noxa,) which contain only the alpha helical BH3 ligand domain and multidomain effector (Bak and Bax) proteins.¹⁹ These proteins all share at least one of the four Bcl-2 homology (BH) domains, which are distinct structural motifs composed of several alpha helices, along with a transmembrane (TM) domain that allows embedment into the mitochondria (Figure 1.2B).²⁰ The effector and anti-apoptotic proteins are classified as multi-domain, as they contain BH domains 1-4. The cluster of alpha-helices that make up the BH1-3 domains form the BH3 binding groove, which is the PPI site that allows the binding of the alpha helical BH3 ligand domain. The PPIs between BH3-only and anti-apoptotic proteins are supported by several conserved hydrophobic residues (h1-4) and a hydrogen bond forming Asp (Figure 1.2C). A key feature of the PPIs between pro- and anti- apoptotic proteins is the differential binding selectivity they have for one another (Figure 1.2A). For instance, some BH3-only proteins act as pan inhibitors, which bind and inhibit all the anti-apoptotic proteins, as in the case of Bim, Puma, and tBid. Other BH3-only proteins only engage subsets of the anti-apoptotic proteins, like Bad and Noxa, for example, that selectively bind either Bcl-2/Bcl-xL/Bcl-w or Mcl-1/Bfl-1, respectively. In addition, Hrk is selective for Bcl-xL and does not inhibit the other anti-apoptotic proteins.²¹

Intrinsic apoptosis is initiated by cellular stress signals such as hypoxia, growth factor withdrawal, DNA damage, drug treatments, etc., which trigger transcription factors like p53 to induce the expression of BH3-only pro-apoptotic proteins, allowing for the Bcl-2 protein family balance to tip towards death. This BH3-only protein increase activates the irreversible apoptotic switch of mitochondrial outer membrane permeabilization (MOMP) induced by the effector proteins, Bak and Bax which form holes in the mitochondria.¹³ There have been two models to explain the mechanism of Bak and Bax induced MOMP, the direct and indirect activation models.^{19,22,23} In the direct activation model, certain BH3-only proteins known as activators (Bim and tBid) are capable of directly binding to Bak and Bax and triggering the conformational change necessary to promote pore forming oligomers that induce MOMP. The indirect model involves the PPI disruption of anti-apoptotic proteins that have locked up and prevented Bak and Bax from activating, once free, Bak/Bax oligomers can form and carry out MOMP.¹⁹ The more likely scenario is that both the direct and indirect models apply and form the unified model, which takes into account both mechanisms operating together. After MOMP has commenced, mitochondrial proteins, such as cytochrome-c and Smac/Diablo, are released into the cytosol and interact with the apoptogenic protein APAF-1, which aids in the formation of the apoptosome.²⁴ The apoptosome unit is then able to initiate the caspase cascade, starting with the activation of caspase-9, then the executioner caspases 3 and 7, which carry out the ultimate steps in apoptosis of DNA fragmentation and degradation of cytoskeletal proteins.²⁵ Along with the important role the Bcl-2 family plays in normal physiological apoptosis, these proteins are commonly aberrant in a variety of diseases. Various neurodegenerative and hematologic diseases

are the result of Bcl-2 protein levels being skewed in a manner that favors an increase in apoptotic signaling.²⁶ On the converse, upregulated anti-apoptotic proteins impede apoptosis and contribute to diseases such as cancer.²⁷

1.3 Bcl-2 proteins are therapeutic targets in cancer

Resistance to cell death is a *bona fide* hallmark of cancer and cells advantageously hijack Bcl-2 family apoptotic machinery to promote malignancy and therapeutic resistance.¹¹ Various genetic abnormalities in cancer cells contribute to anti-apoptotic protein overexpression, including chromosomal translocations and constitutively activated upstream promoters.²⁷ The founding member of the Bcl-2 protein family, Bcl-2 itself, was first discovered in B-cell lymphoma where it was shown to promote cancer progression.²⁸ The homologous Bcl-xL protein also has a prominent role in promoting aggressive malignancy, particularly in solid tumors, and has been specifically shown to promote cancer cell stemness in RAS driven tumors.^{29,30} Meanwhile, Mcl-1 is one of the top 10 most common genetic aberrations across a wide spectrum of cancers and is a notorious resistance factor to many chemo and targeted therapies.^{31,32} Clinically relevant biological discoveries regarding the role of Bcl-2 in cancer have further promoted its status as an additional therapeutic target, especially in cancers like melanoma and lymphoma.³³ All of these examples highlight the need to develop a selective quiver of anti-apoptotic inhibitors that can be used clinically to combat a variety of cancers. The therapeutic value in targeting the Bcl-2 anti-apoptotic proteins has been long sought after as the biological data continues to support their role as cell death suppressors in cancer.

The variable selectivity of endogenous BH3-only proteins to their anti-apoptotic binding partners (Figure 1.2A) highlights possible benefits of inhibiting certain anti-apoptotic proteins over the others in particular circumstances. The fact that nature has conceived a method to selectively antagonize specific anti-apoptotic proteins highlights the therapeutic potential of developing selective inhibitors and provides rationale for the biological relevance of doing so.³⁴ Additionally, the structural basis of BH3-only protein specificity provides a template for small molecule discovery and design.

1.4 Drugging the Bcl-2 proteins with BH3 mimetics

In the past, PPIs were considered undruggable, but new advances in developing small molecules that effectively inhibit these proteins have broken previously conceived limits. The main challenges in developing PPI inhibitors come from the large hydrophobic surface area without well-defined pockets on these PPI interfaces (Figure 1.3A), unlike what is faced with kinase inhibitors that have well defined ligand binding sites.³⁵ Structural information from nuclear magnetic resonance (NMR) and x-ray crystallography were vital for the mapping of PPI hotspots and defining key anchoring interactions with conserved residues (Figure 1.2C) that has helped focus drug design.³⁶ Strategies utilizing *in silico*, peptidomimetic, and fragment-based screens and designs have aided in the discovery of novel PPI inhibitor scaffolds. The development of small molecule inhibitors targeting the anti-apoptotic proteins of the Bcl-2 family has been accelerating at an exciting pace over recent years.³⁷ This class of inhibitors have been appropriately coined as BH3 mimetics, named for their mimicry of BH3-only protein binding into the BH3 binding groove of the anti-apoptotic proteins.³⁸ Analyzing the

interactions between BH3-only and anti-apoptotic proteins provides information on crucial interactions that drive ligand affinity. The BH3 binding groove is composed of several hydrophobic pockets (p1-4), that are defined by conserved interactions of the BH3-only peptides like Bim, which also forms an anchoring hydrogen bond that occurs between its conserved Asp residue and the Arg of the anti-apoptotic protein (Figure 1.3B).³⁹ Mimicking these hydrophobic interactions and the Arg hydrogen bond with chemical functionalities that span the most important areas of the BH3 binding groove can effectively disrupt endogenous PPIs, as seen with the Mcl-1 selective BH3 mimetic, S63845, which represents the strategy employed by inhibitors of the other anti-apoptotic proteins (Figure 1.3C).³⁷

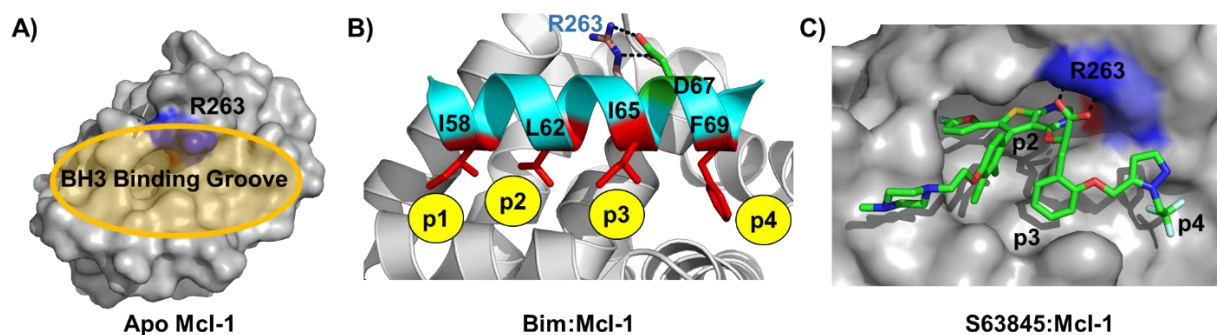


Figure 1.3 BH3 binding site of anti-apoptotic proteins

A) Apo Mcl-1 crystal structure (PDB: 4WMS), with Arg263 in blue and the BH3 binding groove highlighted in orange, as a representation of all the anti-apoptotic proteins. **B)** Crystal structure of the Bim:Mcl-1 complex (PDB: 2NL9). Key hydrophobic interactions of Bim residues (red) that define the pockets p1-p4. Hydrogen bond depicted between Arg263 of Mcl-1 and conserved Asp67 on Bim. **C)** Co-crystal structure of Mcl-1 and the Mcl-1 selective BH3 mimetic, S63845.

1.5 Development of pan and Bcl-2/Bcl-xL dual and selective inhibitors

Natural products have historically played an important role in discovering new therapeutics⁴⁰ and the discovery of the natural gossypol molecule from cotton seed oil

was a vital step in the field of BH3 mimetics. Gossypol was identified as a pan Bcl-2 family inhibitor⁴¹ and through structure activity relationship (SAR) studies was developed into various analogues, such as AT-101 and TW-37, which displayed efficacy in several types of cancer (Figure 1.4).^{42,43} Additionally, obatoclox (Figure 1.4) is another pan-Bcl-2 family inhibitor that was independently discovered through high throughput screening (HTS) and was clinically evaluated for treating various oncological diseases, however off-target toxicities have limited its success, necessitating more rationally designed selective Bcl-2 protein inhibitors.⁴⁴⁻⁴⁶

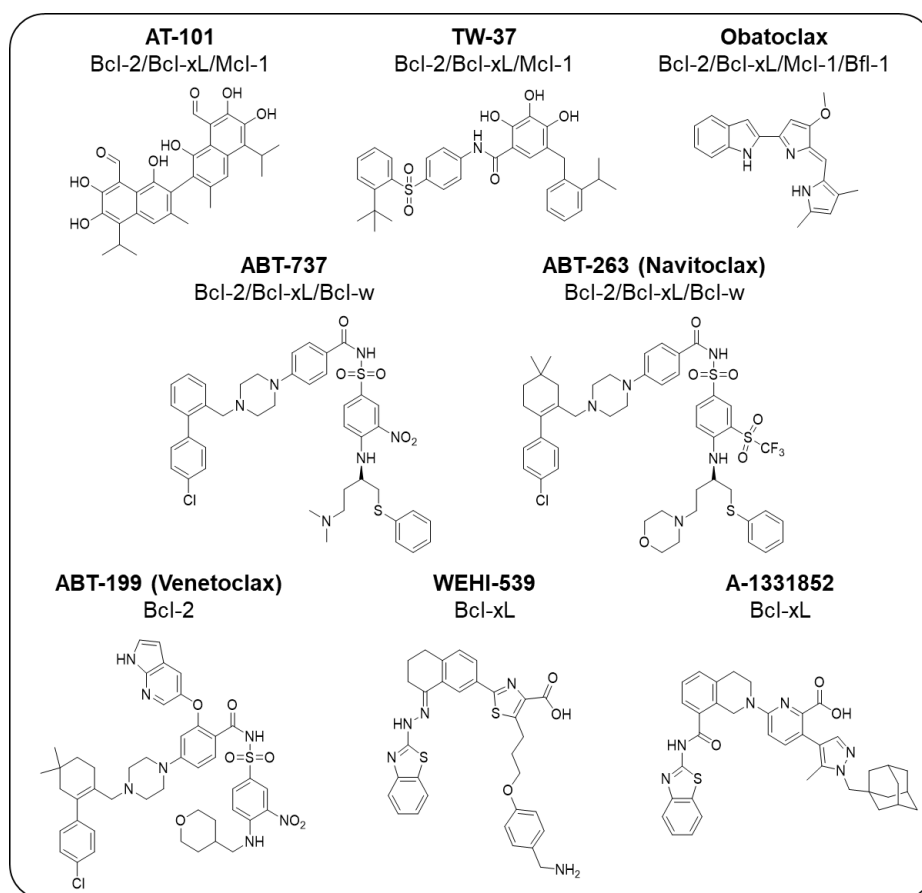


Figure 1.4 Bcl-2 family pan and Bcl-2/Bcl-xL dual and selective inhibitors

Abbott Laboratories (now Abbvie) utilized the “SAR by NMR” method⁴⁷ to discover and develop new scaffolds as potent BH3 mimetics. ABT-737 (Figure 1.4), a Bad mimetic that selectively inhibits Bcl-2, Bcl-xL, and Bcl-w, was developed by fragment-based design which consisted of linking two fragments that bind in the p2 and p4 pockets of these proteins, resulting in a potent PPI inhibitor.⁴⁸ This molecule displayed potent efficacy in various cancer models, including solid tumor *in vivo* xenografts. An important and challenging balance to maintain during the development of BH3 mimetics is between retaining sufficient hydrophobicity required for high affinity and efficient drug-like physicochemical properties. To this point, ABT-263 (Figure 1.4) was developed which maintains potent Bad-like binding selectivity but with an improved pharmacokinetic (PK) profile, including oral bioavailability, which made it suitable for evaluation in clinical trials (Figure 1.4).⁴⁹ Although ABT-263 displayed efficacy in many Bcl-2 and Bcl-xL dependent cancers, it induced on-target dose-limiting thrombocytopenia from the inhibition of Bcl-xL in platelet cells.⁵⁰ To eliminate these toxicity concerns, Abbvie focused on developing selective Bcl-2 inhibitors, leading to ABT-199 (venetoclax) which possess a similar chemical scaffold as ABT-737 and ABT-263 (Figure 1.4).²³ ABT-199 was a first in-class orally bioavailable selective Bcl-2 inhibitor that produced outstanding clinical results in 17p deleted chronic lymphocytic leukemia, leading to its initial FDA approval in 2016 and is currently being evaluated in numerous clinical trials for various indications as a single agent and in combination regimens.²⁴ Aside from the on-target toxicity concerns of Bcl-xL, it remains an important therapeutic target, especially in solid tumors, therefore development of selective Bcl-xL inhibitors remains an attractive approach. An academic group from the Walter and Eliza

Hall Institute developed a potent and selective Bcl-xL inhibitor, WEHI-539, and later worked with Abbvie to optimize additional inhibitors of Bcl-xL, including A-1155463 and the orally bioavailable analogue A-1331852, which displayed robust *in vivo* efficacy in tumor xenograft models (Figure 1.4).^{53–55} Along with these marquee Bcl-2 and/or Bcl-xL inhibitors are compounds of similar potency developed by Servier⁵⁶ and the Wang laboratory at the University of Michigan^{57,58}. These early successes and lessons learned in developing BH3 mimetics targeting Bcl-2 and Bcl-xL paved the path of drugging the Bcl-2 family and uncovered the need for selective Mcl-1 and Bfl-1 inhibitors.

1.6 Acquired resistance to Bcl-2/Bcl-xL inhibitors

Cancer cells eventually develop acquired resistance mechanisms in response to prolonged treatment to targeted therapies and BH3 mimetics are no exception.⁵⁹ There are several ways cancer cells can become resistant in order to circumvent the activity of targeted drugs, including binding site mutations, as seen in many kinases,⁶⁰ as well as upregulation of compensatory proteins and pathways.⁶¹ Data of prolonged clinical treatment with venetoclax is sparing, but a novel mutation (G101V) in Bcl-2, which induced a conformational change in the BH3 binding site, was identified in CLL patients receiving venetoclax treatment, which led to its reduced binding affinity and correlated with disease progression.⁶² Additional Bcl-2 binding site mutations were identified in this study using lymphoma mouse models treated with venetoclax, none of which significantly impacted the binding affinities of the BH3-only proteins. These important findings and structural information will be important to fuel the development of venetoclax analogues that can be administered to patients when these mutations are

identified, similar to the strategy used with kinase inhibitors in chronic myelogenous leukemia.⁶³

There have been numerous studies that highlight the role of the uninhibited anti-apoptotic proteins which are upregulated in response to prolonged venetoclax, ABT-737, and ABT-263 treatment, particularly Mcl-1 and Bfl-1. Treatment of initially sensitive B-cell lymphoma cells with ABT-737 led to a dynamic increase in both Mcl-1 and Bfl-1 protein levels, which conferred resistance to ABT-737.⁶⁴ In addition to increased Mcl-1 protein abundance, Mcl-1 phosphorylation and stabilization was identified in leukemia cells in response to ABT-737.⁶⁵ With respect to venetoclax, Mcl-1, Bfl-1, and Bcl-xL upregulation have all been shown to play a role in acquired resistance of non-Hodgkin lymphoma cell lines.^{66,67} Both on the protein and functional levels, Mcl-1 is increased in response to short term venetoclax treatment in AML.⁶⁸ Expression of Bfl-1 was identified as a biomarker of venetoclax resistance in a large genetic study of AML patient samples and was shown to promote resistance.⁶⁹ These reports of resistance to Bcl-2/Bcl-xL targeting BH3 mimetics further highlight the need to develop small molecule inhibitors of all the anti-apoptotic proteins, especially Mcl-1 and Bfl-1, to combat resistance mechanisms.

1.7 Development of selective Mcl-1 inhibitors

The need for selective Mcl-1 inhibitors emerged from the observance of Mcl-1 as a prominent resistance factor to other BH3 mimetics, as well as to many targeted, chemo-, and radio-therapies.⁷⁰ To address this need, numerous groups spanning academia and industry undertook focused efforts to develop selective Mcl-1 inhibitors

with a variety of approaches. Early fluorescence polarization (FP) based HTS campaigns by academic groups yielded important tool compounds such as the hydroxynaphthalen-arylsulfonamide series, including UMI-77 (Figure 1.5) developed by the Nikolovska-Coleska group⁷¹, and MIM1, with thiazolyl core, discovered from Walensky group. UMI-77 selectively inhibits Mcl-1 with a binding constant (K_i) value of 490 nM, with *in vitro* and *in vivo* efficacy in pancreatic cancer models.⁷² Utilizing a similar fragment-based NMR screening approach used to discover venetoclax, Abbvie was able to develop the first selective sub-nanomolar Mcl-1 inhibitor, A-1210477 (Figure 1.5).⁷³ Possessing a 2-carboxyindole core with a tethered hydrophobic moiety from the 3-position to access the p4 pocket and a 4-piperazinyloxy linker to accommodate the p4 pocket, A-1210477 inhibits Mcl-1 with a K_i of 450 pM. Although the biological efficacy of A-1210477 was not as robust as its binding affinity would suggest, it served as an important pharmacological tool to potently inhibit Mcl-1.⁷⁴ A series of reports by the Fesik group from Vanderbilt University culminated in the highly potent and biologically efficacious Mcl-1 inhibitor, VU661013 (Figure 1.5).^{68,75,76} Starting with a fragment screen, two fragments were merged to form a starting compound highly similar to the A-1210477 core 2-carboxyindole.⁷⁵ Through rigorous medicinal chemistry efforts, additional fragments were screened and linked to accommodate the p4 pocket, along with conformational restriction to form a tricyclic indole core.⁷⁶ Through optimization of hydrophobic interactions and adding another hydrogen bond with Asn260 of Mcl-1, VU661013 became the lead compound with a highly potent Mcl-1 K_i of 97 pM and robust biological activity in cancers such as acute myeloid leukemia.⁶⁸

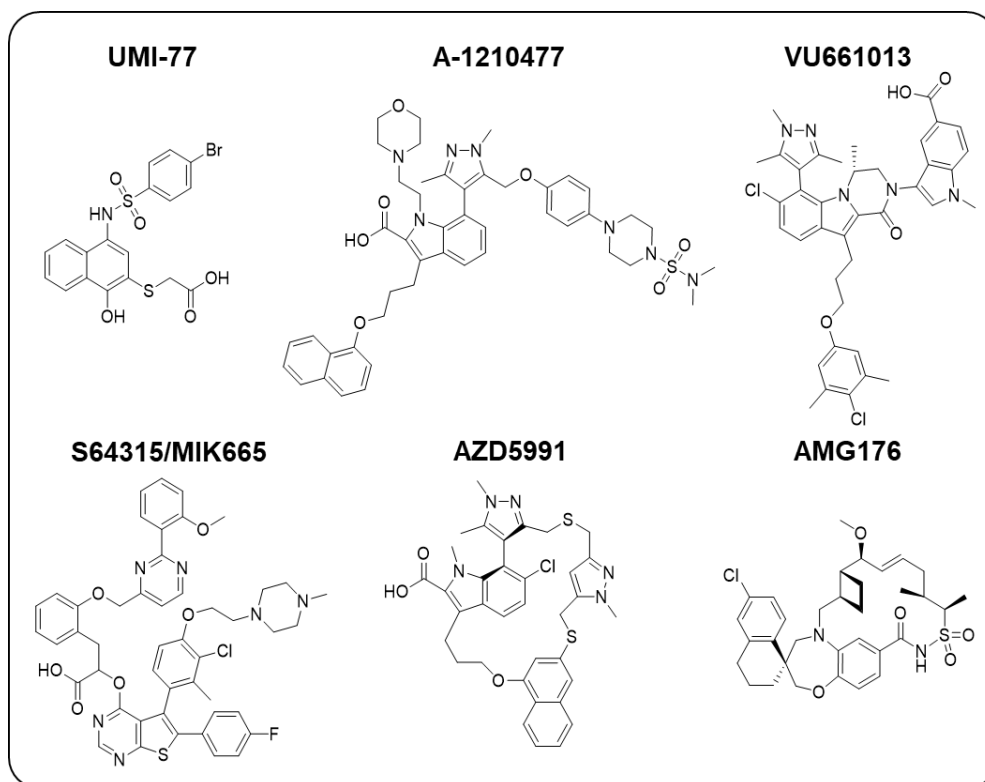


Figure 1.5 Structures of reported Mcl-1 selective inhibitors

The most noteworthy achievements in the efforts of Mcl-1 inhibitor development have come from several compounds that have entered phase I clinical trials for evaluation of safety, PK, pharmacodynamics, and efficacy in a variety of hematologic malignancies (Table 1.1).

Table 1.1 Mcl-1 inhibitors in phase I clinical trials

Mcl-1 Inhibitor	Company sponsor(s)	Indications	ClinicalTrials.org Identifier(s)
S64315/MIK665 (Figure 1.5)	Servier Novartis	MM AML DLBCL MDS Lymphoma	NCT02992483 NCT02979366 NCT03672695
AZD5991 (Figure 1.5)	AstraZeneca	NHL Richter Syndrome CLL SLL T-cell Lymphoma MM AML ALL	NCT03218683
AMG176 (Figure 1.5)	Amgen	MM AML NHL DLBCL	NCT02675452 NCT03797261
AMG397 (structure not disclosed)	Amgen	MM AML NHL DLBCL	NCT03465540
ABBV-467 (structure not disclosed)	Abbvie	MM	NCT04178902

MM=multiple myeloma, AML=acute myeloid leukemia, DLBCL=diffuse large B-cell lymphoma, MDS=myelodysplastic syndrome, NHL=non-Hodkin lymphoma, CLL=chronic lymphocytic leukemia, SLL=small lymphocytic leukemia, ALL=acute lymphocytic leukemia

A thienopyrimidine based Mcl-1 inhibitor was discovered by fragment screening and was developed by industry groups at Servier and Vernalis.⁷⁷ The published lead compound from this series, S63845, was the first reported selective Mcl-1 inhibitor with robust *in vivo* efficacy and showed activity in a wide range of cancer types by inhibiting Mcl-1 with a K_d of 190 pM.⁷⁸ Its closely related analogue S64315/MIK665 (Figure 1.5) is currently in phase I clinical trials as a single agent and in combination with the Bcl-2

inhibitor, venetoclax. Macrocyclic chemical compounds have also proven to produce potent Mcl-1 inhibitors, as with AZD5991 (Figure 1.5) developed by AstraZeneca.⁷⁹ AZD5991 was developed based on the analysis of co-crystal structures of intermediate compounds published from Abbvie's Mcl-1 inhibitor development program. Through cyclizing one of these 2-carboxyindole compounds and SAR investigations, AZD5991 was developed as a clinical candidate. AZD5991 inhibits Mcl-1 with a K_d of 170 pM and displays potent efficacy in hematologic malignancies, as well as solid tumors such as melanoma in combination with MAPK inhibitors.^{80,81} Another clinical stage macrocyclic compound is AMG176 (Figure 1.5) developed by Amgen based on an acylsulfonamide core structure.⁸² AMG176 was originally discovered through a large-scale time-resolved fluorescence resonance energy transfer (TR-FRET) based HTS and was optimized using structure-based design driven by conformational restriction and intricate synthesis. AMG176 selectively inhibits Mcl-1 with a K_i of 60 pM and is capable of inducing rapid tumor regression in hematologic cancer xenograft models with a single oral dose. Amgen also reported activity of AMG176 in combination with MEK inhibitors in KRas driven non-small cell lung cancer models.⁸³ AMG176 is currently being evaluated as a single agent by intravenous dosing (despite its oral bioavailability) and in combination with venetoclax in phase I clinical trials. Additional compounds with undisclosed structures and pre-clinical data that are also in phase I clinical trials are AMG397 from Amgen and ABBV-467 sponsored by Abbvie. Initial efficacy and toxicity data from these clinical trials are highly anticipated by those in the field of targeting the Bcl-2 protein family, especially considering genetic studies that allude to potential cardiotoxicity from Mcl-1 deletion. Additionally, learning about Mcl-1 inhibitor resistance

factors will be important, especially if other anti-apoptotic proteins are up-regulated to compensate.

1.8 Unmet need for Bfl-1 inhibitors

There is still a need to effectively target Bfl-1 with drug-like molecules, as it continues to emerge as an important therapeutic target, especially in regard to acquired resistance.^{33,64,69,84–87} The most potent selective inhibitors remain peptides that were discovered through mutational studies or hydrocarbon stapled derivatives of the natural BH3-only peptide sequences.^{88–91} Bfl-1 is unique in that it is the only anti-apoptotic protein that contains a Cys residue (C55) in its BH3 binding groove, allowing the possibility of developing covalent inhibitors. There have been several reports of covalent peptide inhibitors of Bfl-1 that have shown some on-target effect in cell-based studies.^{88,89} There is one reported small molecule N-acetyltryptophan analogue that covalently binds Bfl-1 through disulfide tethering to C55 and induces on-target intrinsic apoptosis.⁹² Our research group and others, using biochemical screening assays, have identified hit small molecule inhibitors of Bfl-1.^{93,94} A recent study identified bicyclic stapled peptides as dual Mcl-1/Bfl-1 inhibitors with cellular activity and demonstrated an opportunity to develop Noxa-mimetic type inhibitors.⁹⁵ However, there is still a need for a small molecule with high enough affinity to elicit a robust on-target cellular response as seen with other successful BH3 mimetics. A potent and selective Bfl-1 BH3 mimetic is the missing piece to complete the panel of Bcl-2 family antagonists, which then raises the next translational challenge of identifying effective means to guide the application of these therapeutics to the right patient populations.

1.9 BH3 profiling: a functional assay to determine survival dependence

Cell priming is a term used to define a cell's propensity to commit to apoptosis. When a cell is primed for apoptosis, it contains high levels of both pro- and anti-apoptotic proteins that are in a primed state in the form of PPI complexes that would readily trigger the intrinsic apoptotic pathway if a pro-apoptotic stimulus was applied, like chemotherapy or direct BH3 mimetic treatments.⁹⁶ Cancer cells usually exist in a highly primed state due to aberrant Bcl-2 protein family expression, while cells in normal tissues usually contain low amounts of these proteins and are not primed for apoptosis, with the exception of some hematopoietic cells and others with high turnover rates.⁹⁷ Additionally, cells can be primed for dependence on an individual anti-apoptotic protein, such as Bcl-2, Bcl-xL, or Mcl-1. Identifying which anti-apoptotic protein specific cancer cells rely on for survival dependence will help with the selection of BH3 mimetics that would produce apoptotic response.

BH3 profiling is a functional assay designed to detect survival dependence in individual cancer samples and is capable of effectively predicting response to selective BH3 mimetics.^{98,99} Originally developed by the Letai laboratory at the Dana-Farber Cancer Institute, BH3 profiling utilizes the natural selective binding profiles of the BH3-only proteins (Figure 1.2A) to individually antagonize the anti-apoptotic proteins which then elicits a functional response in the form of mitochondrial depolarization or cytochrome-c release from the mitochondria (Figure 1.6).¹⁰⁰ When one of the BH3-only peptides evokes a downstream effect, the functional survival dependence is attributed to its anti-apoptotic binding partner. The promiscuous peptides, Bim and Pima, are

capable of gauging overall baseline apoptotic priming of cells, which has been an effective strategy to determine apoptotic priming and predict the response to chemotherapy and BH3 mimetics in leukemia.^{101–104} The clinical utility of BH3 profiling has been substantiated in clinical trials to identify functional biomarkers of venetoclax response in acute myeloid leukemia.¹⁰⁵ It has also been a useful tool to parse the high heterogeneity of survival dependence in solid tumors, including breast,¹⁰⁶ thyroid,¹⁰⁷ colon,¹⁰⁸ and esophageal¹⁰⁹ cancers.

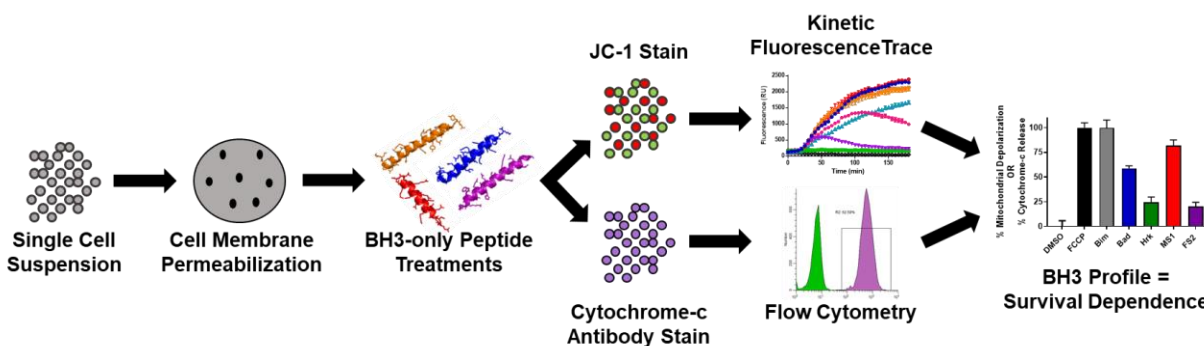


Figure 1.6 BH3 profiling workflow

Dynamic BH3 profiling is an adaptation of this functional technique that monitors the modulation of survival dependence induced by drug treatments.¹¹⁰ Many chemotherapeutics and molecular targeted drugs induce apoptosis in cancer cells through the intrinsic pathway and dynamic BH3 profiling is capable of predicting which drugs will achieve the greatest response in a specific cancer.¹¹¹ This tool is extremely valuable as it provides functional insight into the best drugs to employ before administering to a patient and can increase the success of clinical outcomes, especially in difficult to treat solid tumors.¹¹² Along with identifying specific drugs with the greatest ability to elicit apoptosis, dynamic profiling can also be used to determine if certain

drugs induce survival dependence on individual anti-apoptotic proteins and can therefore be used to design rational combination regimens with BH3 mimetics. Two interesting examples of this come from studies where statins¹¹³ and Bruton's tyrosine kinase inhibitors¹¹⁴ were found to increase Bcl-2 dependence and sensitivity to venetoclax. Overall, the application of BH3 profiling both in the baseline and dynamic setting serves as a valuable tool that can guide the use of BH3 mimetics along with chemotherapy and other targeted agents in the clinic to improve cancer treatments.

1.10 Conclusions and research aims

The field of Bcl-2 protein family targeting for cancer treatment has rapidly progressed over the past decade and continues to provide viable new treatment options for patients with aggressive malignancies. The goal of drugging the Bcl-2 protein family is being realized with an FDA approved Bcl-2 inhibitor and promising Bcl-xL and Mcl-1 inhibitors under clinical trial evaluation, while progress on Bfl-1 inhibitors has been slow but progressing. The broad heterogeneity of survival dependence on the anti-apoptotic proteins necessitated introducing functional methods and identifying biomarkers that can guide the use of BH3 mimetics as single agents and in combination treatments and predict the development of acquired resistance.

The overall aim of this dissertation research is to elucidate and identify trends in cancer survival dependence on the anti-apoptotic proteins, develop novel strategies to overcome resistance, and to develop new BH3 mimetic tools. To accomplish this goal the BH3 profiling assay relying on a set of selective chemical tools, was utilized to discover novel survival trends in a wide spectrum of cancers ranging from hematologic

malignancies to solid tumors. Furthermore, applying dynamic BH3 profiling, the role of anti-apoptotic proteins in acquired resistance to standard-of-care therapies in melanoma was investigated. In addition, the need for Bcl-1 inhibitors has been realized and we undertook substantial medicinal chemistry efforts to produce dual Mcl-1/Bcl-1 small molecule inhibitors to contribute to the advancement of BH3 mimetic development. Taken together, these research endeavors were focused on the ultimate goal of improving the treatment of various cancers and contributing to the alleviation of the pain and suffering that cancer patients continually go through.

1.11 References

1. Hanahan D, Weinberg RA. The hallmarks of cancer. *Cell*. 2000;100(1):57-70. doi:10.1016/S0092-8674(00)81683-9
2. Vogelstein B, Papadopoulos N, Velculescu VE, Zhou S, Diaz LA, Kinzler KW. Cancer genome landscapes. *Science* (80-). 2013;340(6127):1546-1558. doi:10.1126/science.1235122
3. Mroz EA, Rocco JW. The challenges of tumor genetic diversity. *Cancer*. 2017;123(6):917-927. doi:10.1002/cncr.30430
4. Chae YK, Pan AP, Davis AA, et al. Path toward precision oncology: Review of targeted therapy studies and tools to aid in defining “actionability” of a molecular lesion and patient management support. *Mol Cancer Ther*. 2017;16(12):2645-2655. doi:10.1158/1535-7163.MCT-17-0597
5. Collins FS, Varmus H. A New Initiative on Precision Medicine. *N Engl J Med*. 2015;372(9):793-795. doi:10.1056/NEJMp1500523
6. Garraway LA, Verweij J, Ballman K V. Precision oncology: An overview. *J Clin Oncol*. 2013;31(15):1803-1805. doi:10.1200/JCO.2013.49.4799
7. Arteaga CL, Baselga J. Impact of genomics on personalized cancer medicine. In: *Clinical Cancer Research*. Vol 18. ; 2012:612-618. doi:10.1158/1078-0432.CCR-11-2019
8. Friedman AA, Letai A, Fisher DE, Flaherty KT. Precision medicine for cancer with next-generation functional diagnostics. *Nat Rev Cancer*. 2015;15(12):747-756.

doi:10.1038/nrc4015

9. Letai A. Functional precision cancer medicine-moving beyond pure genomics. *Nat Med.* 2017;23(9):1028-1035. doi:10.1038/nm.4389
10. Kim JJ, Tosteson AN, Zauber AG, et al. Cancer Models and Real-World Data: Better Together. *J Natl Cancer Inst.* 2016;108(2). doi:10.1093/jnci/djv316
11. Hanahan D, Weinberg RA. Hallmarks of cancer: the next generation. *Cell.* 2011;144(5):646-674. doi:10.1016/j.cell.2011.02.013
12. Carneiro BA, El-Deiry WS. Targeting apoptosis in cancer therapy. *Nat Rev Clin Oncol.* 2020;17(7):395-417. doi:10.1038/s41571-020-0341-y
13. Elmore S. Apoptosis: A Review of Programmed Cell Death. *Toxicol Pathol.* 2007;35(4):495-516. doi:10.1080/01926230701320337
14. Savill J, Fadok V. Corpse clearance defines the meaning of cell death. *Nature.* 2000;407(6805):784-788. doi:10.1038/35037722
15. Wang X. The expanding role of mitochondria in apoptosis. *Genes Dev.* 2001;15(22):2922-2933.
16. Leibowitz B, Yu J. Mitochondrial signaling in cell death via the Bcl-2 family. *Cancer Biol Ther.* 2010;9(6):417-422. doi:10.4161/cbt.9.6.11392
17. Opferman JT, Kothari A. Anti-apoptotic BCL-2 family members in development. *Cell Death Differ.* 2018;25(1):37-45. doi:10.1038/cdd.2017.170
18. Gross A, Katz SG. Non-apoptotic functions of BCL-2 family proteins. *Cell Death Differ.* 2017;24(8):1348-1358. doi:10.1038/cdd.2017.22
19. Czabotar PE, Lessene G, Strasser A, Adams JM. Control of apoptosis by the BCL-2 protein family: implications for physiology and therapy. *Nat Rev Mol Cell Biol.* 2014;15(1):49-63. doi:10.1038/nrm3722
20. Popgeorgiev N, Jabbour L, Gillet G. Subcellular Localization and Dynamics of the Bcl-2 Family of Proteins. *Front Cell Dev Biol.* 2018;6(FEB):13. doi:10.3389/fcell.2018.00013
21. Opferman JT. Attacking cancer's Achilles heel: antagonism of anti-apoptotic BCL-2 family members. *FEBS J.* 2016;283(14):2661-2675. doi:10.1111/febs.13472
22. Letai A, Bassik MC, Walensky LD, Sorcinelli MD, Weiler S, Korsmeyer SJ. Distinct BH3 domains either sensitize or activate mitochondrial apoptosis, serving as prototype cancer therapeutics. *Cancer Cell.* 2002;2(3):183-192. doi:10.1016/S1535-6108(02)00127-7

23. Adams JM, Cory S. Bcl-2-regulated apoptosis: mechanism and therapeutic potential. *Curr Opin Immunol*. 2007;19(5):488-496. doi:10.1016/j.coi.2007.05.004
24. Yuan S, Akey CW. Apoptosome structure, assembly, and procaspase activation. *Structure*. 2013;21(4):501-515. doi:10.1016/j.str.2013.02.024
25. Brentnall M, Rodriguez-Menocal L, De Guevara RL, Cepero E, Boise LH. Caspase-9, caspase-3 and caspase-7 have distinct roles during intrinsic apoptosis. *BMC Cell Biol*. 2013;14(1):32. doi:10.1186/1471-2121-14-32
26. Singh R, Letai A, Sarosiek K. Regulation of apoptosis in health and disease: the balancing act of BCL-2 family proteins. *Nat Rev Mol Cell Biol*. 2019;20(3):175-193. doi:10.1038/s41580-018-0089-8
27. Yip KW, Reed JC. Bcl-2 family proteins and cancer. *Oncogene*. 2008;27(50):6398-6406. doi:10.1038/onc.2008.307
28. Tsujimoto Y, Finger LR, Yunis J, Nowell PC, Croce CM. Cloning of the chromosome breakpoint of neoplastic B cells with the t(14;18) chromosome translocation. *Science (80-)*. 1984;226(4678):1097-1099. doi:10.1126/science.6093263
29. Trisciuglio D, Tupone MG, Desideri M, et al. BCL-XL overexpression promotes tumor progression-associated properties article. *Cell Death Dis*. 2017;8(12):1-15. doi:10.1038/s41419-017-0055-y
30. Carné Trécesson S De, Souazé F, Basseville A, et al. BCL-XL directly modulates RAS signalling to favour cancer cell stemness. *Nat Commun*. 2017;8(1). doi:10.1038/s41467-017-01079-1
31. Beroukhi R, Mermel CH, Porter D, et al. The landscape of somatic copy-number alteration across human cancers. *Nature*. 2010;463(7283):899-905. doi:10.1038/nature08822
32. Belmar J, Fesik SW. Small molecule Mcl-1 inhibitors for the treatment of cancer. *Pharmacol Ther*. 2015;145:76-84. doi:10.1016/j.pharmthera.2014.08.003
33. Vogler M. BCL2A1: the underdog in the BCL2 family. *Cell Death Differ*. 2012;19(1):67-74. doi:10.1038/cdd.2011.158
34. Chen L, Willis SN, Wei A, et al. Differential Targeting of Prosurvival Bcl-2 Proteins by Their BH3-Only Ligands Allows Complementary Apoptotic Function. *Mol Cell*. 2005;17(3):393-403. doi:10.1016/j.molcel.2004.12.030
35. Arkin MR, Tang Y, Wells JA. Small-molecule inhibitors of protein-protein interactions: Progressing toward the reality. *Chem Biol*. 2014;21(9):1102-1114. doi:10.1016/j.chembiol.2014.09.001

36. Denis C, Sopková-De Oliveira Santos J, Bureau R, Voisin-Chiret AS. Hot-Spots of Mcl-1 Protein. *J Med Chem*. 2020;63(3):928-943. doi:10.1021/acs.jmedchem.9b00983
37. Merino D, Kelly GL, Lessene G, Wei AH, Roberts AW, Strasser A. BH3-Mimetic Drugs: Blazing the Trail for New Cancer Medicines. *Cancer Cell*. 2018;34(6):879-891. doi:10.1016/j.ccell.2018.11.004
38. Delbridge ARD, Strasser A. The BCL-2 protein family, BH3-mimetics and cancer therapy. *Cell Death Differ*. 2015;22(7):1071-1080. doi:10.1038/cdd.2015.50
39. Petros AM, Olejniczak ET, Fesik SW. Structural biology of the Bcl-2 family of proteins. *Biochim Biophys Acta - Mol Cell Res*. 2004;1644(2-3):83-94. doi:10.1016/j.bbamcr.2003.08.012
40. Newman DJ, Cragg GM. Natural Products as Sources of New Drugs from 1981 to 2014. *J Nat Prod*. 2016;79(3):629-661. doi:10.1021/acs.jnatprod.5b01055
41. Kitada S, Leone M, Sareth S, Zhai D, Reed JC, Pellecchia M. Discovery, Characterization, and Structure–Activity Relationships Studies of Proapoptotic Polyphenols Targeting B-Cell Lymphocyte/Leukemia-2 Proteins. *J Med Chem*. 2003;46(20):4259-4264. doi:10.1021/jm030190z
42. Wang G, Nikolovska-Coleska Z, Yang C-Y, et al. Structure-Based Design of Potent Small-Molecule Inhibitors of Anti-Apoptotic Bcl-2 Proteins. *J Med Chem*. 2006;49(21):6139-6142. doi:10.1021/jm060460o
43. Liu G, Kelly WK, Wilding G, Leopold L, Brill K, Somer B. An open-label, multicenter, phase I/II study of single-agent AT-101 in men with castrate-resistant prostate cancer. *Clin Cancer Res*. 2009;15(9):3172-3176. doi:10.1158/1078-0432.CCR-08-2985
44. Nguyen M, Marcellus RC, Roulston A, et al. Small molecule obatoclax (GX15-070) antagonizes MCL-1 and overcomes MCL-1-mediated resistance to apoptosis. *Proc Natl Acad Sci U S A*. 2007;104(49):19512-19517. doi:10.1073/pnas.0709443104
45. Schimmer AD, O'Brien S, Kantarjian H, et al. A phase I study of the pan bcl-2FamilyInhibitor obatoclax mesylate in patients with advanced hematologic malignancies. *Clin Cancer Res*. 2008;14(24):8295-8301. doi:10.1158/1078-0432.CCR-08-0999
46. Liu Q, Wang HG. Anti-cancer drug discovery and development bcl-2 family small molecule inhibitors. *Commun Integr Biol*. 2012;5(6):557-565. doi:10.4161/cib.21554
47. Shuker SB, Hajduk PJ, Meadows RP, Fesik SW. Discovering high-affinity ligands for proteins: SAR by NMR. *Science (80-)*. 1996;274(5292):1531-1534.

doi:10.1126/science.274.5292.1531

48. Oltersdorf T, Elmore SW, Shoemaker AR, et al. An inhibitor of Bcl-2 family proteins induces regression of solid tumours. *Nature*. 2005;435(7042):677-681. doi:10.1038/nature03579
49. Tse C, Shoemaker AR, Adickes J, et al. ABT-263: A Potent and Orally Bioavailable Bcl-2 Family Inhibitor. *Cancer Res*. 2008;68(9):3421-3428. doi:10.1158/0008-5472.CAN-07-5836
50. Sarosiek KA, Letai A. Directly targeting the mitochondrial pathway of apoptosis for cancer therapy using BH3 mimetics - recent successes, current challenges and future promise. *FEBS J*. 2016;283(19):3523-3533. doi:10.1111/febs.13714
51. Souers AJ, Levenson JD, Boghaert ER, et al. ABT-199, a potent and selective BCL-2 inhibitor, achieves antitumor activity while sparing platelets. *Nat Med*. 2013;19(2):202-208. doi:10.1038/nm.3048
52. Roberts AW, Davids MS, Pagel JM, et al. Targeting BCL2 with Venetoclax in Relapsed Chronic Lymphocytic Leukemia. *N Engl J Med*. 2016;374(4):311-322. doi:10.1056/NEJMoa1513257
53. Tao Z-F, Hasvold L, Wang L, et al. Discovery of a Potent and Selective BCL-X_L Inhibitor with *in Vivo* Activity. *ACS Med Chem Lett*. 2014;5(10):1088-1093. doi:10.1021/ml5001867
54. Lessene G, Czabotar PE, Sleebs BE, et al. Structure-guided design of a selective BCL-XL inhibitor. *Nat Chem Biol*. 2013;9(6):390-397. doi:10.1038/nchembio.1246
55. Wang L, Doherty GA, Judd AS, et al. Discovery of A-1331852, a First-in-Class, Potent and Orally-Bioavailable BCL-X_L Inhibitor. *ACS Med Chem Lett*. March 2020. doi:10.1021/acsmchemlett.9b00568
56. Casara P, Davidson J, Claperon A, et al. S55746 is a novel orally active BCL-2 selective and potent inhibitor that impairs hematological tumor growth. *Oncotarget*. 2018;9(28):20075-20088. doi:10.18632/oncotarget.24744
57. Aguilar A, Zhou H, Chen J, et al. A potent and highly efficacious Bcl-2/Bcl-xL inhibitor. *J Med Chem*. 2013;56(7):3048-3067. doi:10.1021/jm4001105
58. Bai L, Chen J, McEachern D, et al. BM-1197: A Novel and Specific Bcl-2/Bcl-xL Inhibitor Inducing Complete and Long-Lasting Tumor Regression In Vivo. Mott JL, ed. *PLoS One*. 2014;9(6):e99404. doi:10.1371/journal.pone.0099404
59. Szakács G, Paterson JK, Ludwig JA, Booth-Genthe C, Gottesman MM. Targeting multidrug resistance in cancer. *Nat Rev Drug Discov*. 2006;5(3):219-234. doi:10.1038/nrd1984

60. Barouch-Bentov R, Sauer K. Mechanisms of drug resistance in kinases. *Expert Opin Investig Drugs*. 2011;20(2):153-208. doi:10.1517/13543784.2011.546344
61. Neel DS, Bivona TG. Resistance is futile: overcoming resistance to targeted therapies in lung adenocarcinoma. *npj Precis Oncol*. 2017;1(1):3. doi:10.1038/s41698-017-0007-0
62. Birkinshaw RW, Gong J nan, Luo CS, et al. Structures of BCL-2 in complex with venetoclax reveal the molecular basis of resistance mutations. *Nat Commun*. 2019;10(1):1-10. doi:10.1038/s41467-019-10363-1
63. Jabbour E, Hochhaus A, Cortes J, La Rosée P, Kantarjian HM. Choosing the best treatment strategy for chronic myeloid leukemia patients resistant to imatinib: Weighing the efficacy and safety of individual drugs with BCR-ABL mutations and patient history. *Leukemia*. 2010;24(1):6-12. doi:10.1038/leu.2009.193
64. Yecies D, Carlson NE, Deng J, Letai A. Acquired resistance to ABT-737 in lymphoma cells that up-regulate MCL-1 and BFL-1. *Blood*. 2010;115(16):3304-3313. doi:10.1182/blood-2009-07-233304
65. Mazumder S, Choudhary GS, Al-harbi S, Almasan A. Mcl-1 phosphorylation defines ABT-737 resistance that can be overcome by increased NOXA expression in leukemic B cells. *Cancer Res*. 2012;72(12):3069-3079. doi:10.1158/0008-5472.CAN-11-4106
66. Choudhary GS, Al-Harbi S, Mazumder S, et al. MCL-1 and BCL-xL-dependent resistance to the BCL-2 inhibitor ABT-199 can be overcome by preventing PI3K/AKT/mTOR activation in lymphoid malignancies. *Cell Death Dis*. 2015;6(1). doi:10.1038/cddis.2014.525
67. Esteve-Arenys A, Valero JG, Chamorro-Jorganes A, et al. The BET bromodomain inhibitor CPI203 overcomes resistance to ABT-199 (venetoclax) by downregulation of BFL-1/A1 in in vitro and in vivo models of MYC+/BCL2+ double hit lymphoma. *Oncogene*. 2018;37(14):1830-1844. doi:10.1038/s41388-017-0111-1
68. Ramsey HE, Fischer MA, Lee T, et al. A Novel MCL1 Inhibitor Combined with Venetoclax Rescues Venetoclax-Resistant Acute Myelogenous Leukemia. *Cancer Discov*. 2018;8(12):1566-1581. doi:10.1158/2159-8290.CD-18-0140
69. Bisailon R, Moison C, Thiollier C, et al. Genetic characterization of ABT-199 sensitivity in human AML. *Leukemia*. 2020;34(1):63-74. doi:10.1038/s41375-019-0485-x
70. Quinn BA, Dash R, Azab B, et al. Targeting Mcl-1 for the therapy of cancer. *Expert Opin Investig Drugs*. 2011;20(10):1397-1411. doi:10.1517/13543784.2011.609167

71. Abulwerdi FA, Liao C, Mady AS, et al. 3-Substituted-N-(4-hydroxynaphthalen-1-yl)arylsulfonamides as a novel class of selective Mcl-1 inhibitors: structure-based design, synthesis, SAR, and biological evaluation. *J Med Chem.* 2014;57(10):4111-4133. doi:10.1021/jm500010b
72. Abulwerdi F, Liao C, Liu M, et al. A novel small-molecule inhibitor of mcl-1 blocks pancreatic cancer growth in vitro and in vivo. *Mol Cancer Ther.* 2014;13(3):565-575. doi:10.1158/1535-7163.MCT-12-0767
73. Bruncko M, Wang L, Sheppard GS, et al. Structure-Guided Design of a Series of MCL-1 Inhibitors with High Affinity and Selectivity. *J Med Chem.* 2015;58(5):2180-2194. doi:10.1021/jm501258m
74. Levenson JD, Zhang H, Chen J, et al. Potent and selective small-molecule MCL-1 inhibitors demonstrate on-target cancer cell killing activity as single agents and in combination with ABT-263 (navitoclax). *Cell Death Dis.* 2015;6(1):e1590. doi:10.1038/cddis.2014.561
75. Friberg A, Vigil D, Zhao B, et al. Discovery of Potent Myeloid Cell Leukemia 1 (Mcl-1) Inhibitors Using Fragment-Based Methods and Structure-Based Design. *J Med Chem.* 2013;56(1):15-30. doi:10.1021/jm301448p
76. Shaw S, Bian Z, Zhao B, et al. Optimization of Potent and Selective Tricyclic Indole Diazepinone Myeloid Cell Leukemia-1 Inhibitors Using Structure-Based Design. *J Med Chem.* 2018;61(6):2410-2421. doi:10.1021/acs.jmedchem.7b01155
77. Szlavik Z, Ondi L, Csékei M, et al. Structure-guided discovery of a selective mcl-1 inhibitor with cellular activity. *J Med Chem.* 2019;62(15):6913-6924. doi:10.1021/acs.jmedchem.9b00134
78. Kotschy A, Szlavik Z, Murray J, et al. The MCL1 inhibitor S63845 is tolerable and effective in diverse cancer models. *Nature.* 2016;538(7626):477-482. doi:10.1038/nature19830
79. Tron AE, Belmonte MA, Adam A, et al. Discovery of Mcl-1-specific inhibitor AZD5991 and preclinical activity in multiple myeloma and acute myeloid leukemia. *Nat Commun.* 2018;9(1):5341. doi:10.1038/s41467-018-07551-w
80. Koch R, Christie AL, Crombie JL, et al. Biomarker-driven strategy for MCL1 inhibition in T-cell lymphomas. *Blood.* 2019;133(6):566-575. doi:10.1182/blood-2018-07-865527
81. Sale MJ, Minihane E, Monks NR, et al. Targeting melanoma's MCL1 bias unleashes the apoptotic potential of BRAF and ERK1/2 pathway inhibitors. *Nat Commun.* 2019;10(1):1-19. doi:10.1038/s41467-019-12409-w
82. Caenepeel S, Brown SP, Belmontes B, et al. AMG 176, a Selective MCL1

- Inhibitor, is Effective in Hematological Cancer Models Alone and in Combination with Established Therapies. *Cancer Discov.* 2018;8(12):CD-18-0387. doi:10.1158/2159-8290.CD-18-0387
83. Nangia V, Siddiqui FM, Caenepeel S, et al. Exploiting MCL1 Dependency with Combination MEK + MCL1 Inhibitors Leads to Induction of Apoptosis and Tumor Regression in KRAS-Mutant Non-Small Cell Lung Cancer. 2018. doi:10.1158/2159-8290.CD-18-0277
 84. Haq R, Yokoyama S, Hawryluk EB, et al. *BCL2A1* is a lineage-specific antiapoptotic melanoma oncogene that confers resistance to BRAF inhibition. *Proc Natl Acad Sci.* 2013;110(11):4321-4326. doi:10.1073/pnas.1205575110
 85. Champa D, Russo MA, Liao X-H, Refetoff S, Ghossein RA, Di Cristofano A. Obatoclox overcomes resistance to cell death in aggressive thyroid carcinomas by countering Bcl2a1 and Mcl1 overexpression. *Endocr Relat Cancer.* 2014;21(5):755-767. doi:10.1530/ERC-14-0268
 86. Morales AA, Olsson A, Celsing F, Österborg A, Jondal M, Osorio LM. High expression of bfl-1 contributes to the apoptosis resistant phenotype in B-cell chronic lymphocytic leukemia. *Int J Cancer.* 2005;113(5):730-737. doi:10.1002/ijc.20614
 87. Olsson A, Norberg M, Ökvist A, et al. Upregulation of bfl-1 is a potential mechanism of chemoresistance in B-cell chronic lymphocytic leukaemia. *Br J Cancer.* 2007;97(6):769-777. doi:10.1038/sj.bjc.6603951
 88. Huhn AJ, Guerra RM, Harvey EP, Bird GH, Walensky LD. Selective Covalent Targeting of Anti-Apoptotic BFL-1 by Cysteine-Reactive Stapled Peptide Inhibitors. *Cell Chem Biol.* 2016;23(9):1123-1134. doi:10.1016/j.chembiol.2016.07.022
 89. Harvey EP, Seo H-S, Guerra RM, Bird GH, Dhe-Paganon S, Walensky LD. Crystal Structures of Anti-apoptotic BFL-1 and Its Complex with a Covalent Stapled Peptide Inhibitor. *Structure.* 2018;26(1):153-160.e4. doi:10.1016/j.str.2017.11.016
 90. Guerra RM, Bird GH, Harvey EP, et al. Precision Targeting of BFL-1/A1 and an ATM Co-dependency in Human Cancer. *Cell Rep.* 2018;24(13):3393-3403.e5. doi:10.1016/j.celrep.2018.08.089
 91. Jenson JM, Ryan JA, Grant RA, Letai A, Keating AE. Epistatic mutations in PUMA BH3 drive an alternate binding mode to potently and selectively inhibit anti-apoptotic Bfl-1. *Elife.* 2017;6. doi:10.7554/eLife.25541
 92. Harvey EP, Hauseman ZJ, Cohen DT, et al. Identification of a Covalent Molecular Inhibitor of Anti-apoptotic BFL-1 by Disulfide Tethering. *Cell Chem Biol.* 2020;27(6):647-656.e6. doi:10.1016/j.chembiol.2020.04.004

93. Mathieu A-L, Sperandio O, Pottiez V, et al. Identification of Small Inhibitory Molecules Targeting the Bfl-1 Anti-Apoptotic Protein That Alleviates Resistance to ABT-737. *J Biomol Screen*. 2014;19(7):1035-1046. doi:10.1177/1087057114534070
94. Mady ASA, Liao C, Bajwa N, et al. Discovery of Mcl-1 inhibitors from integrated high throughput and virtual screening. *Sci Rep*. 2018;8(1):10210. doi:10.1038/s41598-018-27899-9
95. D. de Araujo A, Lim J, Wu K-C, et al. Bicyclic Helical Peptides as Dual Inhibitors Selective for Bcl2A1 and Mcl-1 Proteins. *J Med Chem*. 2018;61(7):2962-2972. doi:10.1021/acs.jmedchem.8b00010
96. Potter DS, Letai A. To prime, or not to prime: That is the question. *Cold Spring Harb Symp Quant Biol*. 2016;81(1):131-140. doi:10.1101/sqb.2016.81.030841
97. Montero J, Letai A. Why do BCL-2 inhibitors work and where should we use them in the clinic? *Cell Death Differ*. 2018;25(1):56-64. doi:10.1038/cdd.2017.183
98. Butterworth M, Pettitt A, Varadarajan S, Cohen GM. BH3 profiling and a toolkit of BH3-mimetic drugs predict anti-apoptotic dependence of cancer cells. *Br J Cancer*. 2016;114(6):638-641. doi:10.1038/bjc.2016.49
99. Touzeau C, Ryan J, Guerriero J, et al. BH3 profiling identifies heterogeneous dependency on Bcl-2 family members in multiple myeloma and predicts sensitivity to BH3 mimetics. *Leukemia*. 2016;30(3):761-764. doi:10.1038/leu.2015.184
100. Ryan J, Letai A. BH3 profiling in whole cells by fluorimeter or FACS. *Methods*. 2013;61(2):156-164. doi:10.1016/j.ymeth.2013.04.006
101. Deng J, Carlson N, Takeyama K, Dal Cin P, Shipp M, Letai A. BH3 Profiling Identifies Three Distinct Classes of Apoptotic Blocks to Predict Response to ABT-737 and Conventional Chemotherapeutic Agents. *Cancer Cell*. 2007;12(2):171-185. doi:10.1016/j.ccr.2007.07.001
102. Pierceall WE, Kornblau SM, Carlson NE, et al. BH3 profiling discriminates response to cytarabine-based treatment of acute myelogenous leukemia. *Mol Cancer Ther*. 2013;12(12):2940-2949. doi:10.1158/1535-7163.MCT-13-0692
103. Vo TT, Ryan J, Carrasco R, et al. Relative mitochondrial priming of myeloblasts and normal HSCs determines chemotherapeutic success in AML. *Cell*. 2012;151(2):344-355. doi:10.1016/j.cell.2012.08.038
104. Chonghaile TN, Sarosiek KA, Vo TT, et al. Pretreatment mitochondrial priming correlates with clinical response to cytotoxic chemotherapy. *Science (80-)*. 2011;334(6059):1129-1133. doi:10.1126/science.1206727
105. Konopleva M, Pollyea DA, Potluri J, et al. Efficacy and biological correlates of

- response in a phase II study of venetoclax monotherapy in patients with acute Myelogenous Leukemia. *Cancer Discov.* 2016;6(10):1106-1117. doi:10.1158/2159-8290.CD-16-0313
106. Goodwin CM, Rossanese OW, Olejniczak ET, Fesik SW. Myeloid cell leukemia-1 is an important apoptotic survival factor in triple-negative breast cancer. *Cell Death Differ.* 2015;22(12):2098-2106. doi:10.1038/cdd.2015.73
 107. Gunda V, Sarosiek KA, Brauner E, et al. Inhibition of MAPKinase pathway sensitizes thyroid cancer cells to ABT-737 induced apoptosis. *Cancer Lett.* 2017;395:1-10. doi:10.1016/j.canlet.2017.02.028
 108. Ishikawa K, Kawano Y, Arihara Y, et al. BH3 profiling discriminates the anti-apoptotic status of 5-fluorouracil-resistant colon cancer cells. *Oncol Rep.* 2019;42(6):2416-2425. doi:10.3892/or.2019.7373
 109. Taylor Ripley R, Surman DR, Diggs LP, et al. Metabolomic and BH3 profiling of esophageal cancers: Novel assessment methods for precision therapy. *BMC Gastroenterol.* 2018;18(1):94. doi:10.1186/s12876-018-0823-x
 110. Montero J, Letai A. Dynamic BH3 profiling-poking cancer cells with a stick. *Mol Cell Oncol.* 2016;3(3). doi:10.1080/23723556.2015.1040144
 111. Montero J, Sarosiek KA, Deangelo JD, et al. Drug-Induced death signaling strategy rapidly predicts cancer response to chemotherapy. *Cell.* 2015;160(5):977-989. doi:10.1016/j.cell.2015.01.042
 112. Bholá PD, Ahmed E, Guerriero JL, et al. High-throughput dynamic BH3 profiling may quickly and accurately predict effective therapies in solid tumors. *Sci Signal.* 2020;13(636). doi:10.1126/scisignal.aay1451
 113. Lee JS, Roberts A, Juarez D, et al. Statins enhance efficacy of venetoclax in blood cancers. *Sci Transl Med.* 2018;10(445). doi:10.1126/scitranslmed.aaq1240
 114. Deng J, Isik E, Fernandes SM, Brown JR, Letai A, Davids MS. Bruton's tyrosine kinase inhibition increases BCL-2 dependence and enhances sensitivity to venetoclax in chronic lymphocytic leukemia. *Leukemia.* 2017;31(10):2075-2084. doi:10.1038/leu.2017.32

Chapter 2

Functional Elucidation and Inhibition of the Bcl-2 Pro-Survival Proteins Unveils Precision Medicine Strategies in a Wide Spectrum of Cancers

2.1 Abstract

Clinical outcomes in oncology have been improved by precision medicine strategies and could be further enhanced by incorporating functional biomarkers. Targeting the Bcl-2 pro-survival proteins holds therapeutic promise in various cancers and has potential to play a role in precision oncology therapy. BH3 profiling distinguishes pro-survival dependence in individual cancers and we further explored its utility as a functional diagnostic. Our results indicate that various hematologic cancer cell lines are sensitive to single agent treatment with Bcl-2 and/or Mcl-1 inhibitors, highlighted by our finding that certain lymphomas subtypes of B-cell and T-cell origin are preferentially dependent upon Bcl-2 and Mcl-1, respectively. These conclusions were further substantiated in primary patient samples. We screened a diverse array of solid tumor cell lines, including ovarian cancer PDX models, and were able to pinpoint single agent BH3 mimetic sensitive cancers. Additionally, we identified that the combination of Bcl-xL and Mcl-1 inhibitors induced robust apoptosis in most solid tumor cell lines. This study outlines a strategy for parsing functional pro-survival culprits in various cancers and provides translational applications for employing BH3 mimetics in precision cancer therapy.

2.2 Introduction

Effective practice of oncology precision medicine relies on distinguishing and targeting unique characteristics of individual cancers.¹ Identifying predictive biomarkers that incorporate functional characteristics of cancers presents a translational opportunity to enhance clinical outcomes.^{2,3} Capabilities of cancer cells are defined by distinct hallmarks, one of which is resistance to cell death through overexpressing Bcl-2 family anti-apoptotic proteins.⁴ The anti-apoptotic proteins, Bcl-2, Bcl-xL, Mcl-1, and Bfl-1, govern mitochondrial mediated programmed cell death by sequestering opposing pro-apoptotic proteins.⁵ Inhibiting protein-protein interactions (PPIs) between anti- and pro-apoptotic proteins in cancer cells leads to sensitization to cell death and apoptosis.⁶ Targeting PPIs is a validated therapeutic approach and development of small molecule inhibitors of these interactions have been a hot area in drug discovery, leading to the FDA-approval of venetoclax (selective Bcl-2 inhibitor), for treating chronic lymphocytic leukemia and promise in various indications.^{7,8} Selective Mcl-1 and Bcl-xL inhibitors have been developed and are being clinically evaluated in diverse cancers, setting the stage for physicians to have selective Bcl-2 family inhibitors to employ in precision medicine.⁹⁻¹² Progress on Bfl-1 small molecule inhibitors has been reported by our group,^{13,14} as well as peptide based inhibitors by others,¹⁵⁻¹⁸ with the aim of completing the arsenal of anti-apoptotic protein antagonists.

In order to parse the heterogeneity of functional survival dependence on Bcl-2 anti-apoptotic proteins, the BH3 profiling assay was established by the Letai laboratory.¹⁹⁻²¹ This assay utilizes the selective binding of endogenous PPIs between BH3-only and anti-apoptotic Bcl-2 proteins to induce mitochondrial depolarization. By

using BH3-only peptides which bind selectively to the anti-apoptotic proteins and measuring the induced mitochondrial depolarization, it can be identified which anti-apoptotic protein promotes survival dependence. This assay has been used in numerous studies and represents an appropriate tool to probe the intrinsic apoptosis pathway in cancer.²²⁻²⁸

In this study we investigated the role of Bcl-2 family proteins in a wide spectrum of cancers from hematologic and solid tumor origins using established and patient derived xenograft (PDX) cell lines and primary patient samples. We validated the up-to-date chemical toolkit of anti-apoptotic protein inhibitors, including the FS2 peptide²⁹ which allowed us to perform novel studies probing for Bfl-1 dependence across various cancer types in the BH3 profiling assay. BH3 profiling effectively identified dependence on Bcl-2, Bcl-xL, Mcl-1, and/or Bfl-1 and predicted sensitivity to selective small molecule BH3 mimetics. Distinct trends were discovered based on a particular cancer's preference for functional dependence on pro-survival proteins. The use of primary patient samples solidifies the clinical utility of this approach and strengthens the rationale for including Bcl-2 family protein targeting in precision medicine by utilizing BH3 profiling to pinpoint potentially responsive cancers. This study builds on previous reports evaluating Bcl-2 protein targeting across various cancer types by focusing on functional analysis with BH3 profiling and using potent, up-to-date BH3 mimetics.³⁰⁻³²

2.3 *In vitro* binding and functional validation of chemical tools

The principle of BH3 profiling is based on exposing the mitochondria to different BH3-only peptides obtained from pro-apoptotic proteins and measuring the resulting

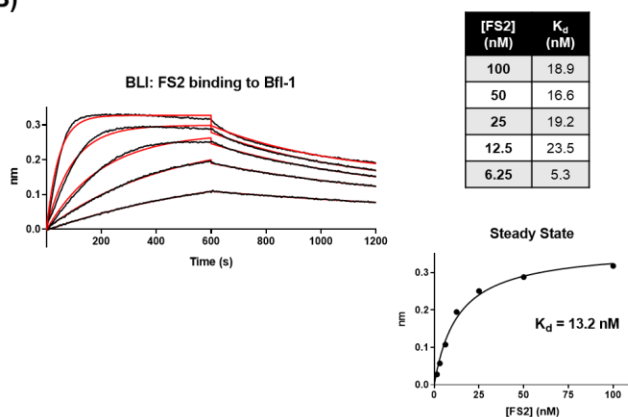
depolarization of the outer mitochondrial membrane. The selective binding profile of these peptides to anti-apoptotic proteins is used to identify dependence on individual members of Bcl-2 family proteins. The following BH3-only peptides were used in this study: Bim, Puma, Bad, Hrk, Noxa, MS1,³³ and FS2²⁹. To verify the binding affinity and selectivity of the peptides, a fluorescence polarization (FP) based binding assay was used (Figure 2.1). The obtained binding results confirm the selective profiles and binding affinities (K_i values) that have been reported in previous studies (Figure 2.1A).³⁴ The recently developed Bfl-1 selective peptide, FS2, was further evaluated for its binding potency by both bio-layer interferometry (BLI) and isothermal titration calorimetry (ITC), providing novel support of the previously reported Bfl-1 affinity only shown in the FP based assay (Figures 2.1B-C).²⁹ These assays provided K_d values of 13.2 nM and 26 nM in the BLI and ITC assays, respectively, consistent with the K_i values as well as reported data. It is important to note that this peptide shows the lowest level of selectivity in comparison with other BH3-only peptides tested. FS2 binds to Mcl-1 with K_i of 179 nM, about 20-fold decreased binding affinity, followed by Bcl-2 (K_i = 860 nM) and Bcl-xL (K_i = 1,040 nM). Understanding the binding affinity and selectivity of the BH3-only peptides is very important for identification of the anti-apoptotic protein on which the cells depend for survival when used in the functional assay. To validate the results obtained from utilizing the BH3-only peptides, the following reported potent and selective small molecule inhibitors were used: ABT-199/venetoclax targeting Bcl-2,⁷ A-1155463, binding to Bcl-xL,¹² and S63845, selective Mcl-1 inhibitor⁹. The FP assay confirmed their binding affinities (Figure 2.1A). Together, this experimental binding data

confirms what has been previously reported, making these tools suitable to study the Bcl-2 anti-apoptotic dependence in functional assays.

A)

	BH3-only Peptides						BH3 Mimetics		
	Bim	Bad	Hrk	Noxa	MS1	FS2	ABT-199	A-1155463	S63845
Bcl-2	<10	<10	>5,000	>5,000	>5,000	860 ± 82	<2		
Bcl-xL	<10	<10	41 ± 5.9	>5,000	>5,000	1,040 ± 310		<2	
Mcl-1	<10	>5,000	>5,000	<10	<10	179 ± 46			<2
Bfl-1	<10	>5,000	>5,000	24 ± 7.5	>5,000	<10			

B)



C)

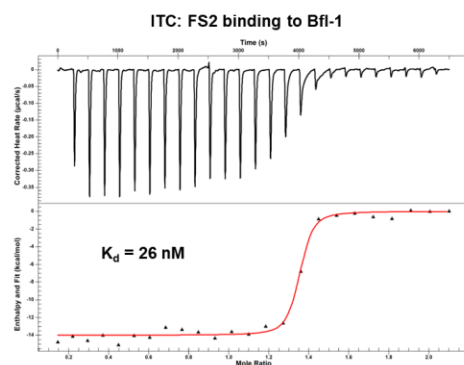


Figure 2.1 Binding affinity and selectivity of anti-apoptotic protein inhibitors

A) K_i binding values (nM) obtained from competitive FP assays of BH3-only peptides and small molecule BH3 mimetics binding to the anti-apoptotic proteins Bcl-2, Bcl-xL, Mcl-1, and Bfl-1. Results are presented as the mean ± SD from three independent experiments. **B)** Bio-layer interferometry (BLI) direct binding of FS2 to Bfl-1, K_d values calculated by both kinetic K_{on}/K_{off} (table) and by steady state saturation curve. **C)** Isothermal titration calorimetry (ITC) of FS2 binding to Bfl-1, with determined K_d .

To further validate these tools for their predictive value within a functional context, BH3 profiling was performed on the Eu-Myc Lymphoma cell lines, which were engineered to overexpress and depend on individual human anti-apoptotic proteins Bcl-2, Bcl-xL, Mcl-1, and Bfl-1.³⁵ As expected, both Bim and Puma, promiscuous BH3-only peptides binding with similar potency to all anti-apoptotic proteins, were able to induce high levels of depolarization in all cell lines, indicating that the cells are well primed for apoptosis (Figure 2.2A). The naturally occurring BH3-only peptides Bad, Hrk, and Noxa,

consistent with their binding profile, maintain a wide selectivity window up to 30 μM , inducing mitochondrial depolarization in the Bcl-2/Bcl-xL, Bcl-xL, and Mcl-1/Bfl-1 cell lines, respectively (Figure 2.3A-C). Importantly, the level of mitochondrial depolarization correlated with their binding affinities. Bad is a potent inhibitor of both, Bcl-2 and Bcl-xL, and induced high depolarization in all three tested concentrations (Fig.2.1A), while predicting the survival dependence on both of these proteins. Hrk, a selective Bcl-xL binder and predictor of Bcl-xL dependence, needs to be used in higher concentrations (30 and 10 μM) to induce depolarization in similar levels because of its moderate binding affinity. Sole Bcl-2 dependence is defined as high Bad and low Hrk depolarization (Figure 2.2A and 2.3A-B). MS1 induces strong depolarization of the Mcl-1 cell line as expected, but loses selectivity at 30 μM , where it begins to depolarize the Bfl-1 cell line (Figure 2.3D). Consistent with its binding profile (Figure 2.1), FS2 exhibits a narrower selectivity window, but maintains selective Bfl-1 inhibition at concentrations below 10 μM , with Mcl-1 being the most prevalent off target binder (Figure 2.3E). These BH3 profiling validation experiments demonstrated that the *in vitro* binding selectivity of BH3-only peptides is recapitulated on the functional cellular level when they are used in a proper concentrations and defined 10 μM of Bad, Hrk, and MS1 and 3 μM of FS2 as the suitable concentrations for subsequent BH3 profiling experiments.

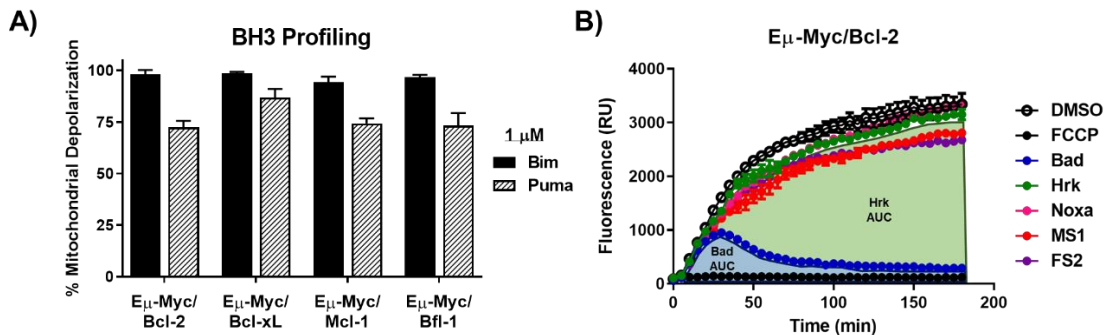


Figure 2.2 Apoptotic priming in E μ -Myc cell lines and example of Bcl-2 dependence

A) Mitochondrial depolarization values of Bim and Puma across the E μ -Myc Lymphoma cell lines. **B)** Kinetic BH3 profile of the E μ -Myc/Bcl-2 cell line (10 μ M peptides) with the area under the curve (AUC) shaded for Bad (blue) and Hrk (green).

To verify that BH3 profiling can predict small molecule sensitivity in the E μ -Myc cell lines we treated intact cells with the selective BH3 mimetics and analyzed cell death induction. As expected, the small molecules ABT-199, A-1155463, and S63845 only induced cell death in the Bcl-2, Bcl-xL, and Mcl-1 cell lines, respectively (Figure 2.3F). BH3 mimetics at 1 μ M fully inhibit their target proteins while remaining selective, making it a suitable concentration for ensuing apoptosis experiments. Importantly, the Bfl-1 cell line remained unharmed by any of the inhibitors, consistent with their binding selectivity that shows no engagement with the Bfl-1 protein at tested concentration (Figure 2.1A). This finding highlights the need of developing drug-like molecules that target Bfl-1; although drugging Bfl-1 has proven challenging, we have reported a class of small molecule dual Mcl-1/Bfl-1 inhibitors that lay a promising foundation to meet this need.¹³ Using the most potent dual Mcl-1/Bfl-1 inhibitor we demonstrated that compound 24 was able to induce cell death only in E μ -Myc lymphoma cell lines that depend on Mcl-1 and Bfl-1 (for more details see Figure 4.8 in Chapter 4).

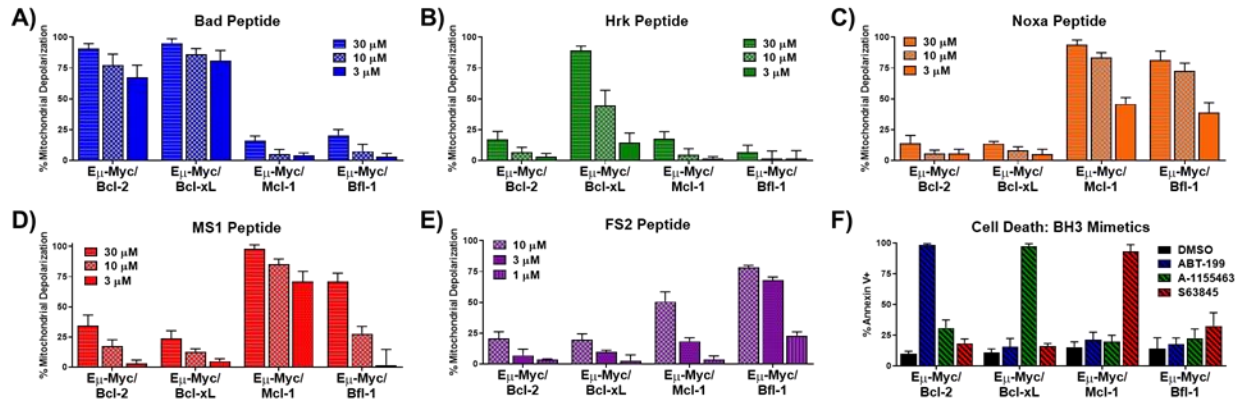


Figure 2.3 Functional assessment of chemical tools in E μ -Myc Lymphoma cell lines

BH3 profiles using varying doses of the natural BH3-only peptides **A)** Bad, **B)** Hrk, and **C)** Noxa and engineered peptides **D)** MS1 and **E)** FS2. **F)** Cell death induced by 1 μ M of the selective small molecule BH3 mimetics ABT-199, A-1155463, and S63845 (24-hour treatments). Cell death analyzed by flow cytometry; % dead cells quantified by violet LIVE/DEAD dye positive populations. All data represented as mean and SEM of three biological replicates.

2.4 Parsing anti-apoptotic dependence in hematologic malignancies

To investigate functional pro-survival trends in blood cancers, we performed BH3 profiling and correlative BH3 mimetic experiments on various cell lines and primary patient samples. The obtained results in acute myeloid leukemia (AML) (Figure 2.4) and lymphoma (Figure 2.5) illustrate distinct trends with potential clinical relevance. BH3 profiling was performed on five commonly used AML cell lines, which represent diverse genetic and clinical backgrounds, including FLT3 and MLL rearrangements and secondary AMLs. We identified that the Bad and MS1 peptides induced the highest levels of depolarization, with minimal effect of Hrk, concluding that both Bcl-2 and Mcl-1 primarily contribute to the apoptotic blockade (Figure 2.4A). Only MS1 was capable of inducing high depolarization in the SKM-1 cell line, which provides an example of a solely Mcl-1 dependent AML sample (Figure 2.4A). On the protein level, the most notable heterogeneity across cell lines were seen with Mcl-1, Bim, and Noxa, and no

observed correlation to functional dependence (Figure 2.4B).³⁶ Confirming our functional assessment of Bcl-2 and Mcl-1 being the main pro-survival players, we identified that 4/5 cell lines are sensitive to both ABT-199 and S63845, while SKM-1 shows sensitivity only to S63845 (Figure 2.4C). Cell viability experiments to determine the effect of the individual inhibitors in Molm-13 and SKM-1, demonstrated a divergence in sensitivity to ABT-199, as expected (Figure 2.4D). This cell viability data also provides important insights into the dual-sensitivity to both ABT-199 and S63845, by Molm-13 showing similar IC₅₀ values of 52 and 35 nM, respectively. Meanwhile in the SKM-1, Mcl-1 dependent cell line, S63845 produced an IC₅₀ of 230 nM, while being relatively insensitive to ABT-199 giving an IC₅₀ ~10 μM. To highlight the clinical applicability of this approach and relevance of conclusions, we performed BH3 profiling on three AML patient samples (Figure 2.4E). The obtained results further confirmed the level heterogeneity of survival dependence in AML patients; one patient displayed a co-Bcl-2/Mcl-1 dependence, similar to 4/5 of the cell lines, while one displayed predominant Bcl-2 dependence, and other was Mcl-1 dependent. This study in AML confirms the anti-apoptotic heterogeneity and predicts sensitivity to BH3 mimetic inhibitors of Bcl-2 and Mcl-1, supplementing current knowledge in targeting Bcl-2 proteins in AML.³⁶⁻³⁸

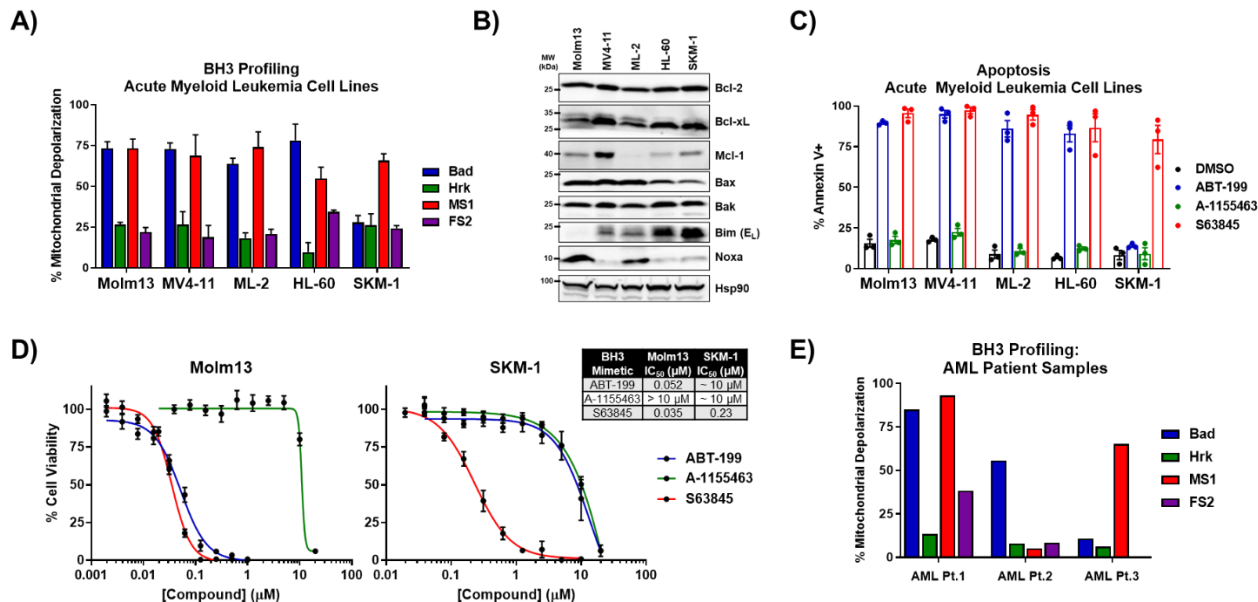


Figure 2.4 Targeting Mcl-1 and Bcl-2 dual dependence in AML

A) BH3 profiling of AML cell lines (10 μM Bad, Hrk, MS1; 3 μM FS2). **B)** Western blot of baseline Bcl-2 family proteins in AML cell line panel. **C)** MTT cell viability experiments of Molm-13 and SKM-1 cell lines following 72-hour BH3 mimetic treatments. **D)** Apoptosis induced by 1 μM of selective BH3 mimetics following 24 hours of treatment. Results presented as mean and SEM of three independent experiments. **E)** BH3 profiling of AML patient samples performed as n=1 due to limited sample.

BH3 profiling of a panel of lymphoma cell lines, segmented into subtypes of B-cell or T-cell origin (Figure 2.5), revealed that B-cell mantle cell lymphoma (MCL) cell lines have predominant dependence on Bcl-2 for survival, while T-cell anaplastic large cell lymphomas (ALCL) rely strongly on Mcl-1, as indicated by selective Bad or MS1 induced depolarization (Figure 2.5A). The baseline Bcl-2 protein expression in the lymphoma cell line panel supports the preferential survival mechanisms, showing that B-cell lymphoma lines express substantially higher amounts of Bcl-2 protein and the T-cell lymphoma lines expressed higher levels of Mcl-1, relative to one another (Figure 2.5B). Bfl-1 protein levels were only detected in T-cell lymphoma cell lines, particularly in SU-DHL-1, which also displayed the highest level of depolarization with the FS2 peptide, likely due to a NPM-ALK driven mechanism that is present in all the ALCL cell

lines tested.³⁹ This trend in preferential survival dependence was supported by small molecule sensitivities, where most B-cell lymphoma cells were sensitive to ABT-199, while T-cell lymphomas are generally more sensitive to S63845, within our panel (Figure 2.5C). In further support of the sensitivity to single agent BH3 mimetics, the Granta-519 (B-cell) and DEL (T-cell) displayed potent, dose dependent caspase-3/7 activation in response to ABT-199 or S63845 treatments, respectively (Figure 2.5D). This novel Bcl-2 family functional data provides rationale for identifying targetable dependencies and clustering lymphoma sub-types based on anti-apoptotic protein preference to inform precision medicine strategies.

To substantiate the translational applicability of these results in cell lines, we performed BH3 profiling on various hematologic cancer patient samples of lymphoid origin (Figures 2.5E-G). BH3 profiling of five chronic lymphocytic leukemia (CLL) patient samples identified Bcl-2 as the predominant functional player (Figure 2.5E), which supports the clinical success of venetoclax in this indication.⁸ In the MCL patient samples we identified a similar trend noted in cell lines, that there is a predominant functional preference for Bcl-2 dependence (Figure 2.5F). Conversely, the T-cell lymphoma primary specimens are majorly Mcl-1 dependent, with increased Bfl-1 involvement (Figure 2.5G).

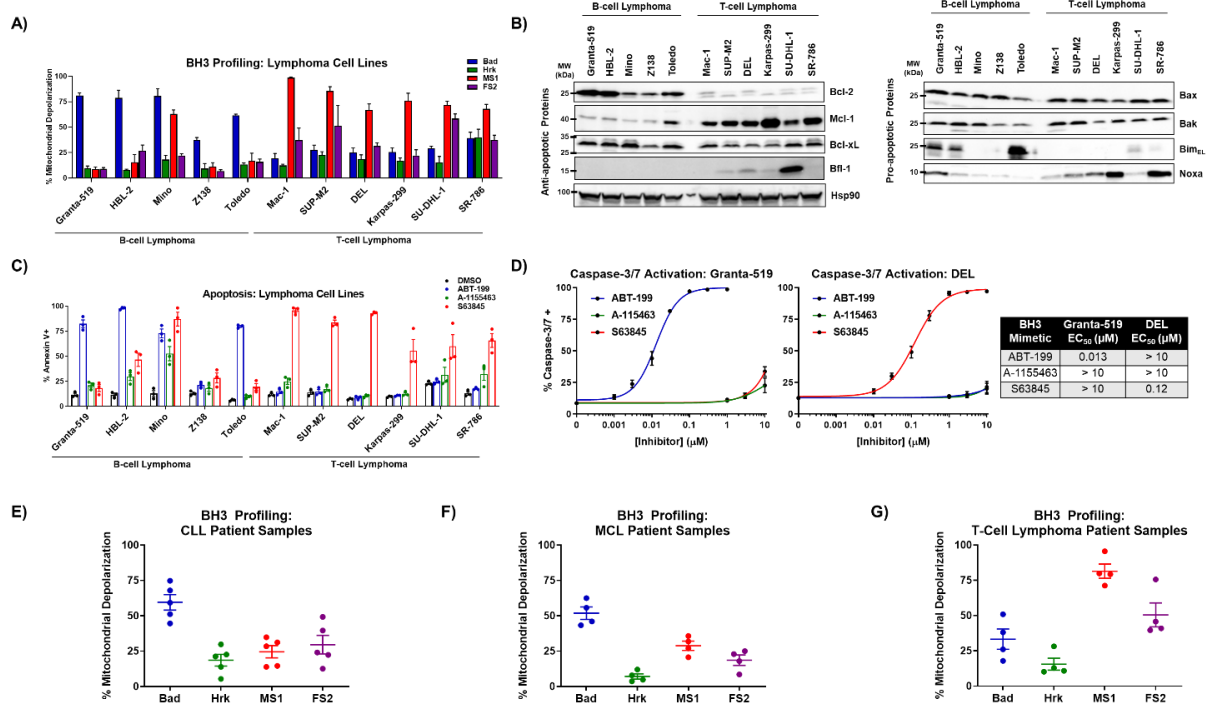


Figure 2.5 Survival dependence trends in B-cell and T-cell lymphoma subtypes

A) BH3 profiling of lymphoma cell line panel (10 μM Bad, Hrk, MS1; 3 μM FS2). **B)** Western blot of baseline Bcl-2 family proteins in lymphoma cell lines. **C)** Apoptosis induced by 1 μM, 24-hour BH3 mimetic treatments. **D)** Caspase-3/7 activation dose response curves of individual BH3 mimetic treatments of the Granta-519 (B-cell) and DEL (T-cell) cell lines. Table indicates average EC₅₀ values. **E)** BH3 profiling performed on primary samples from Chronic Lymphocytic Leukemia (CLL), **F)** Mantle Cell Lymphoma (MCL) and **G)** T-Cell Lymphoma patients. Patient sample BH3 profiling was performed as n=1 for each patient sample in technical triplicates, due to limited cell availability, all other data is from three independent experiments.

Furthermore, we analyzed mRNA expression data from clinical lymphoma specimens available through the Oncomine database,⁴⁰ showing elevated Bcl-2 levels in MCL and DLBCL samples and high Mcl-1 in the T-cell patient samples, which provided additional support to our conclusions (Figure 2.6). Interestingly, Bfl-1 levels were also highly expressed in many of these lymphoma sample. Taken together, this data delineates specific B-cell and T-cell lymphoma subtypes as being predominantly Bcl-2 and Mcl-1 dependent, respectively, which provides further support of the literature

that suggests these trends when lymphoma sub-types have been individually studied, while the role of Bfl-1 requires further investigation.^{25,41,42}

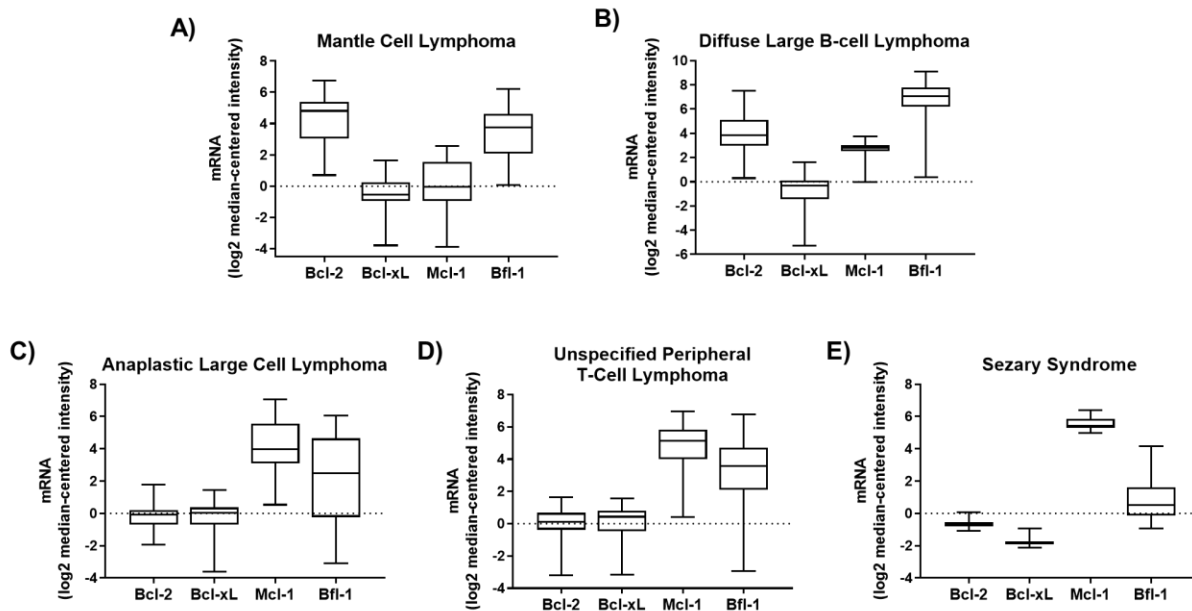


Figure 2.6 mRNA expression of Bcl-2 family anti-apoptotic proteins in lymphomas

Clinical specimen data from B-cell Lymphoma Patients diagnosed with **A)** Mantle Cell Lymphoma (n=95) and **B)** Diffuse Large B-cell Lymphoma (n=91). Data from T-cell Lymphoma patients with **C)** Anaplastic Large Cell Lymphoma (n=52), **D)** Unspecified Peripheral T-cell Lymphoma (n=78), and **E)** Sezary Syndrome (cutaneous lymphoma) (n=32). All data obtained via the OncoPrint database (www.oncoPrint.org).

2.5 Targeting the Bcl-2 proteins in ovarian cancer

Solid tumors are typically less sensitive to apoptosis and present greater therapeutic challenges.⁴³ Due to clinical need for effective therapies and lack of studies of Bcl-2 proteins in ovarian cancer, we further studied the applications of BH3 profiling in this indication with the benefit of having access to patient derived xenograft (PDX) models. Previous reports have performed BH3 profiling in ovarian cancer to measure overall apoptotic priming with promiscuous BH3-only peptides as a means to predict clinical prognosis and chemosensitivity.^{44,45} In this study, we utilize BH3 profiling to dig

deeper into individual anti-apoptotic protein dependencies by using selective peptides on a panel of established and PDX ovarian cancer cell lines (OV81.2⁴⁶ and OV231). The functional data from all cell lines and OV81.2 revealed low levels of depolarization induced by the peptides, which indicates that inhibition of a single anti-apoptotic protein is insufficient to induce apoptosis and may necessitate inhibiting multiple cellular pathways (Figure 2.7A). The results for OV231 were of particular interest, showing high levels of response to MS1, indicating Mcl-1 dependence. In support of the profiling data, OV231 was the only cell line to respond to single agent BH3 mimetic treatment, by displaying robust apoptosis response to S63845, consistent with its determined Mcl-1 dependence (Figure 2.7B). Interestingly, the rest of the cell lines whose BH3 profiles indicated low apoptotic priming and no predominant pro-apoptotic player responded exquisitely to the Mcl-1 and Bcl-xL inhibitor combination (Figure 2.7B). To provide further evidence of dual Mcl-1/Bcl-xL or single agent Mcl-1 inhibitor sensitivity of the at the PDX cell lines, we used dose dependent caspase activation experiments (Figure 2.7C). In OV81.2 a constant ratio of A-1155463 and S63845 produced a caspase activation EC_{50} of 200 nM, while the single agent EC_{50} values were $>10 \mu\text{M}$. Not surprisingly, the basal protein levels had little correlation to the functional data, but OV231 contained slightly lower levels of Bcl-xL compared to the rest of the panel, which has been identified previously as a correlative predictor of Mcl-1 dependence (Figure 2.7D).⁴⁷

We also evaluated a cisplatin resistant subline of OV231 (OV231-CP30) and revealed modulation of Bcl-2 proteins leading to suppressed apoptotic priming (Figures 2.7E-H). We identified that OV231-CP30 contained elevated protein levels of Mcl-1, as

well as a loss of the Bim protein, which has been reported previously as a mechanism of cisplatin resistance (Figure 2.7E).⁴⁸ BH3 profiling of OV231-CP30 showed a decrease in apoptotic priming and loss of Mcl-1 dependence that was seen in the parental line (Figure 2.7F). This was accompanied by a lack of sensitivity to single agent S63845 and A-1155463/S63845 combination noted by apoptosis and caspase activation (Figures 2.7G-H). To further confirm our data, we used a genetic approach to target Bcl-xL and Mcl-1 by using siRNA knockdown studies in the PDX cell lines; knockdown efficiency by siRNA pools was confirmed by western blot (Figure 2.11). The results corroborated our preceding data, confirming that OV81.2 is only sensitive to dual Bcl-xL/Mcl-1 knockdown, while Mcl-1 knockdown alone was sufficient to induce significant apoptosis in OV231 (Figure 2.7I). Importantly, the cisplatin resistant OV231-CP30 shows lack of sensitivity to both Mcl-1 and Bcl-xL/Mcl-1 knockdowns, confirming the results from the functional BH3 profiling and cell viability experiments using this PDX cell line (Figure 2.7I).

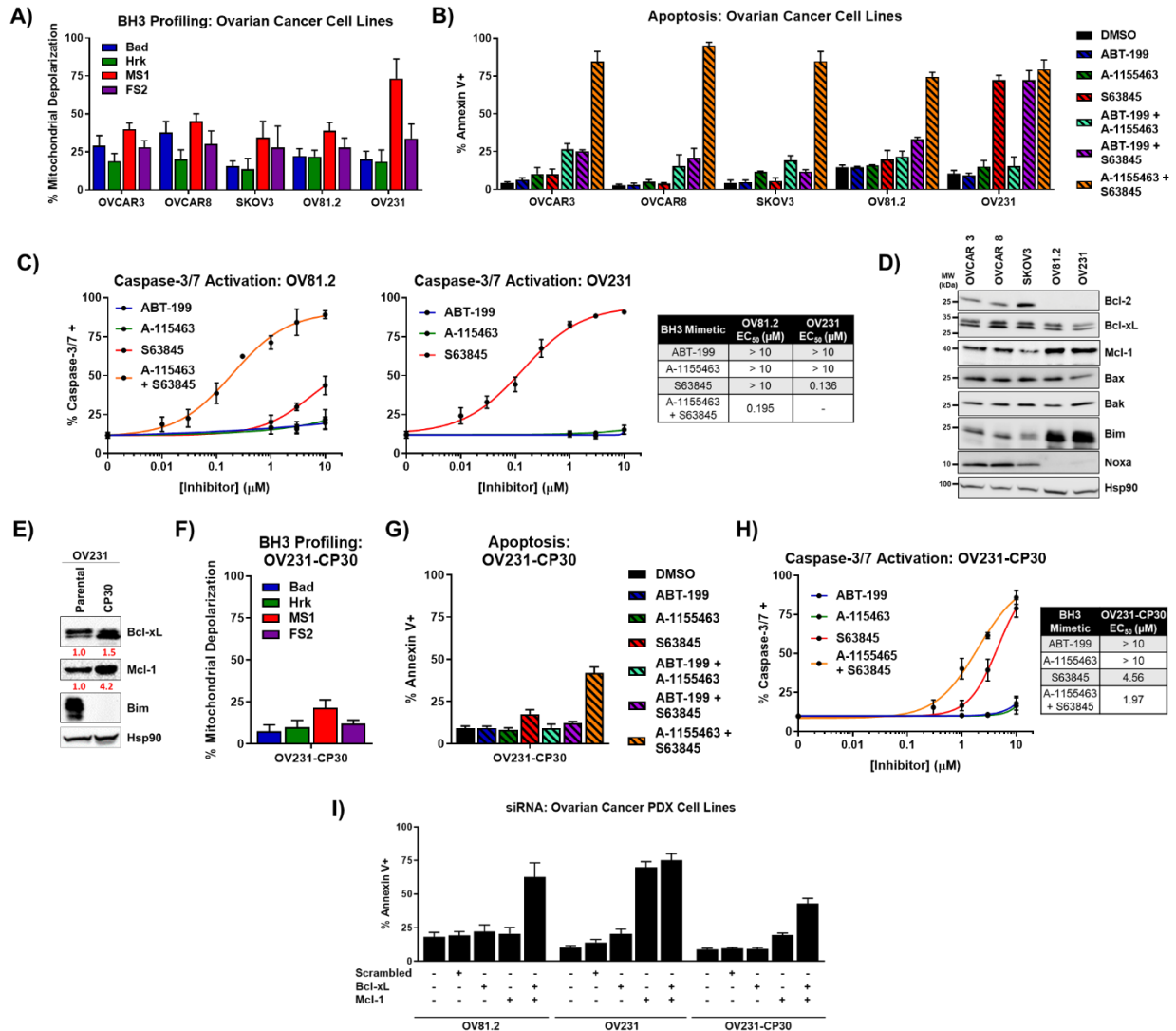


Figure 2.7 Targeting pro-survival proteins in ovarian cancer

A) BH3 profiling (10 μM Bad, Hrk, MS1; 3 μM FS2) of established ovarian cancer cell lines (OVCAR 3, OVCAR 8, and SKOV3) and PDX lines (OV81.2 and OV231). **B)** Apoptosis induced by 1 μM of BH3 mimetics (single agent or in combination) following 24 hours of treatment. **C)** Caspase-3/7 activation induced by 16-hour BH3 mimetic treatments in the PDX cell lines, with EC₅₀ values summarized in the table. **D)** Western blot of baseline Bcl-2 family proteins. **E)** Basal protein western blot of OV231 compared to its cisplatin resistant subline (OV231-CP30), with quantification. **F)** BH3 profiling, **G)** BH3 mimetic apoptosis, and **H)** Caspase-3/7 activation in OV231-CP30. **I)** Apoptosis induced by 48-hour siRNA (25 nM) treatments targeting Bcl-xL and Mcl-1 in PDX lines. All results presented as mean and SEM of three independent experiments.

To have a better understanding for Bcl-2 anti-apoptotic proteins overexpression in ovarian cancer, we analyzed the mRNA data available from 193 clinical samples available through the OncoPrint database. The data showed that Mcl-1 was the highest

expressed anti-apoptotic protein, followed by Bcl-xL (Figure 2.8A). In addition, using a separate dataset from the The Cancer Genome Atlas (TCGA) database, Mcl-1 and Bcl-xL gene copy numbers were shown to be significantly higher in ovarian carcinoma cells compared with non-malignant ovary cells from patients, supporting their prominent role in solid tumors such as ovarian cancer (Figure 2.8B-C).⁴⁹ These novel findings in ovarian cancer provide strong rationale for exploring dual Mcl-1/Bcl-xL inhibition as a therapeutic strategy, as well as utilizing BH3 profiling to identify patients whose tumors are Mcl-1 dependent and may be candidates for Mcl-1 inhibitor treatment.

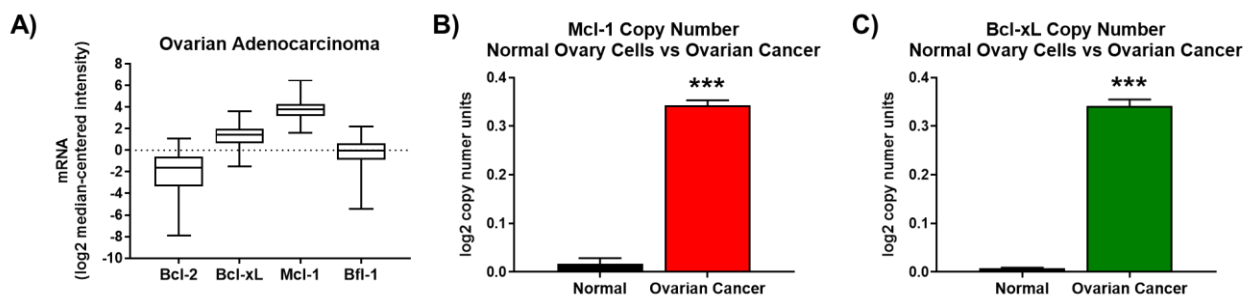


Figure 2.8 Gene expression of Bcl-2 proteins in ovarian cancer patients

A) Clinical specimen data from ovarian cancer patients (n=193), data obtained via the Oncomine database (www.oncomine.org). **B)** Comparison of Mcl-1 and **C)** Bcl-xL gene copy number counts in normal ovary (n=130) and ovarian carcinoma (n=607) patient samples, from the TCGA database. ***p-value < 0.0005.

2.6 Characterizing survival dependence in diverse solid tumors

To investigate if the identified anti-apoptotic dependence and efficacy of Bcl-xL/Mcl-1 inhibition apply across various types of solid tumors, we selected a panel of commonly used cell lines that represent diverse tissues of origin and genetic backgrounds, including non-small cell lung cancer (NSCLC), pancreatic, colorectal, thyroid, and breast cancers. Several of these cancers have been previously evaluated

in depth for their dependence on Bcl-2 family members, including NSCLC,⁵⁰ breast,⁵¹ and thyroid cancer,²⁴ and the studies concluded that Bcl-xL, together with Mcl-1 were the main players in promoting cell survival. Functional BH3 profiling revealed that most cell lines displayed low levels depolarization in response to all peptides, with no apparent predominant anti-apoptotic protein promoting survival (Figure 2.9A). We identified four solid tumor cell lines with BH3 profiles that indicated single anti-apoptotic protein dependence (Figure 2.9A). MS1 induced >50% depolarization in the H23, MiaPaCa-2, and MCF-7 cell lines, indicating strong Mcl-1 dependence, while the MDA-MB-231 breast cancer cell line revealed predominant Bcl-xL dependence (Figure 2.9A). To study the predictive capability of BH3 profiling, these cell lines were treated with BH3 mimetics as single agents and in their combinations and analyzed apoptosis induction (Figure 2.9B). The cell lines that showed no predominant survival dependence were all insensitive to single agent BH3 mimetic treatments but were exquisitely sensitive to the combination of A-1155463 and S63845 (Figure 2.9B). An important finding was that BH3 profiling effectively identified solid tumor cell lines that would respond to single agent BH3 mimetic treatment, with S63845 inducing 75%, 60%, and 50% apoptosis in the, H23, MiaPaCa-2, and MCF-7 (Figure 2.9B). Interestingly, the addition of A-1155463, with S63845 produced an increased apoptotic response in MiaPaCa-2 and MCF-7, but not H23, indicating that H23 survival dependence is solely from Mcl-1, while Bcl-xL still plays a functional role in MiaPaCa-2 and MCF-7. Meanwhile, the addition of ABT-199 in combination with S63845 or A-1155463 did not lead to increased apoptosis. A-1155463 was capable of inducing ~75% apoptosis as a single agent in the MDA-MB-231 cell line, with the addition of neither ABT-199 or S63845 increasing the response,

confirming predominant Bcl-xL dependence. The baseline Bcl-2 protein levels revealed variable expression of both pro- and anti-apoptotic family members and only the M14 melanoma cell line expressed detectable Bfl-1 (Figure 2.9C). Interestingly, the three Mcl-1 dependent cell lines (H23, MiaPaCa-2, and MCF-7) also expressed the lowest levels of Bcl-xL protein, with variable levels of Mcl-1, further supporting the reported trend of low Bcl-xL correlating with Mcl-1 dependence.⁴⁷ Corresponding to the high levels of Bfl-1 protein, M14 showed the highest FS2 induced depolarization, which supports previous studies that highlight increased expression of Bfl-1 in melanoma.^{30,52} This analysis of solid tumor cell lines demonstrated a strategy for identifying cancers with single agent BH3 mimetic sensitivity and revealed broad apoptosis response to dual Bcl-xL/Mcl-1 inhibition.

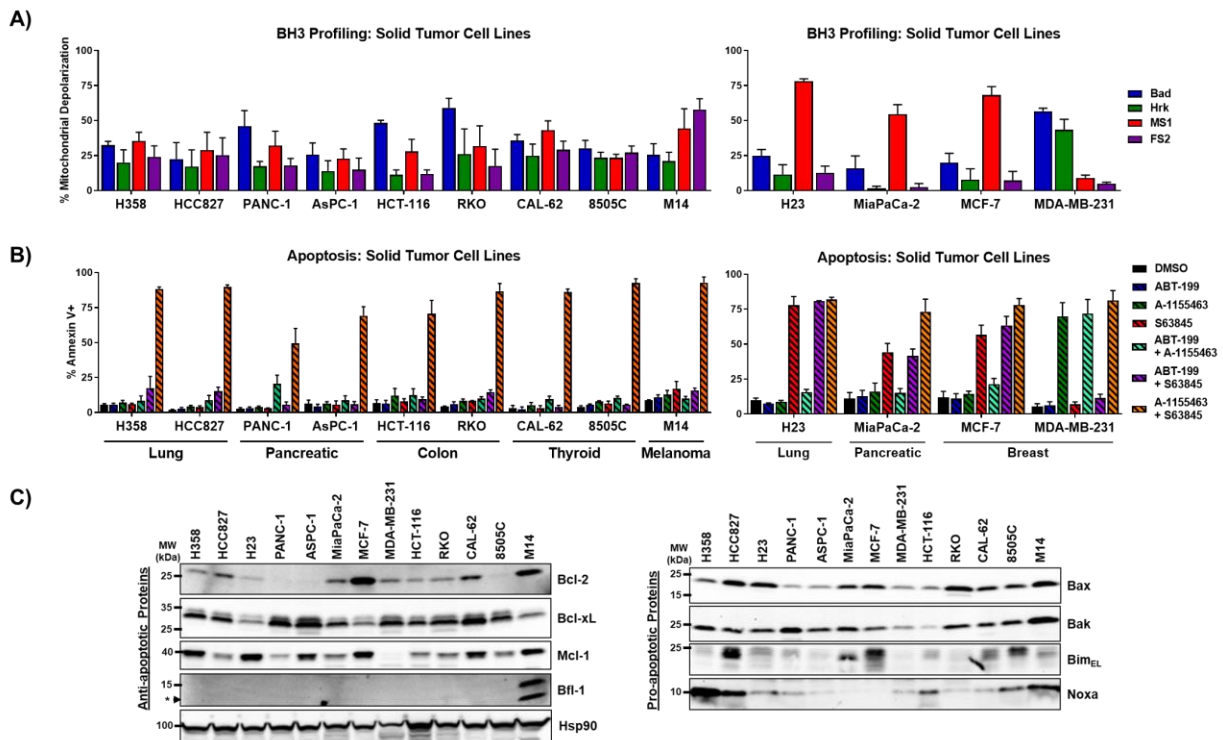


Figure 2.9 Targeting Bcl-2 anti-apoptotic proteins in solid tumor cell lines

A) BH3 profiling of solid tumor cell lines (10 μ M Bad, Hrk, MS1; 3 μ M FS2). **B)** Apoptosis induced by 1 μ M of individual or combinations of BH3 mimetics following 24 hours of treatment. Results presented as mean and SEM of three independent experiments. **C)** Western blot of baseline Bcl-2 family proteins in various solid tumor derived cell lines.

2.7 Dynamic BH3 profiling in solid tumors to target resistance

As previously stated, solid tumors in general present a greater therapeutic challenge, therefore we employed dynamic BH3 profiling to identify efficacious combination regimens with BH3 mimetics. BRAF and MEK inhibitors are the standard frontline therapies for melanoma patients, but resistance is inevitable and additional strategies are typically required to prolong survival.⁵³ We investigated the effect of both the FDA approved BRAF and MEK inhibitors, vemurafenib and cobimetinib, respectively, in modulating the pro-survival dependence of melanoma cells. Melanoma cells pre-treated with vemurafenib or cobimetinib displayed a selective increase in Mcl-1 dependence, as indicated by dynamic BH3 profiling that shows heightened sensitivity to the MS1 peptide, but not the others (Figure 2.10A). This selective increase in Mcl-1 dependence can be partially explained by the changes in baseline protein levels, which shows that vemurafenib and cobimetinib pre-treated cells have slightly Mcl-1 protein levels, accompanied by an increase in Bim and depletion Noxa, which would likely lead to higher levels of Mcl-1:Bim complexes, priming cells for Mcl-1 dependence (Figure 2.10B). This identified priming shows potential for therapeutic advantage as illustrated by vemurafenib pre-treated cells being selectively more sensitive to Mcl-1 inhibitor treatment (Figure 2.10C). Coupling the increased Mcl-1 dependence induced by MAPK inhibitors with an Mcl-1 BH3 mimetic may provide enhanced therapeutic efficacy. In colorectal cancer, insufficient degradation of Mcl-1 by an inactivating mutation in the

ubiquitin ligase, FBW7, was identified as a resistance factor to regorafenib and was modeled using an Mcl-1 knock-in HCT-116 cell line (HCT-116 MCL1-Ki).^{54,55} Using dynamic BH3 profiling,⁵⁶ we further functionally characterize this model system by demonstrating the ability of regorafenib to deplete Mcl-1 dependence in HCT-116 WT cells, with accompanied Mcl-1 protein degradation, while having no effect on Mcl-1 protein or functional dependence in HCT-116 MCL1-Ki cells (Figures 2.10D-E). These findings suggest that in colorectal cancer cells with FBW7 mutations, regorafenib is unable to functionally deplete Mcl-1 that would normally promote its efficacy, therefore the combination of regorafenib with pharmacological inhibition of Mcl-1 may provide restore sensitivity. These dynamic BH3 profiling exercises further enhance our functional study of solid tumor derived cell lines by providing additional avenues of therapeutic intervention using BH3 mimetics.

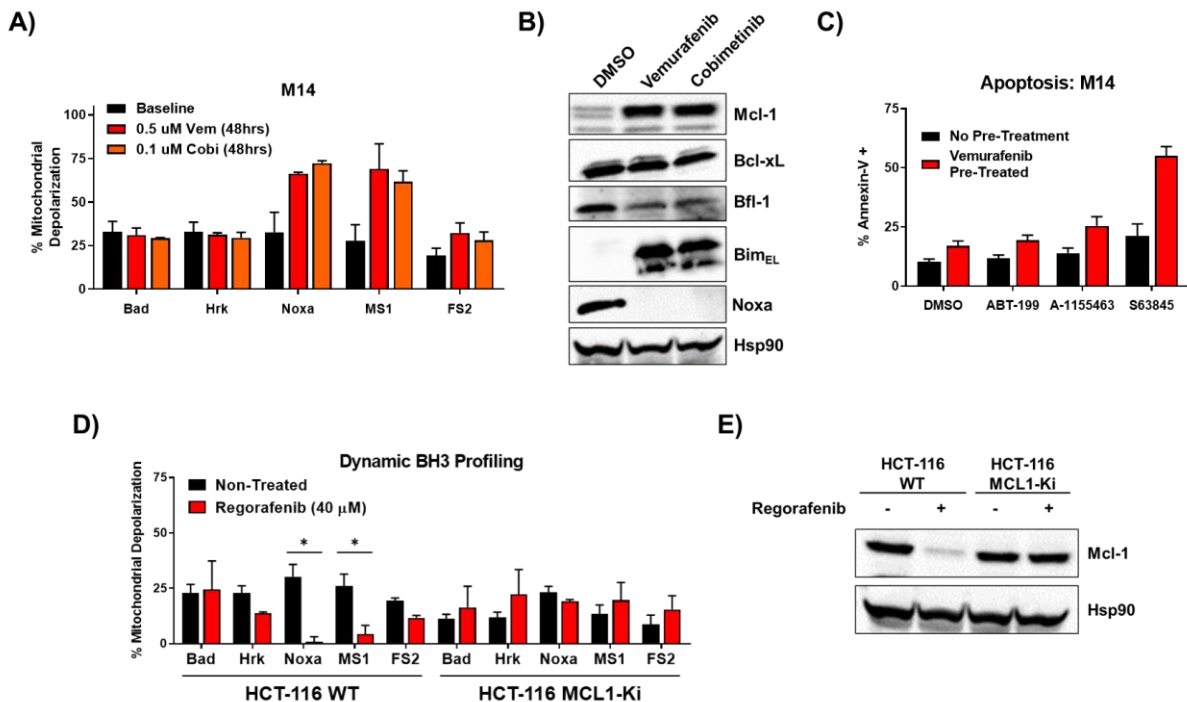


Figure 2.10 Dynamic BH3 profiling in melanoma and colon cancer

A) M14 cell line pre-treated for 48 hr with 0.5 μM vemurafenib (vem) or 0.1 μM of cobimetinib (cobi) and analyzed by dynamic BH3 profiling, **B)** western blotting of Bcl-2 family proteins, and **C)** apoptosis induced by BH3 mimetics (24 hr, 1 μM treatment post vem or cobi pre-treatment, $n=3$). **D)** HCT-116 parental and MCL1-Ki cell lines pre-treated with 20 μM regorafenib for 4 hours and analyzed by dynamic BH3 profiling **E)** western blot. Results presented as mean and SEM of three independent experiments.

2.8 Conclusions

This work outlines a strategy for identifying Bcl-2 family pro-survival dependence across diverse cancer types, covering a wide array of genetic backgrounds, and revealed important trends in functional anti-apoptotic protein preference, allowing for the selection of rationalized BH3 mimetics. The BH3 profiling assay is at the heart of this study and using the model E μ -Myc lymphoma cell lines allowed us to identify optimal concentrations of the BH3-only peptides to probe different cancers. We take advantage of an optimized quiver of BH3 mimetics that inhibit the Bcl-2, Bcl-xL, and Mcl-1 proteins to demonstrate the ability of targeting anti-apoptotic proteins in a wide spectrum of cancers. While a potent and selective small molecule Bfl-1 inhibitor remains elusive, our group has contributed to the progress with hopes one will be available in the future.^{13,14}

We employed BH3 profiling in various hematologic cancer cell lines and patient samples, identifying the predominant involvement of Bcl-2 and Mcl-1. Most AML cell lines tested displayed dependence on both Bcl-2 and Mcl-1, with substantial sensitivity to corresponding inhibitors. Interesting to note is that both Bad and MS1 as single agents induced high levels of depolarization, indicating that both Bcl-2 and Mcl-1 play major roles and inhibition of either protein is sufficient to initiate apoptosis. Across the AML cell lines and patient samples, we provided examples of what the profile of dual Bcl-2/Mcl-1 dependence looks like compared to single dependent cell lines. A key finding in this study was the contrast in survival dependence between B-cell and T-cell

lymphomas. On the protein and functional levels, we found that our panel of B-cell lymphoma cell lines were predominantly Bcl-2 dependent, while lymphomas from T-cell origin had preference for Mcl-1, which correlated with sensitivity to ABT-199 or S63845. This finding was further enhanced by BH3 profiling of patient samples, showing a clear trend of Mantle Cell Lymphoma being mainly Bcl-2 dependent and T-cell Lymphomas relying strongly on Mcl-1. The obtained data is supported by previous literature that demonstrates Bcl-2 overexpression in various B-cell lymphomas and driver mutation enhanced Mcl-1 overexpression in large cohorts of T-cell lymphoma patient samples.^{25,57–59} The Bfl-1 upregulation that we identified in T-cell lymphomas can be explained by NPM-ALK rearrangements in our ALCL cell line panel, which drives Bfl-1 expression, thus presenting a promising precision approach for Bfl-1 or dual Mcl-1/Bfl-1 inhibitors.³⁹

We assembled a diverse panel of solid tumor derived cell lines in order to determine the prominent pro-survival culprits, including the first known functional dissection of individual Bcl-2 anti-apoptotic proteins in ovarian cancer. We discovered that OV231, an ovarian cancer PDX cell line, was highly Mcl-1 dependent and sensitive to S63845 treatment. This novel finding in ovarian cancer presents important clinical implications and could improve the treatment of patients suffering from this disease. From the diverse solid tumor cell panel, we identified NSCLC, pancreatic, and breast cancer cell lines that were sensitive to single agent Bcl-xL or Mcl-1 inhibitor treatments, which was predicted by BH3 profiling. For the rest of the solid tumor cell lines there was no individual anti-apoptotic protein that played a predominant role and single agent BH3 mimetic treatments were insufficient to induce apoptosis. However, significant apoptosis

was induced by a combination of Bcl-xL and Mcl-1 inhibitors across all cancer types tested, which would require more in-depth analysis of potential toxicities to determine clinical relevance. Of the solid tumor cell lines tested, only the M14 melanoma line possesses detectable Bfl-1 with corresponding response to the FS2 peptide, this warrants further studies evaluating the potential of inhibiting Bfl-1 in melanoma as a potential therapeutic route. The applications of dynamic BH3 profiling we demonstrated provides translationally relevant rationale for combination strategies to treat aggressive solid tumors such as melanoma and colorectal cancer.

In conclusion, we successfully screened a wide spectrum of cancers for functional involvement of the Bcl-2 family anti-apoptotic proteins and identified important trends with potential clinical relevance. The results presented in both established cell lines and patient samples highlight the importance of BH3 profiling as a diagnostic method to be used in precision medicine decision making. This translational work promotes the value in harnessing chemical biology to discover new trends in cancer to potentially improve clinical outcomes.

2.9 Materials and methods

Peptide and small molecule inhibitors

BH3-only peptides (Table 2.1) were custom synthesized by GenicBio Limited (Shanghai, China). ABT-199, A-1155463, and S63845 were purchased from ChemieTek (Indianapolis, IN). Peptides and small molecules were dissolved in DMSO at 10 mM and stored at -20°C.

Table 2.1 BH3-only peptide sequences

Peptide	Sequence
hBim (141-166)	DMRPEIWIAQELRRIGDEFNAYYARR
hPuma (132-154)	QWAREIGAQLRRMADDLNAQYER
hBad (102-128)	PNLWAAQRYGRELRRMSDEFVDSFKKG
hHrk (27-47)	SSAAQLTAARLKALGDELHQR
hNoxa (18-43)	PAELEVECATQLRRFGDKLNFRQKLL
MS1 (engineered)	RPEIWMTQGLRRLGDEINAYYAR
FS2 (engineered)	QWVREIAAGLRRRAADDVNAQVER

In vitro binding assays

The details for the fluorescence polarization assays, including recombinant proteins, assay development, and protocols were previously described.¹³ Bio-layer interferometry experiments were also performed as reported in our previous publication.¹³ In short, the FS2 peptide was diluted from 100 to 1.56 nM and tested against individual sensors with immobilized biotinylated-Bfl-1 protein. K_d values were calculated from kinetic K_{on}/K_{off} parameters, along with steady state response plotting. Isothermal titration calorimetry was measured with NanoITC (TA instruments) and analyzed with NanoAnalyze software to calculate K_d values. FS2 peptide (300 μ M) was titrated into 50 μ M protein at 25°C in buffer (25 mM HEPES pH 7.5, 300 mM NaCl, 0.5 TCEP & 5% glycerol).

Cell culture and patient samples

The Eμ-Myc lymphoma cell lines were gifted from Ricky Johnstone at the University of Melbourne; cells were cultured and viability experiments were performed as previously reported.^{13,35} The ovarian PDX cell lines (OV81.2 and OV231) were established by the laboratory of Analisa DiFeo.⁴⁶ Cell lines that were cultured for a cumulative time of >6 months were re-authenticated by short tandem repeat analysis and genetic identity was confirmed. Mycoplasma testing was performed by PCR and confirmed negative.

All patient information from primary samples was de-identified and used under proper IRB protocols from the University of Michigan (Table 2.2). Cryopreserved AML and CLL patient samples with high blast counts (>90%), were acquired from internal biorepositories. MCL samples were cryopreserved from patients with circulating disease, while T-Cell Lymphoma samples were tested fresh. All samples were immediately analyzed by BH3 profiling without *ex vivo* culturing.

Table 2.2 Primary patient sample information

Sample	Disease	Cytogenetics/Mutations	Prior Tx
AML1	Acute Myeloid Leukemia	FLT3 ITD, IDH1, NPM1	Untreated
AML2	Acute Myeloid Leukemia	CEBPA, JAK2, TET2	Untreated
AML3	Acute Myeloid Leukemia	FLT3 ITD, NPM1	Untreated
CLL1	Chronic Lymphocytic Leukemia	Normal FISH	Fludarabine
CLL2	Chronic Lymphocytic Leukemia	11q23	Rituximab
CLL3	Chronic Lymphocytic Leukemia	13q14	Untreated
CLL4	Chronic Lymphocytic Leukemia	13q14	ND
CLL5	Chronic Lymphocytic Leukemia	13q14	Untreated
MCL1	Mantle Cell Lymphoma (B-cell)	Normal karyotype	Untreated
MCL2	Mantle Cell Lymphoma (B-cell)	t(11;14;?15)(q13;q32;q25)	Untreated
MCL3	Mantle Cell Lymphoma (B-cell)	Normal karyotype	Untreated
MCL4	Mantle Cell Lymphoma (B-cell)	Complex karyotype	Untreated
TCL1	Sezary Syndrome (T-cell Lymphoma)	ND	Untreated
TCL2	Sezary Syndrome (T-cell Lymphoma)	ND	Untreated
TCL3	Sezary Syndrome (T-cell Lymphoma)	ND	Untreated
TCL4	Sezary Syndrome (T-cell Lymphoma)	ND	Untreated

BH3 profiling

BH3 profiling was performed using the plate-based kinetic fluorometric procedure.²⁰ 2×10^6 cells were plated the day before running the assay in 10 cm dishes, providing the highest reproducibility. Working buffer was composed of MEB (150 mM mannitol, 10 mM HEPES-KOH pH 7.5, 50 mM KCl, 0.02 mM EGTA, 0.02 mM EDTA, 0.1% BSA, and 5 mM succinate) with the fresh addition of the following: 20 μ M oligomycin, 0.005% (w/v) digitonin, 10 mM β -mercaptoethanol, and 2 μ M JC-1. Peptides and controls were serially diluted in fresh working buffer and 15 μ L/well was added to black, flat bottom 384-well plates (Corning 3573). Cells were harvested, washed once, re-suspended in MEB, then 15 μ L of cell solution was added to each well such that the final cell count was 20×10^3 cells/well in technical triplicates. Plates were immediately analyzed on a BioTek Synergy H1 plate reader at an excitation of 545 nm and emission of 590 nm every 5 minutes for 3 hours at 30°C. The resulting relative fluorescent units were plotted versus time and area under the curve (AUC) values were generated using GraphPad Prism 8.3.0 software. DMSO (1%) and FCCP (10 μ M) controls were used to set 0% and 100% depolarization parameters, respectively. The following equation was used to generate normalized values for treatment samples:

$$\% \text{ mitochondrial depolarization} = 100 - \left[100 \times \left(\frac{\text{Sample AUC} - \text{FCCP AUC}}{\text{DMSO AUC} - \text{FCCP AUC}} \right) \right].$$

Immunoblotting

Confluent plates were harvested and lysed with RIPA buffer containing protease inhibitors. Clarified lysates were quantified using a Bradford assay; loading samples

were normalized and prepared using 4X SDS dye. 40 µg protein was loaded into 4-20% SDS-PAGE gels for electrophoresis. After transfer and blocking, membranes were incubated in primary antibodies (Table 2.3) overnight. Blots were imaged using a Thermo Fisher iBright FL1000 imager.

Table 2.3 Antibodies used for western blotting

Protein	Clone and Species	MW (kDa)	Dilution	Company	Catalog #
Bcl-2	(124) Mouse mAb	26	1:500	Cell Signaling Technologies	15071
Bcl-xL	(54H6) Rabbit mAb	30	1:1,000	Cell Signaling Technologies	2764
Mcl-1	(RC13) Mouse mAb	40	1:500	Invitrogen	AHO0102
Bfl-1	(D1A1C) Rabbit mAb	18	1:500	Cell Signaling Technologies	14093
Bax	(D2E11) Rabbit mAb	20	1:500	Cell Signaling Technologies	5023
Bak	(D4E4) Rabbit mAb	25	1:500	Cell Signaling Technologies	12105
Bim	(C34C5) Rabbit mAb	12, 15, 23	1:500	Cell Signaling Technologies	2933
Noxa	(D8L7U) Rabbit mAb	10	1:250	Cell Signaling Technologies	14766
Hsp90	(H90-10) Mouse mAb	90	1:10,000	Invitrogen	MA1-10892

MTT cell viability assay

Cells (20,000/well) were treated with BH3 mimetics for 72 hours in 96-well plates in duplicate. After treatment, the MTT reagent, 3-(4,5-dimethylthiazol-2-yl)-2,5-diphenyl tetrazolium bromide, was added and incubated at 37°C for 4 hours before adding SDS/HCl solution. Plates were incubated overnight and read on a BioTek Synergy H1 plate reader at 570 nM absorbance. Treated wells were normalized by subtracting media-only control wells and DMSO treated cells as the 100% cell viability parameter. Growth curves were plotted using GraphPad Prism 8.3.0 software and IC₅₀ values were calculated using non-linear regression fitting.

Apoptosis experiments

Suspension cells (200×10^3 /well) were plated into 24-well plates and adherent cells (100×10^3 /well) were seeded in 12-well plates and left to adhere overnight. Cells were treated with BH3 mimetics for 24 hours and stained with Annexin-V/FITC and propidium iodide or CellEvent Caspase-3/7 Green Detection Reagent (Invitrogen, Carlsbad, CA). Cells were run on an Accuri C6 flow cytometer and analyzed using WinList 3.0 software. Percentage of Annexin-V or Caspase-3/7 positive populations were used to report apoptosis induction.

siRNA knockdowns

Cells (50×10^3 /well) were seeded in 12-well plates and left to adhere overnight. ON-TARGETplus siRNA SMARTpools (Dharmacon, Lafayette, CO) were prepared as recommended by manufacturer at a concentration of 25 nM and delivered using Lipofectamine RNAiMAX transfection reagent (Invitrogen). Combination treatments contained 25 nM of each siRNA and scrambled controls were 50 nM. Cells incubated with siRNA for 48 hours before analyzing apoptosis induction. Knockdown efficiency of siRNA pools was evaluated by western blot (Figure 2.11).

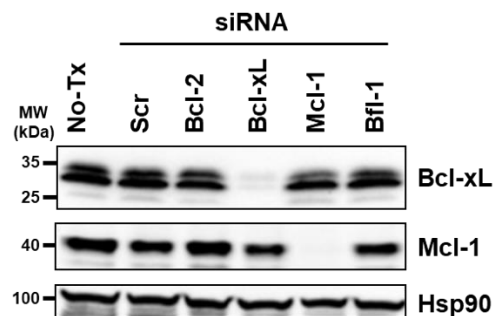


Figure 2.11 siRNA knockdown confirmation in ovarian cancer PDX lines

Western blot of siRNA treatments of OV81.2 PDX cell line with all anti-apoptotic protein siRNA pools. Only Bcl-xL and Mcl-1 protein was detectable, Bcl-2 and Bfl-1 could not be detected.

2.10 Contributions

Karson Kump performed all FP and BLI binding experiments, BH3 profiling, western blotting, apoptosis assays, siRNA knockdowns, and experiments with primary patient samples. Dr. Ejaz Ahmad performed ITC experiments and helped characterize the cell lines. Dr. Charles Foucar performed MTT viability assays and helped with the AML patient sample data collection and analysis. Patient samples and data analysis were provided with the help of Drs Malathi Kandapra, Sami Malek, Tycel Phillips, Ryan Wilcox, Dale Bixby, and Moshe Talpaz. Ovarian cancer PDX models and cell lines were provided by Dr. Analisa DiFeo. Rita Avelar helped with ovarian cancer western blotting and data analysis. Matthew Lieberman assisted in culturing cell lines and performing drug treatments for the apoptosis assays. Dr. Ahmed Mady provided initial assistance in establishing the BH3 profiling assay protocols in our lab and trouble shooting.

2.11 References

1. Garraway LA, Verweij J, Ballman K V. Precision oncology: An overview. *J Clin Oncol.* 2013;31(15):1803-1805. doi:10.1200/JCO.2013.49.4799
2. Letai A. Functional precision cancer medicine-moving beyond pure genomics. *Nat Med.* 2017;23(9):1028-1035. doi:10.1038/nm.4389
3. Friedman AA, Letai A, Fisher DE, Flaherty KT. Precision medicine for cancer with next-generation functional diagnostics. *Nat Rev Cancer.* 2015;15(12):747-756. doi:10.1038/nrc4015
4. Hanahan D, Weinberg RA. Hallmarks of cancer: the next generation. *Cell.* 2011;144(5):646-674. doi:10.1016/j.cell.2011.02.013

5. Adams JM, Cory S. The Bcl-2 apoptotic switch in cancer development and therapy. *Oncogene*. 2007;26(9):1324-1337. doi:10.1038/sj.onc.1210220
6. Yip KW, Reed JC. Bcl-2 family proteins and cancer. *Oncogene*. 2008;27(50):6398-6406. doi:10.1038/onc.2008.307
7. Souers AJ, Levenson JD, Boghaert ER, et al. ABT-199, a potent and selective BCL-2 inhibitor, achieves antitumor activity while sparing platelets. *Nat Med*. 2013;19(2):202-208. doi:10.1038/nm.3048
8. Roberts AW, Davids MS, Pagel JM, et al. Targeting BCL2 with Venetoclax in Relapsed Chronic Lymphocytic Leukemia. *N Engl J Med*. 2016;374(4):311-322. doi:10.1056/NEJMoa1513257
9. Kotschy A, Szlavik Z, Murray J, et al. The MCL1 inhibitor S63845 is tolerable and effective in diverse cancer models. *Nature*. 2016;538(7626):477-482. doi:10.1038/nature19830
10. Caenepeel S, Brown SP, Belmontes B, et al. AMG 176, a Selective MCL1 Inhibitor, is Effective in Hematological Cancer Models Alone and in Combination with Established Therapies. *Cancer Discov*. 2018;8(12):CD-18-0387. doi:10.1158/2159-8290.CD-18-0387
11. Tron AE, Belmonte MA, Adam A, et al. Discovery of Mcl-1-specific inhibitor AZD5991 and preclinical activity in multiple myeloma and acute myeloid leukemia. *Nat Commun*. 2018;9(1):5341. doi:10.1038/s41467-018-07551-w
12. Tao Z-F, Hasvold L, Wang L, et al. Discovery of a Potent and Selective BCL-X_L Inhibitor with *in Vivo* Activity. *ACS Med Chem Lett*. 2014;5(10):1088-1093. doi:10.1021/ml5001867
13. Kump KJ, Miao L, Mady ASA, et al. Discovery and Characterization of 2,5-Substituted Benzoic Acid Dual Inhibitors of the Anti-Apoptotic Mcl-1 and Bfl-1 Proteins. *J Med Chem*. January 2020. doi:10.1021/acs.jmedchem.9b01442
14. Mady ASA, Liao C, Bajwa N, et al. Discovery of Mcl-1 inhibitors from integrated high throughput and virtual screening. *Sci Rep*. 2018;8(1):10210. doi:10.1038/s41598-018-27899-9
15. Dutta S, Chen TS, Keating AE. Peptide Ligands for Pro-survival Protein Bfl-1 from Computationally Guided Library Screening. *ACS Chem Biol*. 2013;8(4):778-788. doi:10.1021/cb300679a
16. Huhn AJ, Guerra RM, Harvey EP, Bird GH, Walensky LD. Selective Covalent Targeting of Anti-Apoptotic BFL-1 by Cysteine-Reactive Stapled Peptide Inhibitors. *Cell Chem Biol*. 2016;23(9):1123-1134. doi:10.1016/j.chembiol.2016.07.022

17. Harvey EP, Seo H-S, Guerra RM, Bird GH, Dhe-Paganon S, Walensky LD. Crystal Structures of Anti-apoptotic BFL-1 and Its Complex with a Covalent Stapled Peptide Inhibitor. *Structure*. 2018;26(1):153-160.e4. doi:10.1016/j.str.2017.11.016
18. D. de Araujo A, Lim J, Wu K-C, et al. Bicyclic Helical Peptides as Dual Inhibitors Selective for Bcl2A1 and Mcl-1 Proteins. *J Med Chem*. 2018;61(7):2962-2972. doi:10.1021/acs.jmedchem.8b00010
19. Deng J, Carlson N, Takeyama K, Dal Cin P, Shipp M, Letai A. BH3 Profiling Identifies Three Distinct Classes of Apoptotic Blocks to Predict Response to ABT-737 and Conventional Chemotherapeutic Agents. *Cancer Cell*. 2007;12(2):171-185. doi:10.1016/j.ccr.2007.07.001
20. Ryan J, Letai A. BH3 profiling in whole cells by fluorimeter or FACS. *Methods*. 2013;61(2):156-164. doi:10.1016/j.ymeth.2013.04.006
21. Del Gaizo Moore V, Letai A. BH3 profiling--measuring integrated function of the mitochondrial apoptotic pathway to predict cell fate decisions. *Cancer Lett*. 2013;332(2):202-205. doi:10.1016/j.canlet.2011.12.021
22. Pan R, Hogdal LJ, Benito JM, et al. Selective BCL-2 inhibition by ABT-199 causes on-target cell death in acute myeloid Leukemia. *Cancer Discov*. 2014;4(3):362-675. doi:10.1158/2159-8290.CD-13-0609
23. Touzeau C, Ryan J, Guerriero J, et al. BH3 profiling identifies heterogeneous dependency on Bcl-2 family members in multiple myeloma and predicts sensitivity to BH3 mimetics. *Leukemia*. 2016;30(3):761-764. doi:10.1038/leu.2015.184
24. Gunda V, Sarosiek KA, Brauner E, et al. Inhibition of MAPKinase pathway sensitizes thyroid cancer cells to ABT-737 induced apoptosis. *Cancer Lett*. 2017;395:1-10. doi:10.1016/j.canlet.2017.02.028
25. Koch R, Christie AL, Crombie JL, et al. Biomarker-driven strategy for MCL1 inhibition in T-cell lymphomas. *Blood*. 2019;133(6):566-575. doi:10.1182/blood-2018-07-865527
26. Taylor Ripley R, Surman DR, Diggs LP, et al. Metabolomic and BH3 profiling of esophageal cancers: Novel assessment methods for precision therapy. *BMC Gastroenterol*. 2018;18(1):94. doi:10.1186/s12876-018-0823-x
27. Lee T, Bian Z, Zhao B, et al. Discovery and biological characterization of potent myeloid cell leukemia-1 inhibitors. *FEBS Lett*. 2017;591(1):240-251. doi:10.1002/1873-3468.12497
28. Pierceall WE, Kornblau SM, Carlson NE, et al. BH3 profiling discriminates response to cytarabine-based treatment of acute myelogenous leukemia. *Mol Cancer Ther*. 2013;12(12):2940-2949. doi:10.1158/1535-7163.MCT-13-0692

29. Jenson JM, Ryan JA, Grant RA, Letai A, Keating AE. Epistatic mutations in PUMA BH3 drive an alternate binding mode to potently and selectively inhibit anti-apoptotic Bcl-1. *Elife*. 2017;6. doi:10.7554/eLife.25541
30. Placzek WJ, Wei J, Kitada S, Zhai D, Reed JC, Pellecchia M. A survey of the anti-apoptotic Bcl-2 subfamily expression in cancer types provides a platform to predict the efficacy of Bcl-2 antagonists in cancer therapy. *Cell Death Dis*. 2010;1(5):e40. doi:10.1038/cddis.2010.18
31. Butterworth M, Pettitt A, Varadarajan S, Cohen GM. BH3 profiling and a toolkit of BH3-mimetic drugs predict anti-apoptotic dependence of cancer cells. *Br J Cancer*. 2016;114(6):638-641. doi:10.1038/bjc.2016.49
32. Soderquist RS, Crawford L, Liu E, et al. Systematic mapping of BCL-2 gene dependencies in cancer reveals molecular determinants of BH3 mimetic sensitivity. *Nat Commun*. 2018;9(1):3513. doi:10.1038/s41467-018-05815-z
33. Foight GW, Ryan JA, Gullá S V., Letai A, Keating AE. Designed BH3 peptides with high affinity and specificity for targeting Mcl-1 in cells. *ACS Chem Biol*. 2014;9(9):1962-1968. doi:10.1021/cb500340w
34. Kong W, Zhou M, Li Q, Fan W, Lin H, Wang R. Experimental Characterization of the Binding Affinities between Proapoptotic BH3 Peptides and Antiapoptotic Bcl-2 Proteins. *ChemMedChem*. 2018;13(17):1763-1770. doi:10.1002/cmdc.201800321
35. Whitecross KF, Alsop AE, Cluse LA, et al. Defining the target specificity of ABT-737 and synergistic antitumor activities in combination with histone deacetylase inhibitors. *Blood*. 2009;113(9):1982-1991. doi:10.1182/blood-2008-05-156851
36. Ewald L, Dittmann J, Vogler M, Fulda S. Side-by-side comparison of BH3-mimetics identifies MCL-1 as a key therapeutic target in AML. *Cell Death Dis*. 2019;10(12). doi:10.1038/s41419-019-2156-2
37. Moujalled DM, Pomilio G, Ghiurau C, et al. Combining BH3-mimetics to target both BCL-2 and MCL1 has potent activity in pre-clinical models of acute myeloid leukemia. *Leukemia*. 2019;33(4):905-917. doi:10.1038/s41375-018-0261-3
38. Ramsey HE, Fischer MA, Lee T, et al. A Novel MCL1 Inhibitor Combined with Venetoclax Rescues Venetoclax-Resistant Acute Myelogenous Leukemia. *Cancer Discov*. 2018;8(12):1566-1581. doi:10.1158/2159-8290.CD-18-0140
39. Piva R, Pellegrino E, Mattioli M, et al. Functional validation of the anaplastic lymphoma kinase signature identifies CEBPB and BCL2A1 as critical target genes. *J Clin Invest*. 2006;116(12):3171-3182. doi:10.1172/JCI29401
40. Rhodes DR, Yu J, Shanker K, et al. ONCOMINE: A Cancer Microarray Database and Integrated Data-Mining Platform. *Neoplasia*. 2004;6(1):1-6. doi:10.1016/s1476-5586(04)80047-2

41. Bentz M, Plesch A, Bullinger L, et al. t(11;14)-positive mantle cell lymphomas exhibit complex karyotypes and share similarities with B-cell chronic lymphocytic leukemia. *Genes Chromosom Cancer*. 2000;27(3):285-294. doi:10.1002/(SICI)1098-2264(200003)27:3<285::AID-GCC9>3.0.CO;2-M
42. Ri M, Iida S, Ishida T, et al. Bortezomib-induced apoptosis in mature T-cell lymphoma cells partially depends on upregulation of Noxa and functional repression of Mcl-1. *Cancer Sci*. 2009;100(2):341-348. doi:10.1111/j.1349-7006.2008.01038.x
43. Vogler M. Targeting BCL2-Proteins for the Treatment of Solid Tumours. *Adv Med*. 2014;2014. doi:10.1155/2014/943648
44. Chonghaile TN, Sarosiek KA, Vo TT, et al. Pretreatment mitochondrial priming correlates with clinical response to cytotoxic chemotherapy. *Science (80-)*. 2011;334(6059):1129-1133. doi:10.1126/science.1206727
45. Montero J, Sarosiek KA, Deangelo JD, et al. Drug-Induced death signaling strategy rapidly predicts cancer response to chemotherapy. *Cell*. 2015;160(5):977-989. doi:10.1016/j.cell.2015.01.042
46. Nagaraj AB, Joseph P, Kovalenko O, et al. Critical role of Wnt/ β -catenin signaling in driving epithelial ovarian cancer platinum resistance. *Oncotarget*. 2015;6(27):23720-23734. doi:10.18632/oncotarget.4690
47. Soderquist RS, Crawford L, Liu E, et al. Systematic mapping of BCL-2 gene dependencies in cancer reveals molecular determinants of BH3 mimetic sensitivity. *Nat Commun*. 2018;9(1):1-13. doi:10.1038/s41467-018-05815-z
48. Wang J, Zhou JY, Wu GS. Bim protein degradation contributes to cisplatin resistance. *J Biol Chem*. 2011;286(25):22384-22392. doi:10.1074/jbc.M111.239566
49. Bell D, Berchuck A, Birrer M, et al. Integrated genomic analyses of ovarian carcinoma. *Nature*. 2011;474(7353):609-615. doi:10.1038/nature10166
50. Zhang H, Guttikonda S, Roberts L, et al. Mcl-1 is critical for survival in a subgroup of non-small-cell lung cancer cell lines. *Oncogene*. 2011;30(16):1963-1968. doi:10.1038/onc.2010.559
51. Goodwin CM, Rossanese OW, Olejniczak ET, Fesik SW. Myeloid cell leukemia-1 is an important apoptotic survival factor in triple-negative breast cancer. *Cell Death Differ*. 2015;22(12):2098-2106. doi:10.1038/cdd.2015.73
52. Hind CK, Carter MJ, Harris CL, Chan HTC, James S, Cragg MS. Role of the pro-survival molecule Bfl-1 in melanoma. *Int J Biochem Cell Biol*. 2015;59:94-102. doi:10.1016/j.biocel.2014.11.015

53. Sullivan RJ, Flaherty K. MAP kinase signaling and inhibition in melanoma. *Oncogene*. 2013;32(19):2373-2379. doi:10.1038/onc.2012.345
54. Tong J, Tan S, Zou F, Yu J, Zhang L. FBW7 mutations mediate resistance of colorectal cancer to targeted therapies by blocking Mcl-1 degradation. *Oncogene*. 2017;36(6):787-796. doi:10.1038/onc.2016.247
55. Tong J, Wang P, Tan S, et al. Mcl-1 degradation is required for targeted therapeutics to eradicate colon cancer cells. *Cancer Res*. 2017;77(9):2512-2521. doi:10.1158/0008-5472.CAN-16-3242
56. Montero J, Letai A. Dynamic BH3 profiling-poking cancer cells with a stick. *Mol Cell Oncol*. 2016;3(3). doi:10.1080/23723556.2015.1040144
57. Rassidakis GZ, Jones D, Lai R, et al. BCL-2 family proteins in peripheral T-cell lymphomas: Correlation with tumour apoptosis and proliferation. *J Pathol*. 2003;200(2):240-248. doi:10.1002/path.1346
58. Spinner S, Crispatzu G, Yi J-H, et al. Re-activation of mitochondrial apoptosis inhibits T-cell lymphoma survival and treatment resistance. *Leukemia*. 2016;30(7):1520-1530. doi:10.1038/leu.2016.49
59. Adams CM, Clark-Garvey S, Porcu P, Eischen CM. Targeting the Bcl-2 family in B cell lymphoma. *Front Oncol*. 2019;9(JAN). doi:10.3389/fonc.2018.00636

Chapter 3

Targeting the Bcl-2 Proteins to Overcome Resistance in Melanoma

3.1 Abstract

Despite therapeutic improvements in treating metastatic melanoma, most patients develop acquired resistance and are left with limited options. Attenuation of intrinsic apoptosis by upregulated pro-survival Bcl-2 proteins plays a prominent role in drug resistance and may be effective targets in melanoma. We functionally analyzed the Bcl-2 proteins using BH3 profiling in a panel of melanoma cell lines. Most cell lines exhibited a strong co-dependence on Mcl-1 and Bcl-xL. A few cell lines displayed sole Mcl-1 or Bcl-xL, which was predictive of single agent Mcl-1 or Bcl-xL inhibitor and siRNA treatment induced apoptosis, while all cell lines responded robustly to the combination of Mcl-1/Bcl-xL inhibitors. Furthermore, we investigated the functional role of Bfl-1 as an emerging therapeutic target and highlight the potential of dual Mcl-1/Bfl-1 inhibition. We identified that vemurafenib acquired resistance in the SK-MEL-239 cell line was substantially more dependent on Mcl-1 than its parent line, which led to heightened sensitivity to Mcl-1 inhibition. Dynamic BH3 profiling revealed that short term treatment of cell lines with BRAF and MEK inhibitors also primed cells for functional Mcl-1 dependence and sensitized to Mcl-1 inhibitor treatment. These studies guided by BH3 profiling highlight the therapeutic potential of targeting the Bcl-2 proteins in melanoma.

3.2 Introduction

Melanoma is the deadliest form of skin cancer and new incidences have increased at a steeper rate than any other malignancy over the last 40 years.¹ In the year 2020 this invasive disease is estimated to be newly diagnosed in 100,350 men and women, resulting in a projected 6,850 deaths, in the United States alone.² Those diagnosed with melanoma after metastasis have dismal 5-year survival rates as low as 19%.³ Previous to 2011 there were only two approved drugs for the treatment of metastatic melanoma, dacarbazine and high doses of IL2, both of which showed limited clinical efficacy and high toxicity.⁴ In the last decade there have been phenomenal leaps in the treatment of metastatic melanoma advent by several new molecular targeted drugs aimed at common oncogenic drivers and immunotherapies that commission the immune system to attack cancer cells.⁵ These new advancements have come namely in the form of BRAF/MEK inhibitors⁶⁻⁸ and anti-PD-1/PD-L1 monoclonal antibodies^{9,10}, and although they have shown clinical efficacy, there is still a need to combat acquired resistance which develops in many patients.¹¹⁻¹³ Cancer is a very heterogeneous disease that is capable of utilizing many physiological avenues to ensure its survival and evasion; melanoma is no exception and it is critical to simultaneously modulate several pathways through combinatorial therapies to ensure efficacy.¹⁴

Previous reports have highlighted the role of the Bcl-2 proteins in melanoma and the promise they hold as therapeutic targets in this disease.¹⁵ Identifying when to deploy inhibitors of the anti-apoptotic proteins will be critical to guiding their use in melanoma therapy. BH3 profiling can be used to identify functional pro-survival dependence and predict response to small molecule Bcl-2 family inhibitors (BH3 mimetics), which will be

a key tool in this study.^{16,17} Additionally, Mcl-1 is suspected to play a role in promoting resistance to MAPK inhibitors in melanoma¹⁸ and we aim to use BH3 profiling to functionally investigate this in the context of acquired resistance to identify combination treatments with BH3 mimetics. This study utilizes the chemical and functional tools available in the form of selective peptides, BH3 mimetics, and BH3 profiling to dissect and target the survival dependence in melanoma. The goal is to define novel treatment strategies to target the Bcl-2 protein family in melanoma in order to provide translational findings that would ultimately improve patient outcomes.

3.3 Functional evaluation of Bcl-2 family proteins in melanoma cell lines

Due to the dynamic nature of Bcl-2 protein family protein-protein interactions (PPIs) their functional roles are difficult to define using absolute protein or mRNA levels alone.^{19,20} Therefore, employing functional methods such as BH3 profiling serves as a much better predictor of survival dependence and sensitivity to BH3 mimetics. We assembled a panel of 11 melanoma derived cell lines, mainly driven by the more common BRAF V600E mutation, with two being NRAS mutant driven (Table 3.1). In addition, alongside this melanoma panel we have dermal cells that were freshly isolated from human foreskin fibroblasts (HFF).

Table 3.1 Melanoma cell line panel

Cell Line	BRAF	NRAS	CDKN2A	p53	PTEN
HFF	WT	WT	WT	WT	WT
M14	V600E	WT	mut	mut	G266E
UACC62	V600E	WT	WT	WT	P248

SK-MEL-1	V600E	WT	WT	WT	WT
Malme-3M	V600E	WT	del	WT	WT
UACC-257	V600E	WT	del	WT	P248
SK-MEL-239	V600E	WT	WT	WT	WT
A2058	V600E	WT	WT	V274F	del
SK-MEL-5	V600E	WT	del	WT	WT
VMM15	V600E	WT	WT	WT	WT
SK-MEL-103	WT	Q61R	P114L	WT	WT
SK-MEL-2	WT	Q61R	WT	G245S	WT

In an effort to define the survival dependence of this panel of melanoma cell lines and therefore predict which BH3 mimetics would produce the greatest apoptotic response, we performed BH3 profiling. We used the promiscuous Puma peptide to gauge overall apoptotic priming and the Bad, Hrk, and MS1 peptides which selectively target Bcl-2/Bcl-xL, Bcl-xL, and Mcl-1, respectively. All the anti-apoptotic proteins being investigated have actionable small molecule inhibitors that can be used for correlative apoptosis analysis. The induced mitochondrial depolarization response from these peptide treatments revealed heterogeneous survival dependence, mainly from Bcl-xL and Mcl-1 (Figure 3.1). The HFF cells displayed the lowest levels of apoptotic priming, as expected from non-malignant cells, while the rest of the melanoma cell lines all showed significant response to the Puma peptide, indicating they are equipped with the required Bcl-2 family machinery to trigger intrinsic apoptosis (Figure 3.1A). Out of the 11 cell lines, seven of them showed very low (<50%) response to the selective peptides with insignificant differences between them, indicating that neither Bcl-2, Bcl-xL, or Mcl-1 alone played a predominant role in survival dependence and selective antagonization is not sufficient to induce mitochondrial depolarization (Figure 3.1B). Knowing that these

seven cell lines are primed for apoptosis, the likely scenario is that they rely on subsets of the anti-apoptotic proteins for survival. In two cell lines (SK-MEL-2 and UACC-62), the MS1 peptide induced high depolarization ($\geq 50\%$) that was significant over Bad and Hrk, indicating sole Mcl-1 dependence. Predominant Bcl-xL dependence was found in two other cell lines (SK-MEL-5 and SK-MEL-103), defined by the Bad and Hrk peptides inducing $\geq 50\%$ depolarization, while remaining insignificant from each other, which signifies that the effect of Bad comes from Bcl-xL binding, and being significantly higher than MS1. This functional exercise utilizing BH3 profiling was able to pinpoint four out of 11 cell lines that displayed sole survival dependence on either Mcl-1 or Bcl-xL, which could be further validated by additional experiments using BH3 mimetics. Additionally, more insight into the co-dependence of the majority of cell lines would need to be investigated before defining the main pro-survival players.

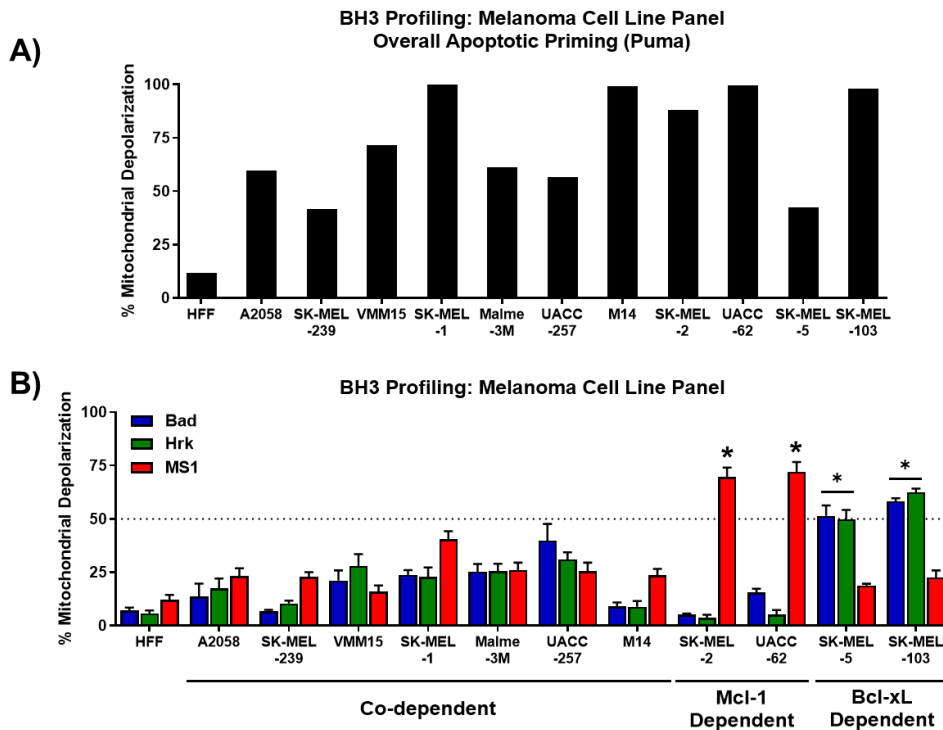


Figure 3.1 BH3 profiling of melanoma cell line panel

A) Overall apoptotic priming gauged by BH3 profiling of a panel of melanoma cell lines and non-malignant dermal fibroblasts (HFF) with the promiscuous Puma peptide (1 μ M) and **B)** the selective Bad, Hrk, and MS1 (12 μ M) peptides to define subgroups of co-dependent and Bcl-xL or Mcl-1 single dependent cell lines. Results from ≥ 2 independent experiments. Significance ($*p < 0.05$) is denoted when data sets $\geq 50\%$ mitochondrial depolarization are different from the others within a cell line, bars over Bad/Hrk indicate difference from MS1, attributing dependence to Bcl-xL.

3.4 Genetic and pharmacological targeting of Bcl-xL and Mcl-1

Following up the functional data provided by BH3 profiling, we treated select cell lines with anti-apoptotic protein targeting siRNAs and BH3 mimetics and monitored apoptosis induction. We performed an siRNA screen targeting Bcl-2, Bcl-xL, Mcl-1 as single and double knockdowns in three of the seven co-dependent cell lines (A2058, Malme-3M, and VMM15) in order to determine the optimal apoptosis inducing combination (Figure 3.2A). Efficient knockdown of each anti-apoptotic protein by siRNA pools was confirmed by western blot (Figure 3.7). All three cell lines did not commit to apoptosis in response to single protein knockdowns, as expected, but all responded robustly to the combination of Bcl-xL and Mcl-1 dual knockdown, but not the combinations with Bcl-2. To corroborate these findings with actionable small molecules, we treated the same cell lines with selective BH3 mimetics and identified a similar phenotype (Figure 3.2B). Single agent BH3 mimetics were insufficient to induce apoptosis, but a strong response was induced by the combination of S63845 and A-1155463, which target Mcl-1 and Bcl-xL, respectively. To verify the dose dependent nature of this combination, we treated the A2058 and Malme-3M cell lines with a 1:1 ratio of S63845 and A-1155463 in doses ranging from 0.003 – 1 μ M (Figure 3.2C-D). The dose dependent apoptosis response generated by this combination produced potent EC₅₀ values ~ 100 nM with near complete induction of apoptosis with as low as

300 nM in both cell lines. These results confirm the Bcl-xL/Mcl-1 co-dependence of the majority of melanoma cell lines tested and identified the combination of S63845 and A-1155463 as a highly potent strategy to combat melanoma. However, these results are limited to cell line studies and the toxicity effects of dual Bcl-xL/Mcl-1 inhibition would need to be evaluated more in depth to determine therapeutic feasibility.

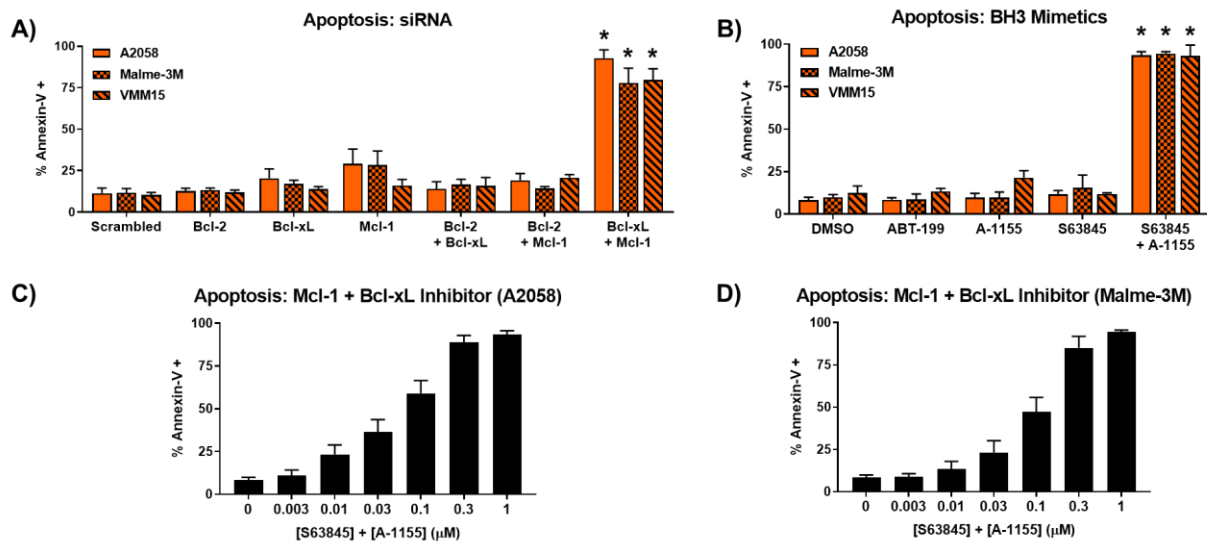


Figure 3.2 siRNA and BH3 mimetic targeting dual Bcl-xL/Mcl-1 dependent cell lines

A) siRNA screen (25 nM, 48 hours) of anti-apoptotic proteins and their combinations in Bcl-xL/Mcl-1 co-dependent cell lines. **B)** The same cell lines treated with selective BH3 mimetics (1 μM, 24 hours) as single agents and the combination of Mcl-1 and Bcl-xL inhibitors producing the same phenotype as siRNA treatments. **C)** Dose dependent apoptosis induction by a 1:1 ratio of S63845 and A-1155 (24-hour treatment) in the A2058 and **D)** Malme-3M cell lines. Cells analyzed by flow cytometry for apoptosis induction (Annexin-V+). Results from ≥ 2 independent experiments, * $p < 0.05$ (significance between both untreated and single agent treatments).

Similar to the previous experimental strategy, we sought to confirm the individual Bcl-xL and Mcl-1 dependence of the remaining cell lines by siRNA and BH3 mimetic induced apoptosis. Indeed, the BH3 profiling determined Bcl-xL dependent cell lines SK-MEL-103 and SK-MEL-5 underwent apoptosis in response to the knockdown of Bcl-xL, but not Bcl-2 or Mcl-1, while the Mcl-1 dependent SK-MEL-2 and UACC62 cell lines

expectedly responded to Mcl-1 knockdown but not the others (Figure 3.3A). Likewise, the siRNA induced apoptotic response was recapitulated by BH3 mimetic treatments, illustrated by A-115463 inducing apoptosis in the Bcl-xL dependent cell lines and S63845 eliciting apoptosis in only the Mcl-1 dependent cell lines, while single agent ABT-199 had no effect. Additionally, potent dose dependent apoptosis was induced by A-1155463 and S63845 in SK-MEL-5 and SK-MEL-2, respectively (Figure 3.3C-D). These experiments validate the ability of BH3 profiling to pinpoint melanoma cell lines that are sensitive to single agent BH3 mimetic treatments, which may have future clinical implications. This data highlights the prominent role of Bcl-xL and Mcl-1 in melanoma either in co-operative or sole dependence and defines a strategy to use BH3 mimetics as potential therapeutics in melanoma.

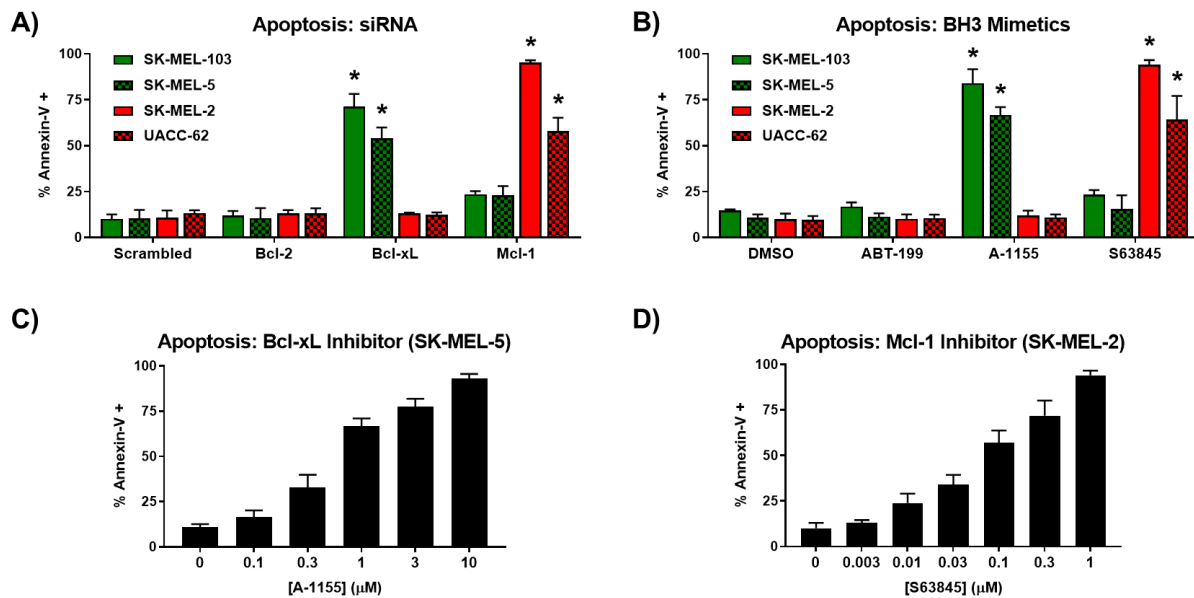


Figure 3.3 Targeting Bcl-xL and Mcl-1 in sole dependent cell lines

A) siRNA screen (25 nM, 48 hours) of anti-apoptotic proteins in Bcl-xL and Mcl-1 dependent cell lines. **B)** The same cell lines treated with selective BH3 mimetics (1 μ M, 24 hours) as single agents, producing the same phenotype as siRNA treatments. **C)** Dose dependent apoptosis induction by A-1155 (24-hour treatment) in the SK-MEL-5 cell line and **D)** S63845 in the SK-MEL-2 cell line. Cells analyzed by flow

cytometry for apoptosis induction (Annexin-V+). Results from ≥ 2 independent experiments, * $p < 0.05$ (significance between both untreated and single agent treatments).

3.5 Functional analysis and targeting of Bfl-1

Up to this point we have focused our efforts on functionally defining and targeting the actionable Bcl-2, Bcl-xL, and Mcl-1 anti-apoptotic proteins in melanoma, which have potent and selective small molecule inhibitors. However, the homologous Bfl-1 protein has been shown to play an important role in contributing to the survival of melanoma cells and is the disease where Bfl-1 is most prevalent.^{21,22} Using the Bfl-1 selective peptide, FS2, we performed BH3 profiling and ranked the cell lines based on their mitochondrial depolarization response (Figure 3.4A). The M14 cell line stood out as displaying the greatest functional dependence on Bfl-1 and was selected for further follow-up studies to investigate the targeting of Bfl-1. In addition to Bfl-1, M14 showed some dependence on Mcl-1 as well, indicated by dose dependent depolarization induced by both MS1 and FS2 (Figure 3.4B). When Mcl-1 and Bfl-1 were individually knocked down by siRNA in the M14 cell line the apoptotic response was minimal, but was further enhanced by their double knockdown (% Annexin-V+ = ~50%), indicating an efficacious strategy for dual inhibition of these two proteins (Figure 3.4C). Since there are no potent and biologically active Bfl-1 inhibitors available, the combination of Bfl-1 siRNA and the Mcl-1 inhibitor, S63845, was tested. Knocking down the Bfl-1 protein potentiated the apoptotic response induced by S63845 in a dose dependent manner, revealing a strategy to combat melanomas with high functional dependence on Bfl-1. This dual Mcl-1/Bfl-1 inhibition approach defined in the M14 cell line highlights the need for Bfl-1 selective or dual inhibitors with Mcl-1 to combat certain subsets of malignant

melanomas. Although we have identified certain cell lines that respond well to single or combination anti-apoptotic protein inhibition, the more relevant therapeutic strategy may be to combine these approaches with standard-of-care treatments in melanoma to combat resistance.

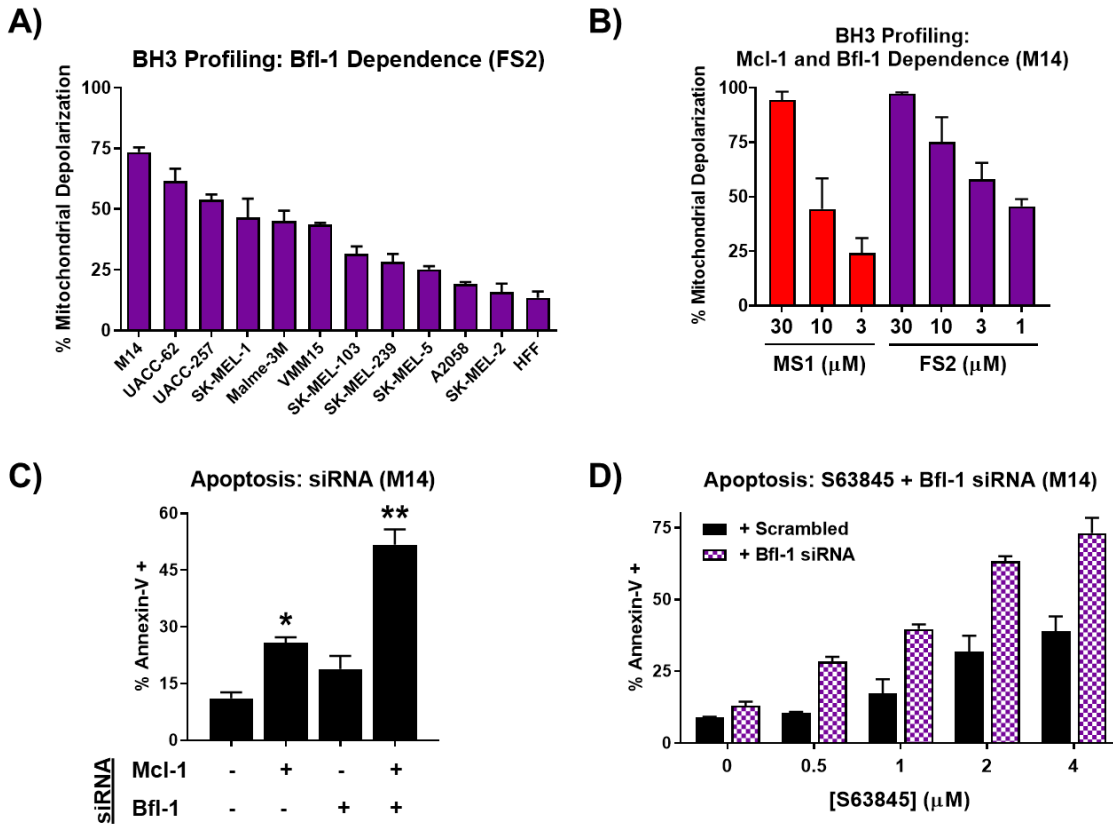


Figure 3.4 Targeting Bfl-1 in the M14 cell line

A) BH3 profiling of melanoma cell line panel with the Bfl-1 selective FS2 peptide (12 μM). **B)** Dose dependent mitochondrial depolarization from BH3 profiling of the M14 cell line with MS1 and FS2. **C)** Apoptosis induction (Annexin-V+) induced by Mcl-1 and/or Bfl-1 siRNA treatments (25 nM, 48 hours). **D)** Apoptosis induced by treatment of M14 with S63845 (24 hours) after 48 hours of scrambled or Bfl-1 siRNA treatment. Results from ≥2 independent experiments. * p < 0.05; ** p < 0.005.

3.6 Vemurafenib resistance selectively increases Mcl-1 dependence

To effectively treat most solid tumors, several oncogenic cellular signaling pathways usually need to be attenuated simultaneously.²³ BRAF and MEK inhibitors are

routinely used to treat metastatic melanoma, but acquired resistance inevitably develops in the vast majority of patients.¹³ To investigate the functional role of the Bcl-2 family of proteins in response to acquired resistance to the BRAF inhibitor, vemurafenib, we utilized the SK-MEL-239 cell line and its vemurafenib resistant sub-line that was developed through chronic vemurafenib treatment. Cell viability curves using a dose range of vemurafenib identified high sensitivity in the parental SK-MEL-239 cell line ($IC_{50} = 324 \text{ nM}$) and confirmed resistance in the resistant subline that was no longer sensitive to vemurafenib treatment ($IC_{50} > 10 \text{ }\mu\text{M}$) (Figure 3.5A). Additionally, the western blot of baseline level proteins in the parental and resistant sublines shows hyperactivated Erk (pErk), confirming that vemurafenib is no longer capable of inhibiting the MAPK pathway (Figure 3.5B). Regarding the Bcl-2 protein family, there are slight decreases in Bcl-2 and Bcl-xL levels and a depletion of the Noxa protein, with no changes in Mcl-1 in the resistant subline. The comparison of BH3 profiles also identified a distinct difference in pro-survival dependence, where the vemurafenib resistant subline displayed a significantly higher level of Mcl-1 dependence compared to the parental cell line, illustrated by increased MS1 depolarization and no significant differences in the effect of the other peptides (Figure 3.5C). This increased Mcl-1 dependence also translated to heightened sensitivity to Mcl-1 inhibition by both siRNA and S63845 treatments, which were both able to elicit robust apoptosis (Figure 3.5C-D). A mechanistic explanation for the increased Mcl-1 dependence can come from the Noxa depletion (Figure 3.5B) which would free up endogenous Mcl-1 and allow it to bind to Bim or other pro-apoptotic activators, priming the cells for Mcl-1 dependence. Additionally, there may be a post translational stabilizing effect of Mcl-1, reducing its

turnover rate. To investigate this, we performed cycloheximide (CHX) half-life experiments in the parental and vemurafenib resistant cell lines. CHX inhibits protein synthesis and the short half-life of Mcl-1 was confirmed by treating the parental cell line with CHX and monitoring its degradation over time, giving an Mcl-1 half-life of 1.2 hours, similar to what has been reported (Figure 3.5F-G).²⁴ Interestingly, the half-life of Mcl-1 was prolonged in the vemurafenib resistant cell line to a half-life > 4 hours, indicating that Mcl-1 is in fact being stabilized in the cell. The PEST domain on Mcl-1 contains several phosphorylation sites that allow for post-translational modification²⁵ and it is possible that an isomerase such as Pin1, which is regulated by the MAPK pathway, contributes to a stabilized state of Mcl-1, increasing its functional activity.²⁶ These important findings highlight the functional role of Mcl-1 in contributing to vemurafenib resistance in melanoma and define a strategy for using Mcl-1 inhibitors to overcome vemurafenib resistance.

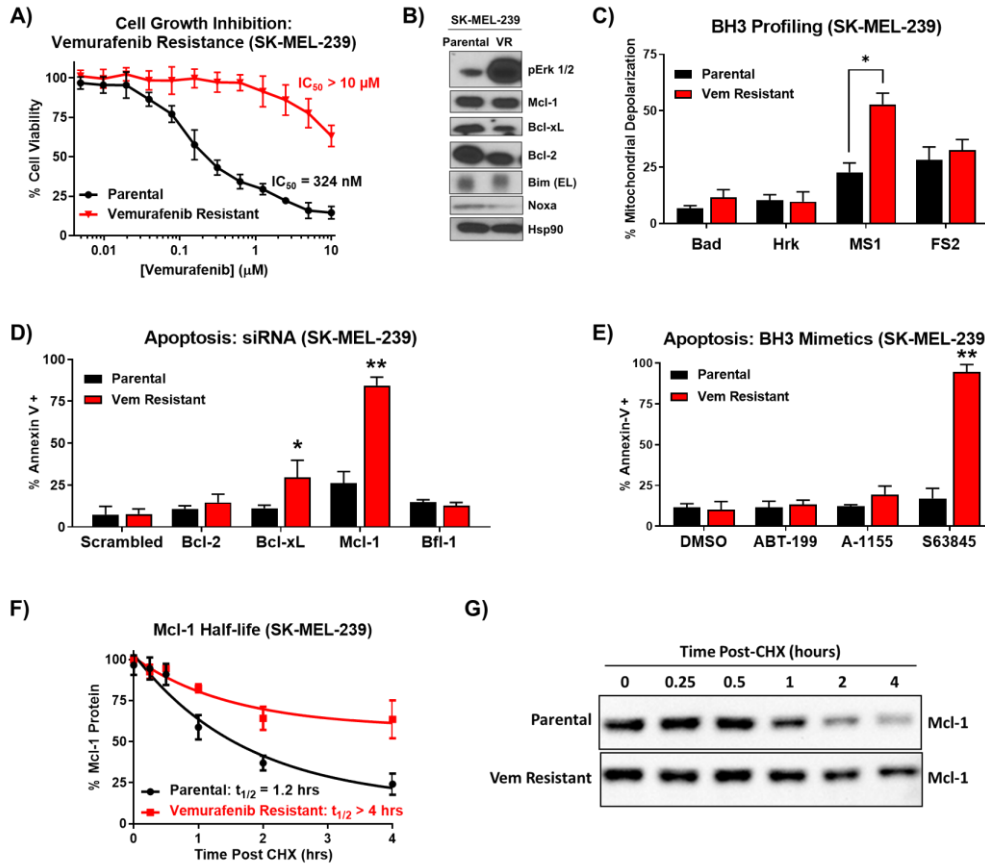


Figure 3.5 Vemurafenib acquired resistance increases Mcl-1 dependence

A) Cell viability curves measuring sensitivity to vemurafenib in the parental and vemurafenib resistant sublines. **B)** Western blot of baseline Bcl-2 family proteins. **C)** BH3 profiling of the parental and vemurafenib resistant lines (12 μ M peptides). **D)** Apoptosis elicited by siRNA (25 nM, 48 hours) and **E)** BH3 mimetic (1 μ M, 24 hours) treatments. **F)** Half-life curves measuring degradation of Mcl-1 protein after CHX treatments in both sublines, **G)** with accompanied representative western blot of Mcl-1.

* $p < 0.05$; ** $p < 0.005$.

3.7 Short term BRAF/MEK inhibitor treatment primes for Mcl-1 dependence

We utilized dynamic BH3 profiling to determine whether melanoma cells need to develop long term resistance in order to increase Mcl-1 dependence, in order to develop combination treatment strategies to kill melanoma cells more effectively before resistance sets in. The A2058 melanoma cell line was treated for 48 hours with vemurafenib or the MEK inhibitor, PD-0325901 (PD-901) before performing BH3 profiling and comparing with the baseline profile. The results from this dynamic BH3

profiling experiment reveals that Mcl-1 functional dependence is indeed increased after a short-term treatment with BRAF or MEK inhibitors (Figure 3.6A). By examining the Bcl-2 protein changes in response to these treatments, we can identify a mechanistic explanation for the increased Mcl-1 dependence. Both MAPK inhibitors slightly increased Mcl-1 levels, dramatically increased Bim, and depleted Noxa, with no apparent change in Bcl-xL, which would favor an increase in Mcl-1:Bim complexes that prime cells for Mcl-1 dependence (Figure 3.6B). As expected, the vemurafenib pre-treatment of A2058 cells selectively potentiated the cells to S63845 treatment, inducing a robust apoptosis response (Figure 3.6C). This combination approach resulted in a dose dependent increase in S63845 sensitivity with a significantly improved apoptotic response with as low as 100 nM of S63845 (Figure 3.6D). These results suggest that a more effective strategy is to treat melanomas with Mcl-1 inhibitors early in the process of MAPK inhibitor administration, before acquired resistance develops, which may further enhance patient outcomes.

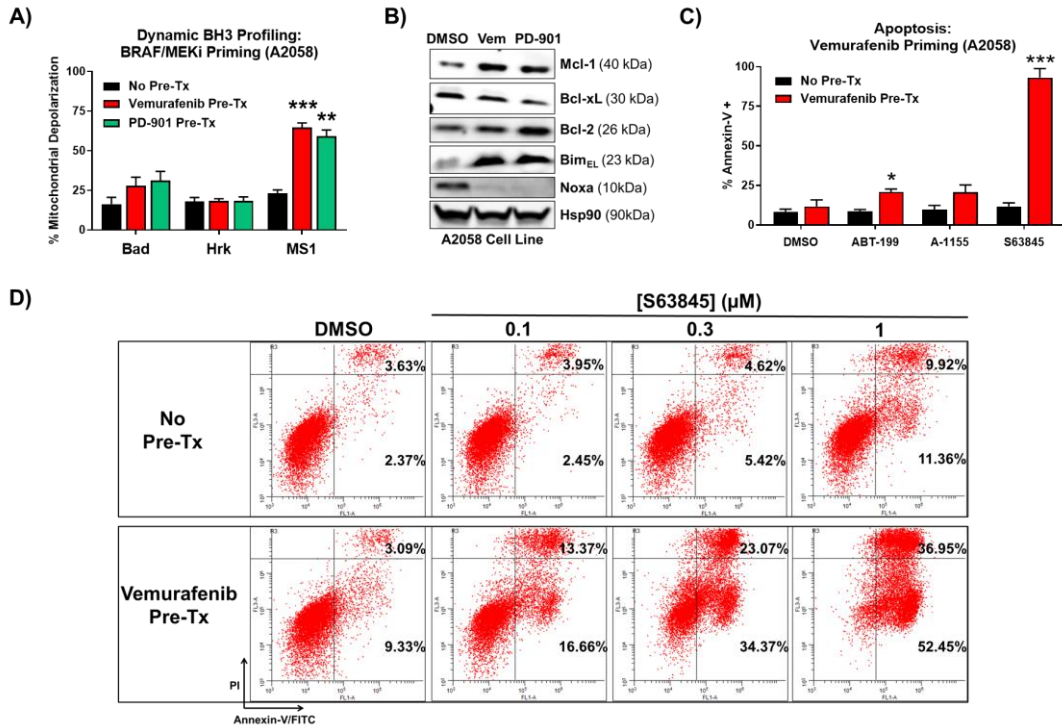


Figure 3.6 MAPK inhibitors selectively prime for Mcl-1 dependence

A) Dynamic BH3 profiling (12 μM peptides) after 48-hour pre-treatment with the BRAF inhibitor vemurafenib (0.5 μM) and the MEK inhibitor PD-901 (0.1 μM). **B)** Western blot of Bcl-2 family proteins before and after treatment with vemurafenib and PD-901. **C)** Apoptosis induced by BH3 mimetics (1 μM, 24 hours) before and after vemurafenib treatment. **D)** Dose dependent apoptosis induction by S63845 depicted by flow cytometry plots of PI and Annexin-V quadrants before and after vemurafenib treatment. * p < 0.05; ** p < 0.005; *** p < 0.0005.

3.8 Conclusions

Guided by BH3 profiling we were able to dissect the functional survival dependence of a panel of melanoma cell lines that represent the most common genetic drivers of the disease. We determined that Bcl-xL and Mcl-1 were the most prevalent pro-survival supporters, either working in co-dependence or individually. Additionally, we investigated the functional role of Bfl-1 and identified co-inhibition strategies with Mcl-1 in the M14 cell line. The majority of cell lines were insensitive to single agent inhibition of the anti-apoptotic proteins and the intrinsic apoptosis pathway was only activated by a combination of Bcl-xL and Mcl-1 inhibition, either by siRNA or A-1155463

and S63845 BH3 mimetic treatments. BH3 profiling effectively identified a small subset of cell lines that displayed sole dependence on Bcl-xL or Mcl-1, which correspondingly exhibited sensitivity to single agent siRNA or BH3 mimetic inhibition of their respective dependent proteins. This approach utilizing BH3 profiling highlights the advantage of elucidating survival dependence in order to identify efficacious BH3 mimetic treatments.

In the setting of acquired resistance in melanoma, we identified the increased pro-survival role of Mcl-1 which promoted therapeutic resistance to the BRAF inhibitor, vemurafenib. The functional increase in Mcl-1 dependence was determined by BH3 profiling and provided an opportunity of heightened Mcl-1 inhibitor sensitivity, which induced robust apoptosis response in the vemurafenib resistant subline, but not the SK-MEL-239 parental cell line. We demonstrated that vemurafenib and the MEK inhibitor, PD-0325901, are capable of increasing Mcl-1 dependence after short term treatments and identified an efficacious combination treatment approach with S63845 before resistance develops.

These studies, functionally guided by BH3 profiling, offer several strategies to target the Bcl-2 protein family in melanoma. Identifying single agent responsive Bcl-xL and Mcl-1 dependent melanomas provide an attractive approach to use BH3 mimetics in a personalized medicine setting. The robust apoptosis activation induced by combination of Bcl-xL and Mcl-1 inhibitors warrants further *in vivo* efficacy and toxicity studies to validate its potential as a therapeutic approach. Furthermore, we highlight the important need of selective Bcl-1 or dual Mcl-1/Bcl-1 inhibitors that may be efficacious in cancers such as melanoma.

3.9 Materials and methods

Peptide and small molecule inhibitors

BH3-only peptides were custom synthesized by GenicBio Limited (Shanghai, China). ABT-199, A-1155463, and S63845 were purchased from ChemieTek (Indianapolis, IN). Peptides and small molecules were dissolved in DMSO at 10 mM and stored at -20°C.

BH3 profiling

BH3 profiling was performed using the plate-based kinetic fluorometric procedure.¹⁶ 2×10^6 cells were plated the day before running the assay in 10 cm dishes, providing the highest reproducibility. Working buffer was composed of DTEB (135 mM Trehalose, 10 mM HEPES-KOH pH 7.5, 50 mM KCl, 0.02 mM EGTA, 0.02 mM EDTA, 0.1% BSA, and 5 mM succinate) with the fresh addition of the following: 20 μ M oligomycin, 0.005% (w/v) digitonin, 10 mM β -mercaptoethanol, and 2 μ M JC-1. Peptides and controls were serially diluted in fresh working buffer and 15 μ L/well was added to black, flat bottom 384-well plates (Corning 3573). Cells were harvested, washed once, re-suspended in MEB, then 15 μ L of cell solution was added to each well such that the final cell count was 20×10^3 cells/well in technical triplicates. Plates were immediately analyzed on a BioTek Synergy H1 plate reader at an excitation of 545 nm and emission of 590 nm every 5 minutes for 3 hours at 30°C. The resulting relative fluorescent units were plotted versus time and area under the curve (AUC) values were generated using GraphPad Prism 8.3.0 software. DMSO (1%) and FCCP (10 μ M) controls were used to set 0% and 100% depolarization parameters, respectively. The following equation was

used to generate normalized values for treatment samples:

$$\% \text{ mitochondrial depolarization} = 100 - \left[100 \times \left(\frac{\text{Sample AUC} - \text{FCCP AUC}}{\text{DMSO AUC} - \text{FCCP AUC}} \right) \right].$$

siRNA knockdowns

Cells (50×10^3 /well) were seeded in 12-well plates and left to adhere overnight. ON-TARGETplus siRNA SMARTpools (Dharmacon, Lafayette, CO) were prepared as recommended by manufacturer at a concentration of 25 nM and delivered using Lipofectamine RNAiMAX transfection reagent (Invitrogen). Combination treatments contained 25 nM of each siRNA and scrambled controls were 50 nM. Cells incubated with siRNA for 48 hours before analyzing apoptosis induction. Knockdown efficiency of siRNA pools was evaluated by western blot in the M14 cell line (Figure 3.7).

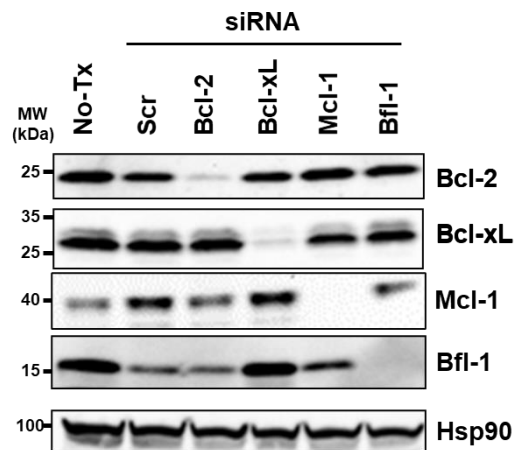


Figure 3.7 siRNA knockdown validation in melanoma

M14 melanoma cell line treated with siRNA pools (25 nM) targeted at individual anti-apoptotic proteins for 48 hours before knockdown efficiency evaluated by western blot.

Apoptosis experiments

Cells (100×10^3 /well) were seeded in 12-well plates and left to adhere overnight. Cells were treated with BH3 mimetics for 24 hours and stained with Annexin-V/FITC and propidium iodide. Cells were run on an Accuri C6 flow cytometer and analyzed using WinList 3.0 software. Percentage of Annexin-V positive populations were used to report apoptosis induction.

MTT cell viability assay

Cells (10,000/well) were treated with BH3 mimetics for 72 hours in 96-well plates in duplicate. After treatment, the MTT reagent, 3-(4,5-dimethylthiazol-2-yl)-2,5-diphenyl tetrazolium bromide, was added and incubated at 37°C for 4 hours before adding SDS/HCl solution. Plates were incubated overnight and read on a BioTek Synergy H1 plate reader at 570 nM absorbance. Treated wells were normalized by subtracting media-only control wells and DMSO treated cells as the 100% cell viability parameter. Growth curves were plotted using GraphPad Prism 8.3.0 software and IC_{50} values were calculated using non-linear regression fitting.

Cyclohexamide (CHX) experiment

SK-MEL-239 parental and vemurafenib resistant cells (1×10^6) were plated in 6-well plates and left to adhere overnight. Cycloheximide (CHX) was added at a concentration of 100 μ g/mL and wells were harvested at respective time points. Cells were lysed and subjected to western blot analysis, probing for Mcl-1.

3.10 References

1. Chudnovsky Y, Khavari PA, Adams AE. Melanoma genetics and the development of rational therapeutics. *J Clin Invest*. 2005;115(4):813-824. doi:10.1172/JCI24808
2. Siegel RL, Miller KD, Jemal A. Cancer statistics, 2020. *CA Cancer J Clin*. 2020;70(1):7-30. doi:10.3322/caac.21590
3. Miller KD, Nogueira L, Mariotto AB, et al. Cancer treatment and survivorship statistics, 2019. *CA Cancer J Clin*. 2019;69(5):363-385. doi:10.3322/caac.21565
4. Jang S, Atkins MB. Which drug, And when, For patients with BRAF-mutant melanoma? *Lancet Oncol*. 2013;14(2). doi:10.1016/S1470-2045(12)70539-9
5. Domingues B, Lopes J, Soares P, Populo H. Melanoma treatment in review. *ImmunoTargets Ther*. 2018;Volume 7:35-49. doi:10.2147/itt.s134842
6. Chapman PB, Hauschild A, Robert C, et al. Improved survival with vemurafenib in melanoma with BRAF V600E mutation. *N Engl J Med*. 2011;364(26):2507-2516. doi:10.1056/NEJMoa1103782
7. Flaherty KT, Robert C, Hersey P, et al. Improved survival with MEK inhibition in BRAF-mutated melanoma. *N Engl J Med*. 2012;367(2):107-114. doi:10.1056/NEJMoa1203421
8. Robert C, Grob JJ, Stroyakovskiy D, et al. Five-Year Outcomes with Dabrafenib plus Trametinib in Metastatic Melanoma. *N Engl J Med*. 2019;381(7):626-636. doi:10.1056/NEJMoa1904059
9. Robert C, Schachter J, Long G V., et al. Pembrolizumab versus ipilimumab in advanced melanoma. *N Engl J Med*. 2015;372(26):2521-2532. doi:10.1056/NEJMoa1503093
10. Larkin J, Chiarion-Sileni V, Gonzalez R, et al. Five-Year Survival with Combined Nivolumab and Ipilimumab in Advanced Melanoma. *N Engl J Med*. 2019;381(16):1535-1546. doi:10.1056/NEJMoa1910836
11. Vennepureddy A, Thumallapally N, Nehru VM, Atallah J-P, Terjanian T. Novel Drugs and Combination Therapies for the Treatment of Metastatic Melanoma. *J Clin Med Res*. 2016;8(2):63-75. doi:10.14740/jocmr2424w
12. Fares CM, Van Allen EM, Drake CG, Allison JP, Hu-Lieskovan S. Mechanisms of Resistance to Immune Checkpoint Blockade: Why Does Checkpoint Inhibitor Immunotherapy Not Work for All Patients? *Am Soc Clin Oncol Educ B*. 2019;(39):147-164. doi:10.1200/edbk_240837
13. Rossi A, Roberto M, Panebianco M, Botticelli A, Mazzuca F, Marchetti P. Drug

- resistance of BRAF-mutant melanoma: Review of up-to-date mechanisms of action and promising targeted agents. *Eur J Pharmacol.* 2019;862. doi:10.1016/j.ejphar.2019.172621
14. Sullivan RJ, Flaherty KT. New strategies in melanoma: Entering the era of combinatorial therapy. *Clin Cancer Res.* 2015;21(11):2424-2435. doi:10.1158/1078-0432.CCR-14-1650
 15. Lee EF, Harris TJ, Tran S, et al. BCL-XL and MCL-1 are the key BCL-2 family proteins in melanoma cell survival. *Cell Death Dis.* 2019;10(5). doi:10.1038/s41419-019-1568-3
 16. Ryan J, Letai A. BH3 profiling in whole cells by fluorimeter or FACS. *Methods.* 2013;61(2):156-164. doi:10.1016/j.ymeth.2013.04.006
 17. Friedman AA, Letai A, Fisher DE, Flaherty KT. Precision medicine for cancer with next-generation functional diagnostics. *Nat Rev Cancer.* 2015;15(12):747-756. doi:10.1038/nrc4015
 18. Fofaria NM, Frederick DT, Sullivan RJ, Flaherty KT, Srivastava SK. Overexpression of Mcl-1 confers resistance to BRAFV600E inhibitors alone and in combination with MEK1/2 inhibitors in melanoma. *Oncotarget.* 2015;6(38):40535-40556. doi:10.18632/oncotarget.5755
 19. Placzek WJ, Wei J, Kitada S, Zhai D, Reed JC, Pellecchia M. A survey of the anti-apoptotic Bcl-2 subfamily expression in cancer types provides a platform to predict the efficacy of Bcl-2 antagonists in cancer therapy. *Cell Death Dis.* 2010;1(5):e40. doi:10.1038/cddis.2010.18
 20. Lucantoni F, Lindner AU, O'donovan N, Düssmann H, Prehn JHM. Systems modeling accurately predicts responses to genotoxic agents and their synergism with BCL-2 inhibitors in triple negative breast cancer cells article. *Cell Death Dis.* 2018;9(2). doi:10.1038/s41419-017-0039-y
 21. Haq R, Yokoyama S, Hawryluk EB, et al. *BCL2A1* is a lineage-specific antiapoptotic melanoma oncogene that confers resistance to BRAF inhibition. *Proc Natl Acad Sci.* 2013;110(11):4321-4326. doi:10.1073/pnas.1205575110
 22. Vogler M. BCL2A1: the underdog in the BCL2 family. *Cell Death Differ.* 2012;19(1):67-74. doi:10.1038/cdd.2011.158
 23. Vogler M. Targeting BCL2-Proteins for the Treatment of Solid Tumours. *Adv Med.* 2014;2014. doi:10.1155/2014/943648
 24. Perciavalle RM, Opferman JT. Delving deeper: MCL-1's contributions to normal and cancer biology. *Trends Cell Biol.* 2013;23(1):22-29. doi:10.1016/j.tcb.2012.08.011

25. Thomas LW, Lam C, Edwards SW. Mcl-1; the molecular regulation of protein function. *FEBS Lett.* 2010;584(14):2981-2989. doi:10.1016/j.febslet.2010.05.061
26. Chen Y, Wu Y ran, Yang H ying, et al. Prolyl isomerase Pin1: a promoter of cancer and a target for therapy. *Cell Death Dis.* 2018;9(9):1-17. doi:10.1038/s41419-018-0844-y

Chapter 4

Discovery and Characterization of Mcl-1 and Bfl-1 Dual Inhibitors

4.1 Abstract

Anti-apoptotic Bcl-2 family proteins are overexpressed in a wide spectrum of cancers and have become well validated therapeutic targets. Cancer cells display survival dependence on individual or subsets of anti-apoptotic proteins that could be effectively targeted by multimodal inhibitors. We designed a 2,5-substituted benzoic acid scaffold that displayed equipotent binding to Mcl-1 and Bfl-1. Structure based design was guided by several solved co-crystal structures with Mcl-1, leading to the development of compound **24**, which binds both Mcl-1 and Bfl-1 with K_i values of 100 nM and shows appreciable selectivity over Bcl-2/Bcl-xL. The selective binding profile of **24** was translated to on-target cellular activity in model lymphoma cell lines. These studies lay a foundation for developing more advanced dual Mcl-1/Bfl-1 inhibitors that have potential to provide greater single agent efficacy and broader coverage to combat resistance in several types of cancer than selective Mcl-1 inhibitors alone.

4.2 Introduction

Development of small molecule inhibitors of the Bcl-2 family of proteins has become a well validated therapeutic approach over recent years, highlighted by the 2016 FDA-approval of the Bcl-2 selective inhibitor, venetoclax.^{1,2} Potent and selective

inhibitors of Bcl-xL and Mcl-1 have also reached clinical evaluation and hold promise of improved clinical outcomes in various cancers.³⁻⁶ Of the validated therapeutic anti-apoptotic targets in the Bcl-2 family, Bfl-1 remains without a potent drug-like inhibitor and represents an important unmet need.

Bfl-1 is considered an “underdog” in the Bcl-2 family, being one of the less studied anti-apoptotic proteins, but there is a growing body of evidence suggesting its value as a therapeutic target, particularly in cancers such as leukemia, lymphoma, and melanoma.^{7,8} Mcl-1 target validation is well established in a wider spectrum of cancers⁹ and shares structural and functional features with Bfl-1, along with the shared selective binding partner, Noxa.¹⁰⁻¹² The close relationship between Mcl-1 and Bfl-1 has been evaluated by phylogenetic analysis, separating the two from the other anti-apoptotic proteins.¹³ The concurrent genetic silencing of Mcl-1 and Bfl-1 led to enhanced apoptosis of melanoma cell lines, while leaving non-malignant skin cells unharmed.¹⁴ Mcl-1 and Bfl-1 have both been identified as resistant factors to other BH3 mimetics in lymphoma^{15,16} and to MAPK inhibitors in melanoma,^{17,18} which was circumvented by genetic modulation in each case. Additionally, concurrent overexpression of Mcl-1 and Bfl-1 in poorly differentiated thyroid cancers was identified to be responsible for *de novo* therapeutic resistance and was overcome with the pan Bcl-2 inhibitor, obatoclax.¹⁹ Thus, compounds that selectively target both Mcl-1 and Bfl-1 hold clinical promise in treating several types of hematological and solid cancers.

Our recent work utilizing an integrated high throughput and virtual screening approach yielded several scaffolds that showed binding to Mcl-1 and Bfl-1, including compound **19** (here referred to as **19SR**).^{20,21} Our screening strategy using the Noxa

pharmacophore to funnel high throughput hits likely selected for molecular scaffolds that display a dual Mcl-1/Bfl-1 binding profile.²¹ In this manuscript, we describe the further development of this hit molecule, **19SR**, by re-designing the chemical core structure (Figure 4.1A). The difuryl-triazine core was replaced with a 2,5-substituted aromatic benzoic acid core, allowing variable chemical functionalization possibilities. The resulting molecule **1** displayed equipotent binding to Mcl-1 and Bfl-1, with selectivity over Bcl-2 and Bcl-xL (Figure 4.1A). Guided by structural information obtained via HSQC-NMR and crystallography, the 2,5-substituted benzoic acid class of inhibitors was developed and led to compound **24** with 15-fold improved binding to both Mcl-1 and Bfl-1, while maintaining a selective profile against other anti-apoptotic proteins. The obtained biological data suggests that both Mcl-1 and Bfl-1 are selectively targeted by **24**, by binding to the endogenous proteins and inducing cell death in engineered lymphoma cells that depend on these two proteins for their survival. This class of molecules displays a Noxa-like, dual selective binding profile that provides key structural information which could lead to the development of more advanced dual Mcl-1/Bfl-1 inhibitors.

4.3 Design of a 2,5-substituted benzoic acid scaffold that inhibits Mcl-1/Bfl-1

We have recently reported a class of small molecule Mcl-1 inhibitors with a difuryl-triazine core scaffold, based on the validated hit molecule **19SR** identified by integrated high throughput and virtual screening strategy.²¹ The structure-activity relationship (SAR) studies of this series of compounds provided two important findings for their binding to the Mcl-1 protein: the conserved hydrogen bond with Arg263 formed

with one of the furan rings and substituting the amide with a flexible carbon linker. In addition to our own findings, we analyzed reported promising Mcl-1 lead compounds, in particular two distinct structural classes derived from biphenyl sulfonamide and salicylic acid cores discovered in an NMR-based fragment screen.²² Comparing these scaffolds to our difuryl-triazine core provided us with additional insights in redesigning the hit molecule **19SR**²¹ to increase the functionalization of this core and synthesize a more diverse molecule library (Figure 4.1A). These biphenyl sulfonamide and salicylic acid fragments, as well as most of the reported classes of Mcl-1 inhibitors,^{4,23–26} have a carboxylic group in their core structures which anchor them into the BH3 binding groove through the conserved hydrogen bond with the Mcl-1 Arg263 residue. Based on this well-known interaction, the triazine core was replaced with a 2,5- substituted benzoic acid and one of the furan rings was replaced with a carboxyl group to preserve and increase the strength of the essential hydrogen bond with Arg263. The 2,5- substituents were inspired from our SAR data for the difuryl-triazine analogues²¹ and the available structural information for the aryl sulfonamide and salicylic acid based inhibitors.²² Thus, the second furan ring at the position 2 of **19SR** was replaced with a phenylsulfonamide group, while the 5- thiol substituent was preserved, where the amide was replaced with a methylene linker to increase the flexibility of the substituent at this position, resulting in compound **1** (Figure 4.1A). We were pleased to determine that the new compound **1** shows equipotent binding to both Mcl-1 and Bfl-1 proteins with 2- and 3-fold improvement, respectively, in comparison with **19SR** (Figure 4.1A and Table 4.1). Importantly, compound **1** has >20-fold selectivity to Bcl-2 and Bcl-xL, with no binding observed in the tested concentrations.

The direct binding of **1** to the Mcl-1 and Bfl-1 proteins was confirmed by HSQC-NMR spectroscopy and the obtained spectra showed concentration-dependent perturbations of the backbone amide residues (Figures 4.1B and 4.1D). The analysis of the HSQC chemical shift changes of **1** in complex with Mcl-1 showed that the residues forming the Mcl-1 BH3-binding groove were primarily affected and provided strong evidence that it binds at the same site where the conserved BH3-only proteins interact with the Mcl-1 protein. To gain structural understanding of the ligand-protein interactions, we predicted the binding model of **1** in complex with Mcl-1 by molecular docking. The predicted model revealed that the phenethylthio moiety occupies the p2 pocket and participates in hydrophobic interactions with the Leu267, Val253, Val243 and Leu235 residues (Figure 4.1C), which showed significant chemical shift perturbations (Figure 4.1B). The carboxyl group forms a hydrogen bond with the Arg263, mimicking the conserved aspartate in the pro-apoptotic BH3 only proteins, confirmed by the HSQC-NMR spectrum of the Mcl-1:1 complex where Arg263 showed a significant chemical shift perturbation. The predicted model showed that the phenylsulfonamide is placed above the p3 pocket, making weak interactions with Thr266, Ala277, and Phe228 (Figure 4.1C). In a similar way, the HSQC-NMR studies with the Bfl-1 protein showed that compound **1** binds to Bfl-1 through several key residue perturbations (Figure 4.1D). Along with a noticeable shift of Arg88, which corresponds to Arg263 of Mcl-1, the residues from the hydrophobic p2 pocket displayed significant perturbations, including Ala94, Phe95, and Ile98, as well as additional identified shifts by Val44 and Lys46 on the α 3 helix. The docking model of compound **1** to Bfl-1 (Figure 4.1E) predicts similar binding as to Mcl-1, with the 5-phenethylthio

moiety occupying the p2 pocket and interaction with Arg88 through the acid group. The phenylsulfonamide substituent appears to be pointed toward the α 4 helix and solvent exposed. Taken together, biophysical HSQC-NMR experiments in combination with *in silico* docking studies strongly suggest that compound **1** binds to the BH3-binding groove of both the Mcl-1 and Bfl-1 proteins.

This dual selective binding profile of compound **1** matches that of the endogenous pro-apoptotic Noxa protein, which also selectively binds only Mcl-1 and Bfl-1. Importantly, the hit molecule **19SR**, based on which the compound **1** was designed, was identified in our integrated screening approach using the Noxa BH3 labeled peptide,²¹ demonstrating that using the Noxa pharmacophore contributed in selecting compounds with molecular scaffolds that display a dual Mcl-1/Bfl-1 binding profile. Since Bfl-1 is an emerging therapeutic target and there is an unmet need for small molecules that inhibit this protein, we sought to further explore the SAR of its inhibition together with Mcl-1.

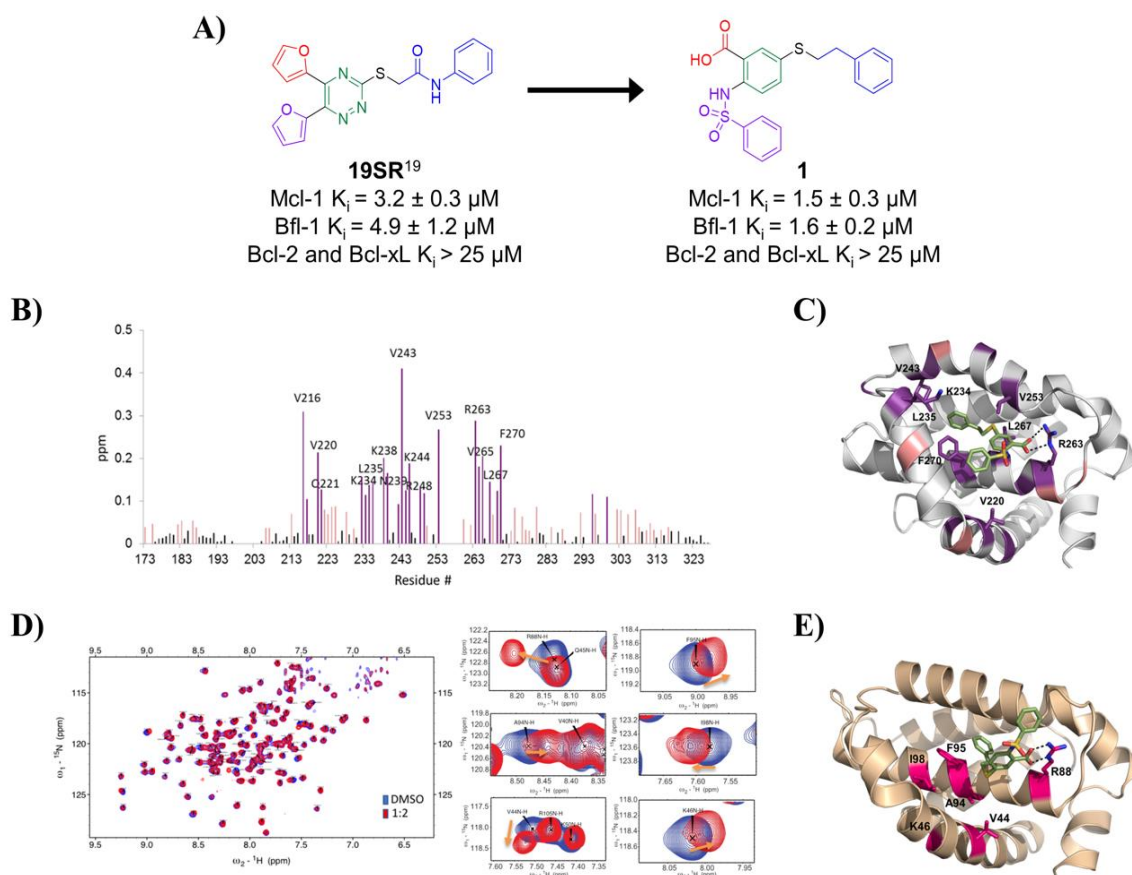


Figure 4.1 Compound 1 design and HSQC-NMR guided binding mode to Mcl-1/Bfl-1

A) Chemical structures and binding affinity of compounds **19SR²¹** and **1**, against Bcl-2 family anti-apoptotic proteins (distinct structural features color coded). **B)** HSQC-NMR chemical shift perturbations of Mcl-1 residues in the presence of **1**. **C)** Predicted binding pose of **1** in the BH3 binding site of Mcl-1 (PDB ID: 4HW2 was used for docking); key residue shifts highlighted corresponding to shift intensity noted in HSQC-NMR experiments. **D)** Superimposed ¹⁵N-HSQC spectra of Bfl-1 in the absence (blue) and presence (red) of compound **1** with close up view of select residue shifts. **E)** Predicted binding pose of **1** to Bfl-1 (PDB ID: 3MQP used for docking) with highlighted residues shifted in HSQC-NMR spectra.

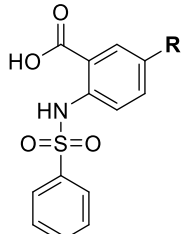
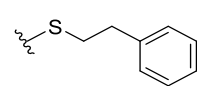
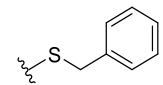
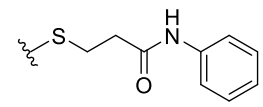
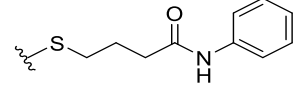
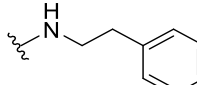
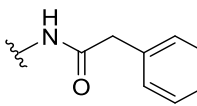
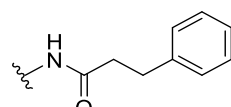
4.4 SAR of novel Mcl-1/Bfl-1 dual inhibitors

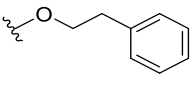
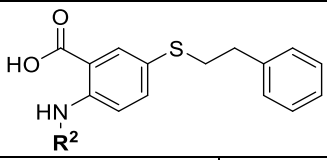
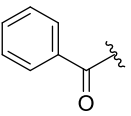
The first series of compounds was synthesized to explore the importance and binding affinity contribution of the 5-phenethylthio (R^1) and 2-phenylsulfonamide (R^2) substituents to the Mcl-1 and Bfl-1 proteins (Table 4.1). Deletion of the phenethylthio substituent in compound **2** resulted in an over 30- and 60-fold decrease in binding affinity to Mcl-1 and Bfl-1, respectively, demonstrating that this group significantly

contributes to the Mcl-1/Bfl-1 binding potency. These findings are consistent with the predicted binding model showing that the phenethylthio substituent is accommodated into the p2 pockets of both Mcl-1 and Bfl-1, maintaining a network of hydrophobic interactions (Figures 4.1C and 4.1E). One carbon reduction of the aliphatic chain at the R¹ position to a phenyl methylthio substituent resulted in compound **3** with similar binding affinities to Mcl-1 and Bfl-1. Several compounds were synthesized to investigate the importance of the ethylthio linker, its length and nature. Reducing the flexibility of the ethyl chain by introducing an amide group in compound **4**, resulted in 10-fold decreased binding to both, Mcl-1 and Bfl-1, consistent with the SAR studies of the difuryl-triazine series, based on the **19SR** hit molecule.²¹ Extending the carbon chain in compound **5** resulted in further significant decreases in binding to both Mcl-1 and Bfl-1. Replacement of the sulfur with an amine linker, as in **6**, resulted in a 6-fold loss in binding to Mcl-1. Replacing the sulfur with an amide linker having different carbon chain lengths, as in **7** and **8**, resulted in a substantial loss of binding affinity to Mcl-1 and an even greater loss in Bfl-1 binding. Furthermore, a 5- ether analogue was synthesized to compare against the sulfur and amine linked compounds to find that compound **9** displayed a 4- and 6-fold affinity decrease for Mcl-1 and Bfl-1, respectively. Importantly, deletion of the R² phenylsulfonamide substituent in compound **10** or changing the sulfonamide to an amide linker in compound **11** did not have significant effect on binding (Table 4.1). These results together with the predicted binding model demonstrate the importance of the phenethylthio substituent in preserving the carbon chain length and its flexibility, as well as keeping the sulfur linker at the 5- substitution site of the core benzoic acid. In

addition, it seems that the sulfur linker is necessary to preserve equipotent binding to Mcl-1/Bfl-1, as the affinities deviate when a direct amide linker is used (**7** and **8**).

Table 4.1 SAR of 2-,5-substituents of benzoic acid core

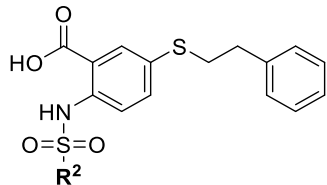
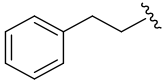
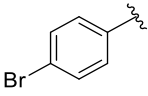
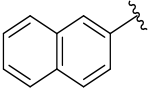
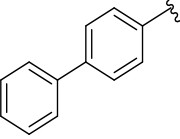
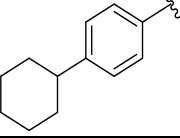
			
Compound	R ¹	Mcl-1 K _i (μM)	Bfl-1 K _i (μM)
1		1.5 ± 0.3	1.6 ± 0.2
2	H	47.8 ± 3.9	>100
3		2.6 ± 0.4	3.0 ± 0.4
4		13.1 ± 2.4	14.8 ± 2.7
5		32.8 ± 4.9	>70
6		4.7 ± 0.7	3.8 ± 1.1
7		70.4 ± 5.4	>70
8		19.0 ± 1.2	62.0 ± 1.8

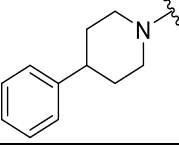
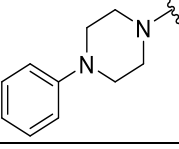
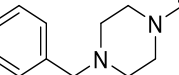
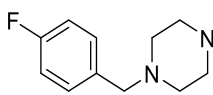
9		6.1 ± 1.0	10.6 ± 1.2
			
Compound	R²	Mcl-1 K_i (μM)	Bfl-1 K_i (μM)
10	H	3.4 ± 0.4	3.7 ± 0.4
11		2.7 ± 0.6	4.6 ± 0.5

Based on these results, we synthesized a series of inhibitors where the R¹ phenethylthio group was fixed at the 5- position and proceeded to probe the SAR of the substituents at the R² position (Table 4.2). Extending the phenyl group away from the sulfonamide linker by two carbons (compound **12**) resulted in no changes in binding affinity. Bioisosteric replacement of the phenyl group with the thiophene moiety, as in **13**, gave a similar Mcl-1 binding affinity with a 2-fold decrease in Bfl-1 binding. Introducing a small hydrophobic substituent at the *para* position of the phenyl ring, such as bromine in compound **14**, led to a 2-fold improvement over **1**, alluding to the possibility of introducing more hydrophobicity at this site. Indeed, substituting the phenyl for a bulkier naphthalene ring resulted in compound **15**, with 6- and 3- fold increases in binding potency to Mcl-1 and Bfl-1, respectively. Introducing a biphenyl substituent in compound **16**, which was beneficial in our previously reported series of Mcl-1

inhibitors,²³ proved again to be a favorable moiety for targeting these protein-protein interactions (PPIs) and led to 15-fold improvements in binding affinity to Mcl-1 ($K_i = 0.09 \pm 0.02 \mu\text{M}$), as well as to Bfl-1 ($K_i = 0.15 \pm 0.02 \mu\text{M}$). Replacing the distal phenyl ring with a saturated cyclohexyl group in compound **17** resulted in similar potent binding to both Mcl-1 and Bfl-1 ($K_i = 0.087 \pm 0.03 \mu\text{M}$ and $K_i = 0.15 \pm 0.03 \mu\text{M}$, respectively).

Table 4.2 SAR of 5-(phenethylthio)-2-(arylsulfonamido)benzoic acid compounds

			
Compound	R ²	Mcl-1 K _i (μM)	Bfl-1 K _i (μM)
12		1.7 ± 0.5	1.7 ± 0.3
13		2.0 ± 0.2	3.4 ± 0.3
14		0.81 ± 0.2	0.81 ± 0.2
15		0.22 ± 0.03	0.57 ± 0.1
16		0.090 ± 0.02	0.15 ± 0.02
17		0.087 ± 0.03	0.17 ± 0.04

18		0.20 ± 0.04	0.28 ± 0.05
19		0.33 ± 0.06	0.39 ± 0.1
20		0.57 ± 0.1	0.76 ± 0.1
21		0.84 ± 0.1	1.0 ± 0.2
22		0.77 ± 0.2	0.90 ± 0.2

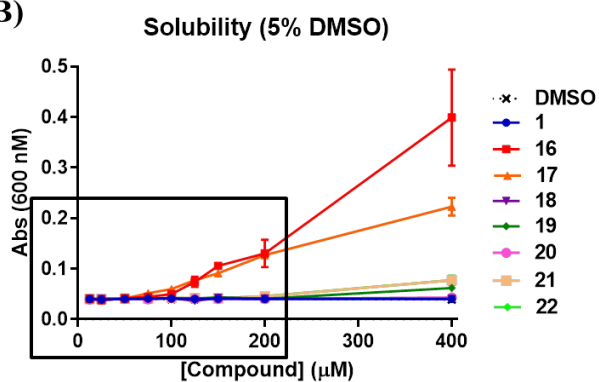
It is well known that anti-apoptotic proteins, including Mcl-1 and Bfl-1, have a prominent hydrophobic groove, thus it is required for ligands to have high lipophilicity to achieve potent affinity to the BH3 binding site. However, compounds with high binding affinity that is primarily driven by lipophilic interactions are likely to be less selective, with potential off-target effects and toxicity. Replacing flat aromatic rings with 3D heteroatom containing rings has been shown to improve many qualities of small molecules, including increasing solubility and decreasing promiscuity.^{27,28} In an effort to balance the lipophilic properties of the newly designed dual inhibitors, and improve physicochemical properties, the R² proximal phenyl ring in **16** was replaced with the heterocyclic pyridine (**18**), piperidine (**19**), and piperazine (**20**) moieties. Compounds **18** and **19** both displayed slightly decreased binding affinities, but improved aqueous solubility compared to **16** (Figure 4.2). Compound **20** showed a 5- to 6-fold decrease in

binding to Mcl-1 and Bfl-1, compared to **16**, which can be explained by the presence of hydrophilic piperazine in the predominantly hydrophobic environment of the Mcl-1 binding pocket. Introducing a methylene spacer between the piperazine moiety and the phenyl substituent in compound **21** and a *para*-fluoro-phenyl derivative, **22**, showed similar binding affinities to Mcl-1 and Bfl-1 as the parent compound **20**. Importantly, as expected, compounds **20** and **22** showed improved solubility and calculated physicochemical properties in comparison with **16** and **17** (Figure 4.2). This improved solubility allowed us to successfully obtain complex structures with the Mcl-1 protein, discussed below.

A)

Compound	cLogP (ChemDraw)	cLogP (DataWarrior)	cLogS (DataWarrior)	Experimental Turbidity Range (μM)
1	5.82	3.85	-5.17	>400
16	7.74	5.51	-7.26	100-125
17	8.47	5.99	-6.94	75-100
18	7.38	4.60	-6.16	>400
19	7.14	5.19	-6.15	>400
20	6.26	3.89	-5.37	>400
21	4.28	2.89	-4.86	>400
22	4.42	2.99	-5.17	>400

B)



C)

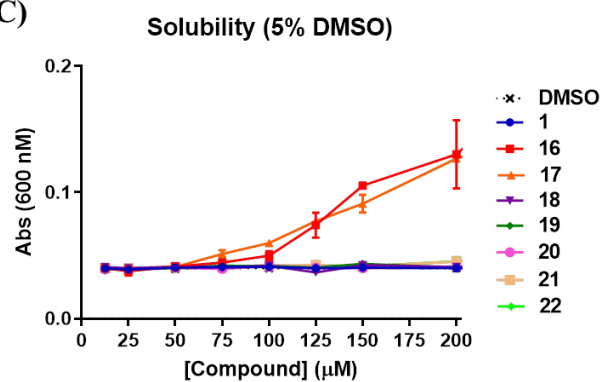
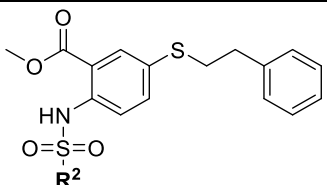
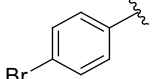
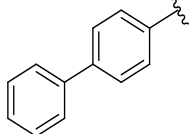
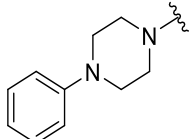


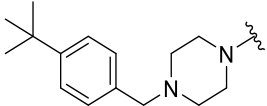
Figure 4.2 Physicochemical evaluation of dual inhibitors

A) Select compounds from **Table 2** and their associated cLogP (ChemDraw and DataWarrior), cLogS (DataWarrior), and experimentally determined turbidity ranges. **B)** Curves from turbidity assay to identify maximum aqueous solubility of compounds. **C)** Zoomed in section from box shown in **B)** to identify more accurate loss of solubility. Turbidity range determined by identifying the inflection point where absorbance significantly deviates from DMSO control.

To verify the importance of the carboxyl acid interaction with the conserved Arg263 and Arg88 residues on Mcl-1 and Bfl-1, respectively, we tested several esterified analogues of compounds in Table 4.2 and as expected no binding was observed to both Mcl-1 and Bfl-1 at the tested concentrations (Table 4.3).

Table 4.3 Mcl-1 and Bfl-1 binding of methyl ester analogues

			
Compound	R ²	Mcl-1 K _i (μM)	Bfl-1 K _i (μM)
30a		>80	>70
30g		>80	>70
30h		>80	>70
30j		>80	>70
30n		>80	>70

30r		>80	>70
-----	---	-----	-----

4.5 Co-crystallography and structure-based design of optimized inhibitors

To drive further development of these inhibitors and provide structural insight into their binding modes, co-crystal structures of **20** and **22** bound to Mcl-1 were solved to 2.55 Å and 2.10 Å resolution, respectively (Figure 4.3). The plasticity of the Mcl-1 BH3 binding site has been noted in previous studies which illustrate its ability to change conformation upon ligand binding, forming a deeper p2 pocket.^{22,24,29} Mcl-1 conformational changes induced by binding of compounds **20** and **22** were compared to the apo-MBP-Mcl-1 (PDB ID: 4WMS) protein (Figure 4.3A). The structures were aligned to **22** by the SSM algorithm in Coot,³⁰ providing root mean square deviations (RMSD) of 1.193 Å for apo and 0.775 Å for **20**. The most notable difference between the aligned structures is the position of the α 4 helix (Figure 4.3A). The displacement of this helix widens the canonical BH3 binding groove to accommodate the ligand in the hydrophobic p2 pocket.²⁴ Both compounds **20** and **22** have an anchoring hydrogen bond between their carboxyl group and the Arg263 side chain of Mcl-1, mimicking the interaction observed between Arg263 and the conserved aspartic acid in pro-apoptotic proteins (Figure 4.3B).

The aromatic 2,5-substituted benzoic acid core is oriented perpendicular in the junction between the p2 and p3 pockets within the BH3 binding groove. The R² piperazine-containing substituents in compounds **20** and **22** occupy the p2 hydrophobic binding pocket, while the phenethylthio moiety is directed towards the p1 pocket. The

phenylpiperazine-sulfonamido substituent in **20** interacts with the side chains of Leu267 and Val253 from the p2 pocket and Leu235 from the p1 pocket through hydrophobic interactions with the distal phenyl group. The addition of the CH₂ linker in the R² substituent of **22** provides additional length and flexibility of the terminal 4-fluoro phenyl moiety, placing it deeper in the p2 binding site in comparison with **20**, and forming hydrophobic interactions with the side chains of Phe270, Met250, and Leu290. The R¹ phenethylthio moiety in both complexes is found near the α 3 helix and has hydrophobic interactions with Met231, Leu235, and Val253 (Figure 4.3B). π - π stacking of the two distal phenyl groups in **20** help stabilize its folded conformation. These structural findings validate the vital Mcl-1 binding features of hydrogen bonding with Arg263 and occupancy of the p2 hydrophobic pocket, which provide insights into further optimization.

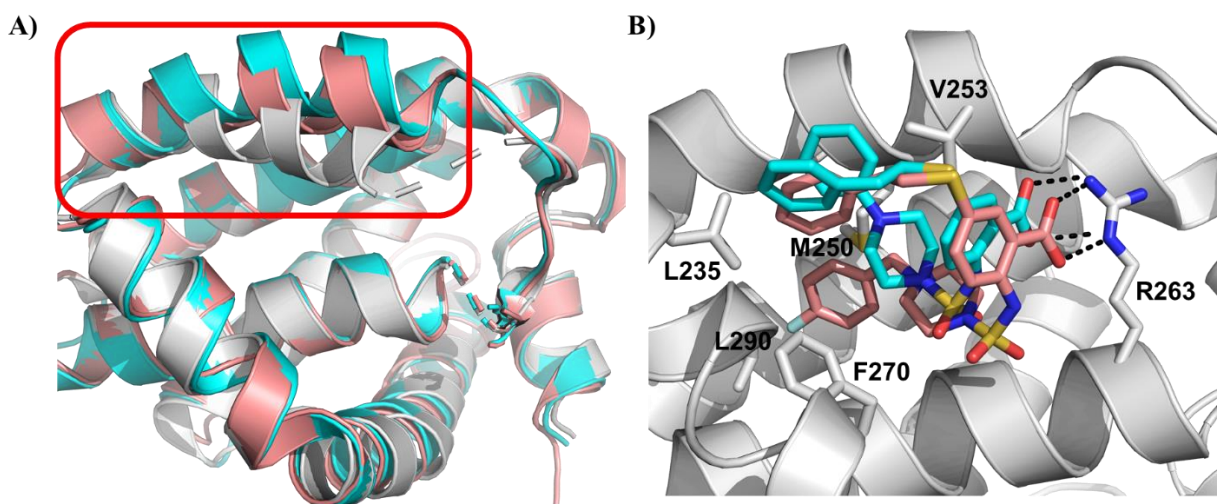
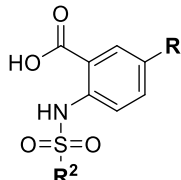
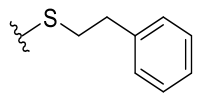
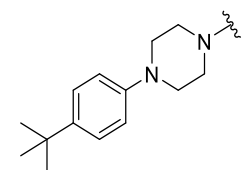
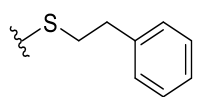
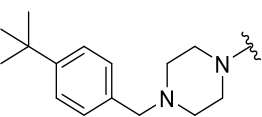


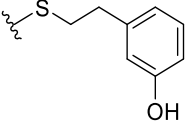
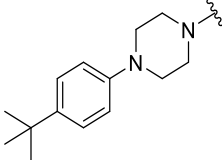
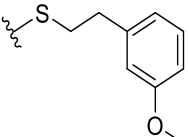
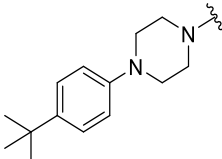
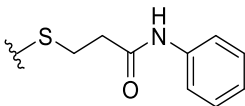
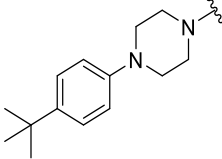
Figure 4.3 Co-crystal structures of compounds **20 and **22** with Mcl-1**

A) Overlay of the C α traces of Mcl-1 in complex with **20** (PDB ID: 6U64) (cyan), **22** (PDB ID: 6U65) (pink), and apo-MBP-Mcl-1 (PDB ID: 4WMS) (gray) depicting movement in the α 4-helix (circled in red) upon ligand binding. X-ray crystallography complex of Mcl-1 with compounds **B)** **20** (cyan) and **22** (pink). The side chains of selected interacting Mcl-1 residues are labeled and dashed lines represent hydrogen bonds.

Based on the experimentally determined binding modes of these inhibitors and knowing that optimal occupancy of the p2 hydrophobic pocket is essential for improved binding affinity to Mcl-1 protein,²⁴ compounds **23** and **24** were synthesized by introducing a bulky *tert*-butyl group in the *para* position on the distal phenyl group of the R² substituent (Table 4.4). Indeed, both compounds, **23** and **24**, displayed an 8-fold increase in the binding affinity to Mcl-1 with K_i values of 73 nM and 94 nM, respectively, compared to their counterparts **20** and **21**, which lack the *tert*-butyl. Importantly, tighter binding affinities of **23** and **24** were also determined for Bfl-1 protein with K_i values of 84 nM and 100 nM, respectively. Similar improvement was also identified in comparison with **22** which has a fluorine at the same position. This finding confirmed the importance of the hydrophobic interactions in the p2 pocket and optimizing its occupancy.

Table 4.4 Optimized dual inhibitors with terminal R² *tert*-butyl moiety

				
Compound	R ¹	R ²	Mcl-1 K _i (μM)	Bfl-1 K _i (μM)
23			0.073 ± 0.02	0.084 ± 0.04
24			0.094 ± 0.01	0.10 ± 0.02

25			0.29 ± 0.01	0.25 ± 0.05
26			0.074 ± 0.01	0.10 ± 0.04
27			0.95 ± 0.08	1.1 ± 0.4

To further validate the direct binding of compounds **23** and **24** to the Mcl-1 and Bfl-1 proteins, we employed the biophysical method of bio-layer interferometry (BLI). Using immobilized biotin-labeled anti-apoptotic proteins, **23** and **24** were tested and demonstrated dose dependent binding against Mcl-1 with K_d values of 490 nM and 670 nM, respectively, calculated by using steady state analysis (Figures 4.4A and 4.4B). Compounds **23** and **24** gave similar K_d values for Bfl-1, 920 nM and 1,270 nM, respectively (Figures 4.4C and 4.4D). To support the FP obtained SAR data, compound **22**, with about 9-fold weaker binding affinity to both proteins (Table 4.2), showed similar decrease in the K_d values determined by BLI (Figures 4.4E and 4.4F).

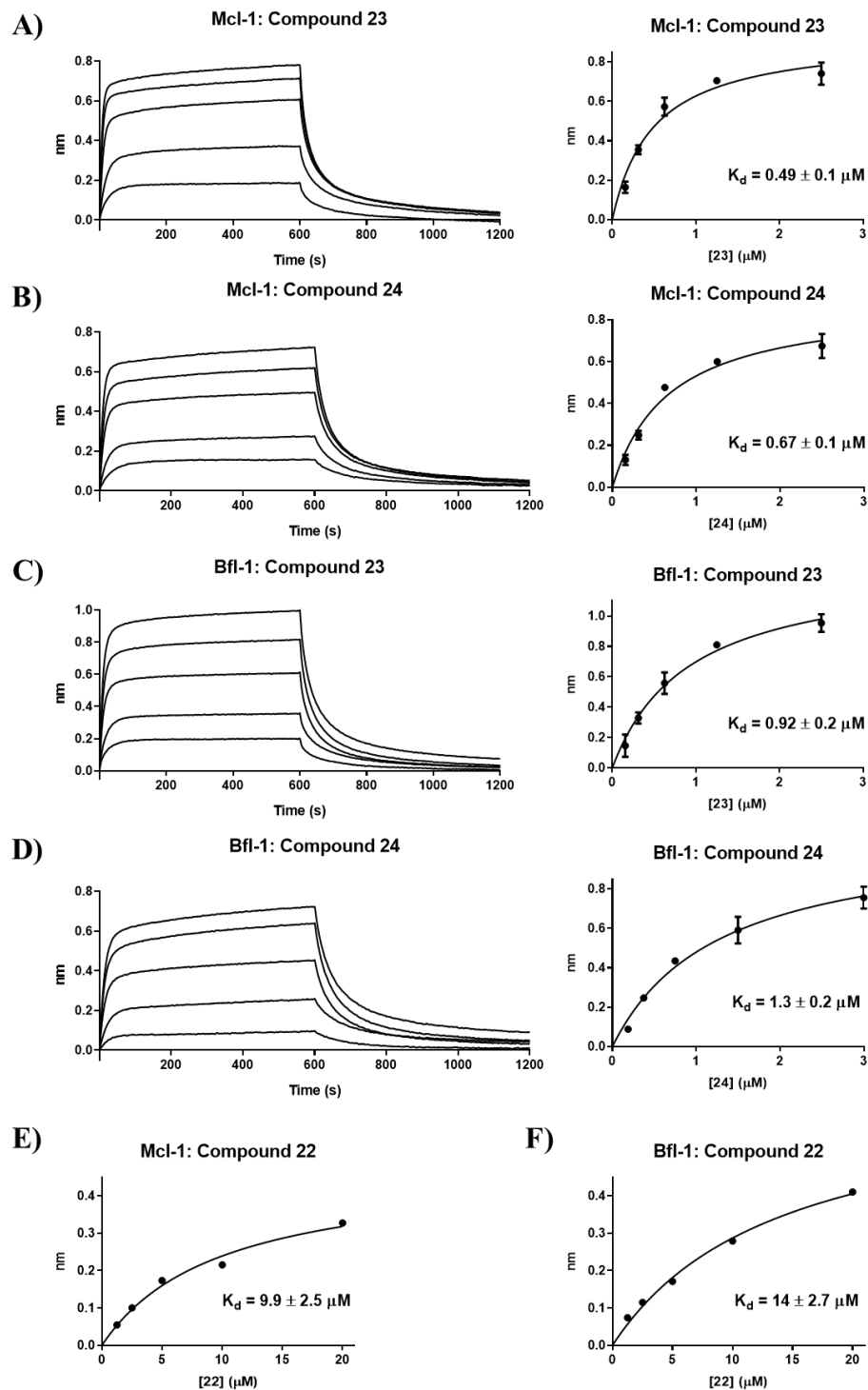


Figure 4.4 Binding affinity determination by BLI

Sensorgrams and steady state plots for Mcl-1 binding with compounds **A) 23** (2.5, 1.25, 0.625, 0.3125, and 0.156 μM) and **B) 24** (2.5, 1.25, 0.625, 0.3125, and 0.156 μM). Corresponding sensorgrams and steady state plots for Bfl-1 binding with compounds **C) 23** (2.5, 1.25, 0.625, 0.3125, and 0.156 μM) and **D) 24** (3, 1.5, 0.75, 0.375, and 0.1875 μM). Steady state plots of compound **22** (20, 10, 5, 2.5, and 1.25 μM) binding to **E) Mcl-1** and **F) Bfl-1**. K_d values were calculated from steady state analysis. Figures are representative of ≥ 3 independent experiments.

We successfully obtained the crystal structure of compound **24** in complex with Mcl-1 (Figure 4.5A), showing a similar binding pose as **22**, with the Arg263-carboxyl group interaction acting as the main anchoring point and aromatic scaffold interacting with Met231. The *tert*-butyl phenyl moiety is deeply accommodated into the p2 pocket, which becomes larger and more opened in complex with **24**. The *tert*-butyl group forms hydrophobic interactions with the side chains of Met250, Ile237, Val243 and Leu290, while the phenyl group interacts with the Phe270 which constitutes the bottom of the p2 pocket. Overall the *tert*-butyl phenyl group shifts towards the α 4 helix and distorts it between residues 245-247. The R¹ phenethylthio substituent is directed towards the p1 pocket and the distal phenyl ring makes hydrophobic interactions with Leu235, leading to opening and merging of the p1 and p2 pockets.

To investigate the contribution and interactions of the R¹ substituent, several compounds were synthesized by modifying the distal phenyl ring as well as the flexibility of the methylene linker. Adding a polar hydroxyl group on the R¹ phenethylthio substituent illustrates the necessity to preserve hydrophobicity at this site, as compound **25** gives a 3- to 4- fold decrease in binding affinity. Methylation of the phenolic hydroxyl group in **26** restored the binding, confirming the unfavorable interactions of the polar hydroxyl group. Furthermore, we tested the importance of the linker geometry of the R¹ substituent. Introducing an amide linker in compound **27** resulted in more than a 10-fold decrease in the binding affinity against both Mcl-1 and Bfl-1. We successfully solved the complex structure of **27** with the Mcl-1 protein (Figure 4.5B). This binding pose is very similar to the Mcl-1:**24** co-crystal structure, showing the Arg263-carboxyl group interaction and the *tert*-butyl phenyl piperazine moiety deeply accommodated in the p2

pocket, forming the hydrophobic interactions with Val243, Leu246 and Leu290 residues. However, the thioethylamide phenyl substituent is solvent exposed and lacks interactions with the p1 pocket. These results confirm the contribution of the R¹ substituent by directly interacting with the Mcl-1 protein, as well as partially stabilizing of the folded conformation of these inhibitors by the π - π stacking between the two distal phenyl groups in the R¹ and R² substituents.

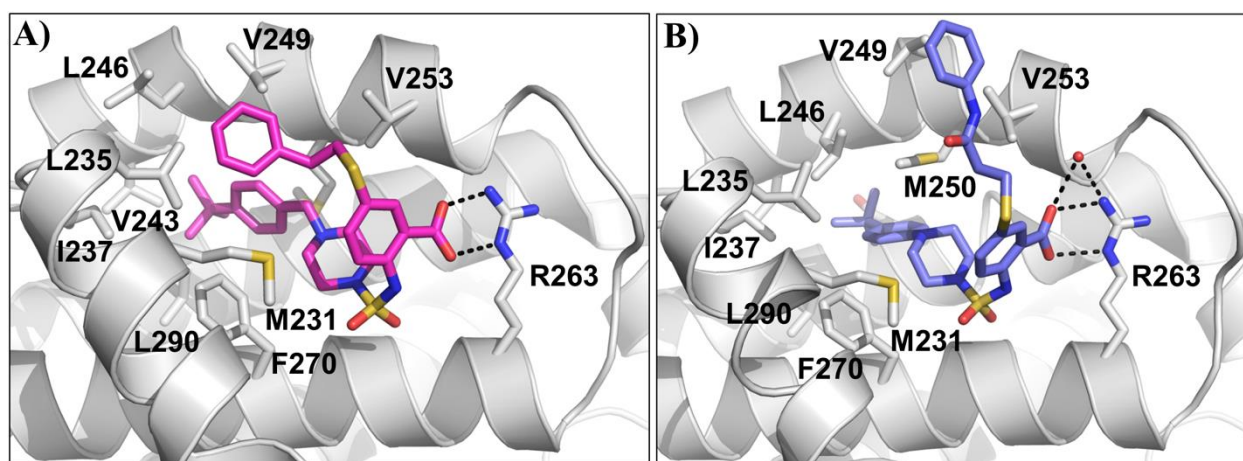


Figure 4.5 Co-crystal structures of compounds 24 and 27 bound to Mcl-1

A) Mcl-1:24 x-ray complex structure (PDB ID: 6U6F). **B)** Mcl-1:27 x-ray complex structure (PDB ID: 6U67), water molecule involved in hydrogen binding appears as a red sphere. Key residues on protein are labeled and hydrogen bonds depicted as black dashed lines.

4.6 Elucidation of dual inhibitors binding to Bfl-1 by HSQC-NMR and docking

Recently, the apo-Bfl-1 structure, as well as complex structures of Bfl-1 and BH3 peptides have been reported.^{31,32} The alignment of the Bfl-1 structures bound to peptides available in the PDB database shows a predominantly uniform conformation of the targeted binding site (Figure 4.6A). As members of the Bcl-2 protein family, Mcl-1 and Bfl-1 contain four BH domains with conserved tertiary structure forming the canonical hydrophobic BH3 binding site where the pro-apoptotic proteins bind.³³ The

structures of apo Bfl-1 and Mcl-1 are largely similar, although Mcl-1 and Bfl-1 display marginal overall sequence identities of approximately 20%. The alignment of the Mcl-1 structure with the Bfl-1 protein showed that the highest degree of sequence similarity is found in their BH3 binding pocket, with several corresponding Mcl-1/ Bfl-1 residue pairs involved in interactions with BH3 domain and inhibitors, including Arg263/Arg88, Met250/Met75, Val274/Leu99 and Phe270/Phe95, indicated comparable overall topology of both binding sites (Figure 4.6B). The most conserved region identified in the loop between α 4 and α 5 (residues 81-84 in Bfl-1 and 256-259 in Mcl-1) and the N-terminus of helix α 5 (residues 85-91 in Bfl-1 and 260-266 in Mcl-1). In addition, the size of the BH3-binding pocket is very similar in apo structures of Mcl-1 and Bfl-1. However, as it was established from numerous Mcl-1 protein crystallography studies, including experiments presented in this work, the amino acid conformations in Mcl-1 binding pocket can be greatly affected by the ligand binding, in particular the α 4 helix adjusted its side chain conformations in response to different binding partners (Figure 4.3A). Thus, a similar conformational change of the Bfl-1 BH3 binding site can also be predicted upon ligand binding. Indeed, a recently reported complex structure of a stapled peptide inhibitor displayed a conformational change upon binding in comparison with the apo-structure by opening the binding groove by displacement of α 2, α 3 and α 4 helices.³¹ Thus, it was not surprising when in our first docking attempts using the complex structure of Noxa BH3 peptide bound to Bfl-1 (PDB ID: 3MQP), we were not able to obtain reasonable binding modes. In order to take the conformational change of the protein into consideration, we used our co-crystal structure of the Mcl-1 in complex with compound **24** and aligned it with the Noxa-bound Bfl-1 protein (PDB ID: 3MQP). In

this way we determined the initial coordinates and conformation of compound **24** bound to the Bfl-1 protein, followed by energy minimization of the produced complex. After the minimization, the most notable conformational change observed was the side chain movements of the Phe71, Met75, and Phe95 residues, which enabled a wider opening of the Bfl-1 p2 pocket to accommodate the compound (Figure 4.6C). Subsequent redocking of compounds **23** and **24** into the resulted Bfl-1 structure, followed by minimization, provided the predicted binding mode, displayed in Figure 4.7A. The predicted binding of compounds **23** and **24** resembles poses observed in the Mcl-1 co-crystal complex structures with other inhibitors from this series. As expected, Arg88 served as the main anchoring residue. In a similar way, the R² substituent was predicted to be buried deep into the Bfl-1 p2 pocket through a network of hydrophobic interactions. The *tert*-butyl group makes contacts with Val122, Ala67, Ile118, Phe121, and Leu99, and the distal phenyl group with Phe71, Ile92 and Phe95. Interestingly the R¹ phenethylthio moiety was oriented towards the α 4 helix of the BH3 binding groove for both compounds **23** and **24**, making hydrophobic interactions between the side chain methylene groups of Lys77 and the distal aromatic ring. The predicted models of Bfl-1 in complex with compounds **23** and **24** suggest that the ligands can accommodate the BH3 pocket by rotating certain binding-site side-chains leading to the opening of a hydrophobic cavity in particular the p2 pocket (Figure 4.7A).

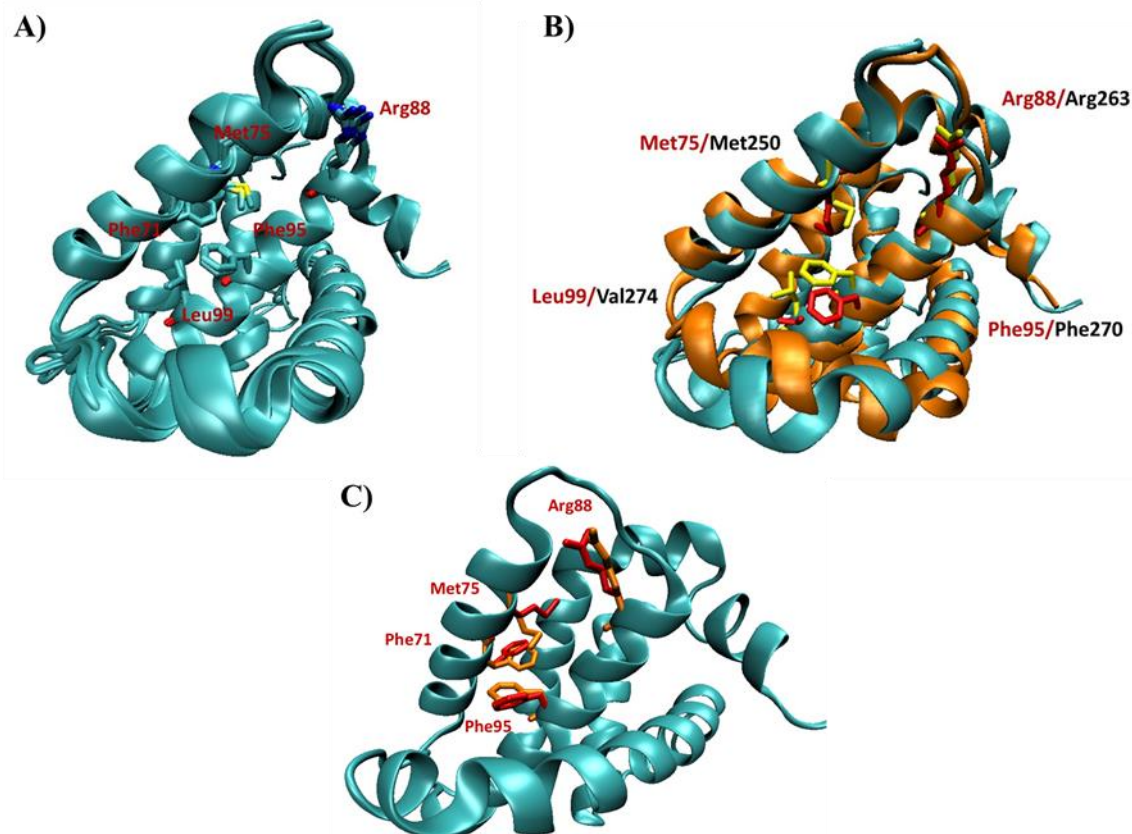


Figure 4.6 Bfl-1 protein alignments and minimization

A) Alignment of several available Bfl-1 crystal structures with outlined residues (PDB IDs: 3MQP, 6MBB, 5UUK, 5WHH). **B)** Alignment of Bfl-1 crystal structure conformation bound with Noxa (PDB ID: 3MQP), protein shown in green and residues in red, and Mcl-1 crystal structure also bound to Noxa (PDB: 2NLA) with protein shown in orange and residues in yellow. **C)** Observed movement of the sidechains in the Bfl-1 crystal structure (PDB ID: 3MQP) after minimization with the placed initial conformation of compound **24** in the BH3 binding site. The original positions of the marked amino acid residues are shown in orange and the new positions after minimization are shown in red.

Currently there are no reported co-crystal structures of the Bfl-1 protein with small molecules in the literature. Our attempts to determine the complex structure between our inhibitors and Bfl-1 were unsuccessful. Thus, we proceeded with Bfl-1 HSQC-NMR studies to provide further evidence to support the molecular docking and predicted binding mode of the analogues in this series. We were successful in obtaining HSQC-NMR data demonstrating that compound **23** binds and interacts with Bfl-1 protein (Figure 4.7B). By performing a titration of different concentration ratios between

compound **23** and the Bfl-1 protein, we identified key residue perturbations that substantiate our evidence of Bfl-1 binding. The important anchoring hydrogen bond interaction with Arg88 was confirmed by chemical shifts with this residue, along with Phe95 and Ala94 in the p2 pocket. Future structural studies of Bfl-1 in complex with these compounds are needed in order to provide in-depth and empirical insights into how this class of inhibitors bind Bfl-1.

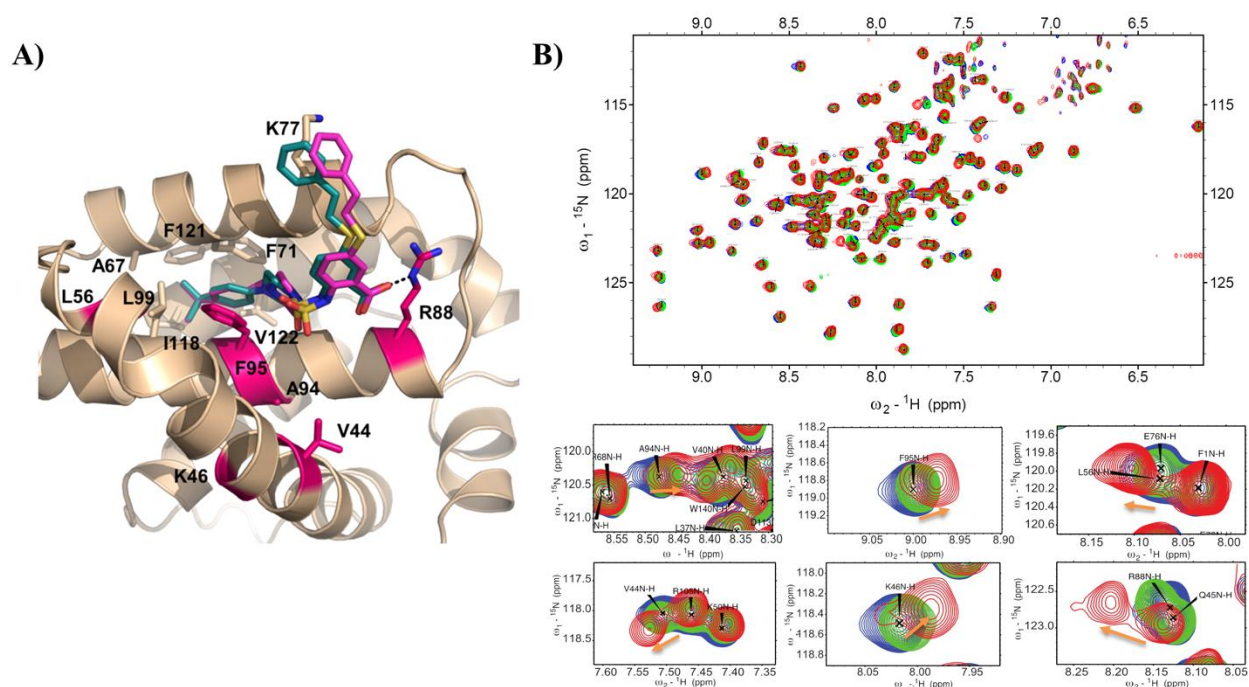


Figure 4.7 HSQC-NMR and docking of optimized compounds with Bfl-1

A) Docking model of compounds **23** and **24** to Bfl-1 (PBD ID: 3MQP was used for docking); residues with chemical-shift perturbations upon **23** binding are highlighted in red. **B)** Superposition of ^{15}N HSQC spectra of labeled Bfl-1, free and in complex with compound **23** in different ratio (DMSO = blue; 1:1 = green; 1:2 = red). Close up view of select residues with noticeable chemical shifts.

4.7 Binding selectivity to anti-apoptotic Bcl-2 family proteins

The overall goal of the design and development of these inhibitors was to have molecules that bind to Mcl-1 and Bfl-1 with selectivity over Bcl-2 and Bcl-xL. Several key

inhibitors were tested for binding against the homologous Bcl-2 and Bcl-xL anti-apoptotic proteins (Table 4.5). The initially designed molecule **1** displayed substantial selectivity with K_i values for Bcl-2/Bcl-xL greater than 25 μ M. Optimized compounds **15**, **20**, and **27** maintained at least 10-fold selectivity, while **22** gave K_i values for Bcl-2/Bcl-xL greater than 25 μ M. Along with the increase in potency for Mcl-1/Bfl-1, compounds **23** and **26** maintained at least a 15-fold selectivity over Bcl-2/Bcl-xL. Compound **24** displayed the greatest selectivity window with K_i values against Bcl-2 and Bcl-xL both being greater than 25 μ M and was selected for further biological evaluation.

Table 4.5 Binding selectivity to anti-apoptotic proteins

Compound	Mcl-1 K_i (μM)	Bfl-1 K_i (μM)	Bcl-2 K_i (μM)	Bcl-xL K_i (μM)
1	1.5 \pm 0.3	1.6 \pm 0.2	>25	>25
15	0.22 \pm 0.03	0.57 \pm 0.1	5.6 \pm 0.7	5.2 \pm 1.1
20	0.57 \pm 0.1	0.76 \pm 0.1	11.7 \pm 3.1	6.6 \pm 1.1
22	0.77 \pm 0.2	0.90 \pm 0.2	>25	>25
23	0.073 \pm 0.02	0.084 \pm 0.04	1.2 \pm 0.4	3.5 \pm 0.5
24	0.094 \pm 0.01	0.10 \pm 0.02	>25	>25
26	0.074 \pm 0.01	0.10 \pm 0.04	1.2 \pm 0.5	6.7 \pm 1.6
27	0.95 \pm 0.08	1.1 \pm 0.4	16.1 \pm 0.9	>25

4.8 Biological evaluation of dual inhibitors

The data presented thus far was focused on binding to recombinant proteins and in order to validate the engagement of Mcl-1 and Bfl-1 in more biologically relevant systems, we moved into cell-based studies. To confirm the endogenous target engagement and PPI disruption capabilities of this class of inhibitors, we employed a biotin-streptavidin pull down assay using a biotin-labeled Bim peptide (BL-Bim) and

whole cell lysate from the M14 melanoma cell line. The M14 cell line was used as it contains high endogenous levels of all anti-apoptotic proteins, particularly Bfl-1, and melanoma cell lines in general are known to display functional dependence on Mcl-1 and Bfl-1.^{14,34} As shown in Figure 4.8A, Mcl-1 and Bfl-1 were pulled down by BL-Bim and the unlabeled Bim peptide served as a positive control to disrupt interactions of BL-Bim and the anti-apoptotic proteins. Incubation with 100 μ M of compound **24** resulted in complete disruption of Mcl-1 and Bfl-1 complexes with BL-Bim, while incubation with 100 μ M of its methyl ester analogue, **30r**, didn't show any effect, consistent with the FP binding data (Figure 4.8A and Table 4.3). The dose dependent and selective PPI disruption capabilities of compound **24** were also evaluated by the pulldown assay (Figure 4.8B). Compound **24** induced dose-dependent disruption of BL-Bim:Mcl-1 and BL-Bim:Bfl-1 interactions, while leaving BL-Bim complexes with Bcl-2 and Bcl-xL unaffected. Compound **23** was also evaluated under these same pulldown assay conditions and demonstrated equivalent potency and selectivity by binding to endogenous Mcl-1 and Bfl-1 and disrupting interactions with BL-Bim BH3 peptide (Figure 4.8C). These results validate the ability of this class of inhibitors to bind endogenous Mcl-1 and Bfl-1 and selectively disrupt PPIs.

The target selectivity of compound **24** was further confirmed using the reported E μ -Myc lymphoma cell lines, which were engineered to overexpress individual anti-apoptotic Bcl-2 proteins with a strong survival dependence on these targets, which makes them excellent tools for testing and characterizing inhibitors of Bcl-2 family proteins.³⁵ Lymphoma cells overexpressing Mcl-1, Bfl-1, Bcl-2, or Bcl-xL were treated with **24** at various concentrations and analyzed for cell death by flow cytometry. E μ -Myc

cells overexpressing Mcl-1 and Bfl-1 showed dose-dependent increase in cell death in response to compound **24** treatment, with significant effect starting from 50 μ M (Figure 4.8D). Importantly, at this concentration, **24** is disrupting about 50% of the PPIs between the pro-apoptotic BH3-only BL-Bim peptide and endogenous Mcl-1 and Bfl-1, but not with other anti-apoptotic proteins. Consistent with these results, cells overexpressing Bcl-2 and Bcl-xL were minimally affected even at the highest tested concentration, 100 μ M, further demonstrating the selective targeting of Mcl-1 and Bfl-1. It is important to note the difference between binding affinity and cellular potency of **24**, which can be attributed to several different factors. For example, it is known that the endogenous BH3-only proteins bind to anti-apoptotic proteins with high affinity, which requires a sub-nanomolar binding affinity of small molecules in order to disrupt these interactions and produce relevant biological activity.^{29,36} Another possible limiting factor is the potential binding to serum proteins, which has been reported as an issue for BH3 mimetics.^{25,37,38} To further evaluate on-target cellular activity of **24**, the negative control, compound **30r**, was tested and did not affect cell viability up to 100 μ M (Figure 4.8D). Furthermore, compound **23**, which has similar binding affinity against Mcl-1 and Bfl-1 as **24**, and only 10- to 15-fold selectivity over Bcl-2 and Bcl-xL, displayed significant cell killing of Mcl-1 and Bfl-1 lymphoma cell lines as expected, but also shows effect on Bcl-2 and Bcl-xL cell lines at the highest doses, consistent with its binding profile (Figure 4.8E and Table 4.4).

To demonstrate that compounds can disrupt PPIs with different pro-apoptotic proteins, we also used biotin labeled Noxa BH3 peptide. As expected, all tested compounds, **15**, **20**, **22**, and **23**, disrupted the interactions between BL-Noxa and

endogenous Mcl-1 with compound **23** being the most potent, corresponding with their binding affinities (Figure 4.8F). In addition, compounds **15**, **20**, and **22** didn't show significant cellular activity at 100 μM (Figure 4.8G), supporting that the increased potency of **23** and **24** contributes to cellular activity. Overall, this biological data confirms that the selective binding profiles of **23** and **24** translate to cellular activity by selectively targeting endogenous Mcl-1 and Bfl-1 in an equipotent manner.

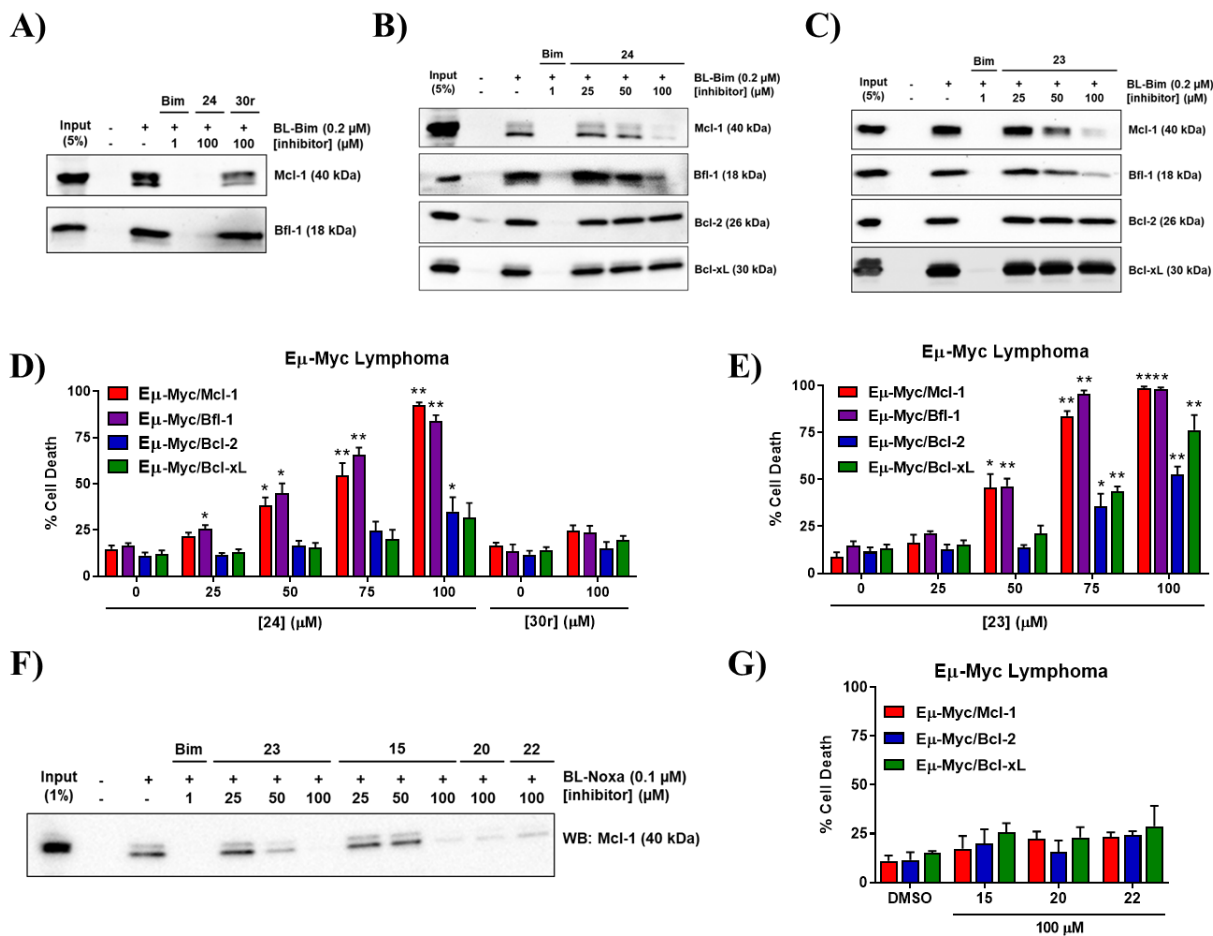


Figure 4.8 Biological evaluation of dual inhibitors

A) Biotin-streptavidin pull-down assay using lysate from the M14 melanoma cell line and biotinylated Bim peptide (BL-Bim) after treatment with 100 μM of compound **24** and its methyl ester analogue, **30r**. Dose dependent and selective disruption of BL-Bim and Mcl-1/Bfl-1 interactions by compounds **B)** **24** and **C)** **23**. Complexes of BL-Bim and endogenous anti-apoptotic proteins were analyzed by western blot. **D)** E μ -Myc lymphoma cell lines (Mcl-1, Bfl-1, Bcl-2, and Bcl-xL) treated for 24 hours with compounds **24** and **30r**

and **E**) **23**, cell death analyzed by flow cytometry. Significance determined by two-tailed t-test compared with DMSO (0 μ M) controls of respective cell lines (*, $p < 0.05$; **, $p < 0.005$). **F**) Pulldown assay using BL-Noxa and 2LMP cell lysate after treatment with compounds **23**, **15**, **20**, and **22**. **G**) Lack of cell death induction by 100 μ M of compounds **15**, **20**, and **22**. Data represents mean and SEM from 3 independent experiments.

4.9 Conclusions

Antagonizing the function of anti-apoptotic proteins constitutes a validated and attractive new paradigm in anticancer therapy and this work contributes to the progress of drugging the Bcl-2 protein family. It is known that cancer cells depend on individual and subsets of Bcl-2 family anti-apoptotic proteins, therefore, development of selective and multimodal inhibitors have therapeutic relevance. Building from our previous reports, we designed a new 2,5-substituted benzoic acid scaffold that enabled further SAR exploration of dual Mcl-1/Bfl-1 inhibition. The binding mode of the designed compound **1** was validated by HSQC-NMR and was shown to have several hydrophobic contacts with key pockets in the BH3 binding groove of Mcl-1 and Bfl-1, anchored by a hydrogen bond between the carboxyl group and Arg263/Mcl-1 or Arg88/Bfl-1.

A series of inhibitors was developed by 2,5-substitutions of the benzoic acid core to explore the binding optimization. Designed compounds comprise the first discovered class of small molecules showing selective inhibition of Mcl-1/Bfl-1 over the remaining anti-apoptotic proteins. While balancing hydrophobic driven increases in potency and hydrophilicity that favored physicochemical properties, several improved molecules were co-crystallized with Mcl-1 and provided valuable structural information that drove further development. The resulting optimized molecule, **24**, was 20-fold more potent for both Mcl-1 and Bfl-1 than compound **1**. Selectivity over Bcl-2/Bcl-xL was preserved and

was demonstrated on the cellular level by the ability of **24** to selectively bind endogenous Mcl-1 and Bfl-1 and to kill Mcl-1 and Bfl-1 dependent cells.

This work contributes to the set of known Bcl-2 family inhibitors and provides small molecules that mimic the binding profile of Noxa as dual Mcl-1/Bfl-1 selective inhibitors. Further optimized dual Mcl-1/Bfl-1 selective inhibitors will have biologically and clinically relevant utility as single agents and in combination for treatment of cancers where Mcl-1 and Bfl-1 have been implicated in their pathogenesis and chemoresistance, including leukemia, lymphoma, and melanoma.

4.10 Materials and methods

Expression and purification of anti-apoptotic proteins

DNA sequences containing human Mcl-1 (residues 171–323 and residues 171-320), human Bfl-1 (residues 1-151), the isoform 2 construct of the human Bcl-2 [Bcl2-2 construct for protein production starts with the Bcl2 sequence of 1-34 aa, followed by the BclxL sequence of 35-50 aa, and ends with the Bcl2 sequence of 92-202aa.], and Bcl-xL (human Bcl-xL protein, which has an internal deletion of the 45-85 amino acid residues and a C-terminal truncation for the amino acid residues 212-233) were cloned into an N-terminal His₆-TEV vector. All constructs were transformed into Rosetta2 DE3 cells. Cultures were grown in Terrific Broth at 37 °C, induced with 0.4 mM IPTG and expressed overnight at 20 °C.

Frozen cell pellets of Mcl-1 were sonicated in 20 mM HEPES pH 7.0, 200 mM NaCl, 0.1% β ME with Leupeptin/Aprotinin mixture and pelleted at 17,000 rpm for 45 min. The soluble fraction was applied to a Ni-NTA resin (Qiagen) for 1 h at 4 °C, the

matrix washed with 20 mM HEPES pH 7.0 and 200 mM NaCl and the protein eluted with 20 mM HEPES pH 7.0, 200 mM NaCl and 500 mM imidazole. The protein was subsequently applied to a Superdex 75 column (GE Healthcare) pre-equilibrated with 20 mM HEPES pH 7.0 and 150 mM NaCl. For crystallography, the tag was removed prior to gel filtration by dialysis against 20 mM HEPES pH 7.0, 150 mM NaCl and 0.1% β ME overnight in the presence of TEV protease.

Bfl-1 cells were lysed with sonication in 50 mM Tris pH 7.5, 200 mM NaCl. The lysate was cleared and loaded onto a Ni-NTA column. The column was washed with lysis buffer containing 10 mM imidazole, then protein eluted in lysis buffer containing 500 mM imidazole. Glycerol was added to the eluate to a final concentration 10%. The tag was cleaved in the presence of TEV protease during an overnight dialysis against 50 mM Tris 7.5, 150 mM NaCl, 0.1% β ME and 10% glycerol. The protein was diluted with 20 mM Tris, pH 7.5, 0.1% β ME and 10% glycerol then loaded onto a Source Q (GE Healthcare). The protein that eluted in the flow through was concentrated and applied to a Superdex 75 (GE Healthcare) preequilibrated with 25 mM HEPES pH 7.5, 300 mM NaCl, 1 mM DTT and 10% glycerol. Protein was concentrated to 1 mg/mL and stored at -80 °C.

To purify Bcl-2 and Bcl-xL proteins, cells were lysed in 25 mM Tris pH 8.5, 200 mM NaCl (Bcl-2), and 50 mM Tris pH 7.5, 200 mM NaCl (Bcl-xL) and applied to a Ni-NTA resin (QIAGEN) pre-equilibrated with lysis buffer containing 10 mM imidazole, then eluted with lysis buffer containing 500 mM imidazole. The His-tag was removed during dialysis overnight against buffer (25 mM Tris pH 8.5, 150 mM NaCl and 0.1% β ME [Bcl-2] and 50 mM Tris 7.5, 150 mM NaCl, 0.1% β ME [Bcl-xL]) containing TEV protease.

Each protein was loaded onto Source 15Q column (GE Healthcare) and eluted with a 0 – 1 M NaCl gradient. Concentrated protein was further purified on a gel filtration column (Superdex 75, Amersham Biosciences) pre-equilibrated with 25 mM Tris pH 8.5, 150 mM NaCl, 0.1% β ME (Bcl-2) or 20 mM Tris pH 7.5, 150 mM NaCl, 0.1% β ME (Bcl-xL). Mcl-1, Bfl-1, Bcl-2, and Bcl-xL were used in fluorescent polarization binding assay. Protein used for HSQC-NMR studies (His-tagged Mcl-1 and His-Bfl-1) were prepared and purified the same way with the exception that the bacteria were grown on M9 minimal media supported with 3 g/L of ^{13}C -glucose and/or 1 g/L of $(^{15}\text{NH}_4)_2\text{SO}_4$.

Heteronuclear single quantum correlation (HSQC) NMR spectroscopy

The Mcl-1 HSQC-NMR studies were performed as previously reported.^{21,23} HSQC NMR experiments with Bfl-1 proceeded as follows, NMR spectra were acquired in NMR Buffer (20 mM $\text{NaH}_2\text{PO}_4/\text{Na}_2\text{HPO}_4$ pH 7.0, 150 mM NaCl, 0.5 mM DTT, and 0.5 mM TECP) supplemented with 10% D_2O and 4% DMSO using 5mm D_2O matched Shigemi NMR tubes. ^{15}N labeled Bfl1-His (50 μM) was incubated with compounds **1** and **23**. All NMR data were collected on a Bruker Avance NEO 600 MHz spectrometer at 298K with a TCI-H&F/C/N cryoprobe. A transverse relaxation optimized spectroscopy (TROSY) with a solvent suppression pulse sequence was used to acquire all HSQC data. NMRPipe³⁹ and Sparky (Goddard and Kneller, Sparky 3, University of California, San Francisco) were used for all NMR data processing and analysis. Assignments of Bfl-1 residues were obtained from the printed HSQC as it was not deposited online by previous studies.⁴⁰

Fluorescence polarization (FP) binding assays

The FP binding assay was optimized for each individual anti-apoptotic protein. The following two fluorescent labeled Bid BH3-only peptides were used as competitive probes: a) Flu-Bid, a fluorescein tagged Bid peptide (Fluorescein-QEDIIRNIARHLAQVGDSMDR-CO₂H) and b) FAM-Bid, a 5-FAM (Abgent, #SP2121) labeled Bid peptide. The buffer for all experiments was composed of 20 mM phosphate (pH 7.4), 50 mM NaCl, 1 mM EDTA, 0.05% Pluronic F68 with a final DMSO concentration of 4%. All experiments were performed in black 96-well plates (Corning #3792) and analyzed using a Synergy H1 Hybrid BioTek plate reader at an excitation wavelength of 485 nm and an emission wavelength of 530 nm.

Dissociation constant (K_d) values were determined by protein saturation experiments where fixed concentrations of the fluorescent probes were mixed with increasing concentrations of the protein and polarization was measured to monitor saturation. K_d values were calculated by fitting the sigmoidal dose-dependent FP increases as a function of protein concentrations using GraphPad Prism 7.0 software. Based on this optimization of peptide probe to protein binding, 2 nM Flu-Bid was used in Mcl-1 assays and 2nM FAM-Bid was used for Bcl-2 and Bcl-xL, while 1 nM FAM-Bid was used for Bfl-1 assays. The following K_d values were determined: 3.24 ± 0.06 nM (Mcl-1), 0.424 ± 0.04 nM (Bfl-1), 18.44 ± 1.40 nM (Bcl-2), and 20.04 ± 2.34 nM (Bcl-xL). Based on saturation curves, the following protein concentrations were used in all FP assays: 10 nM Mcl-1, 2 nM Bfl-1, 60 nM Bcl-2, and 80 nM Bcl-xL.

Competitive binding assays were performed in a final volume of 125 uL and were incubated for three hours at room temperature before analyzing. IC₅₀ values were

determined by nonlinear regression fitting of the competition curves (GraphPad Prism 7.0 Software) and converted into K_i values as previously described.⁴¹

Mcl-1 co-crystallography

For the Mcl-1:**20** complex, prior to crystallization, protein (residues 171-320) was concentrated to 10.66 mg/mL in 20 mM HEPES pH 7.0, 50 mM NaCl and incubated in a 1:1.5 molar ratio with compound **20** at 4 °C for 48 hours. The final DMSO concentration in the protein-ligand sample was 6%. The complex was crystallized in a sitting drop vapor diffusion experiment against well solution of 30% PEG 3350, 0.2 mM MgCl₂ and 0.1 M ADA pH 6.5. The drops consisted of 1.5 uL protein-complex, 0.3 uL of 30% 6-aminohexanoic acid and 1.2 uL of well solution. Crystals grew within 1 day at 20 °C and were cryoprotected in 30% PEG 3350 prior to data collection.

To crystallize Mcl-1:**27** and Mcl-1:**22** complexes, protein (residues 171-323) was concentrated to 10 mg/mL and incubated with compound 1:1.5 ratio for 24 hours at 4 °C. The complex of Mcl-1:**24** was prepared by incubating Mcl-1 at 0.5 mg/mL with compound at 1:4 molar ratio in the presence of 5% DMSO for 12 hours and concentrated to 10 mg/mL. Mcl-1:**27** grew crystals from drops containing equal volumes of protein and well solution setup against 23 % PEG 3350, 0.1 M Tris pH 8.0 and 20% (w/v) PEG-1000, 0.1 M Tris pH 7.0, respectively. Mcl-1:**22** and Mcl-1:**24** grew crystals from drops containing equal volumes of protein and well solution setup against 18% PEG 3350, 200 mM NH₄ Acetate, 100 mM Bis-Tris pH 6.5. All crystals were cryoprotected in well solution containing 25% ethylene glycol.

Diffraction data were collected on LS-CAT 21-ID-D (**17**) and 21-ID-G (**15**, **27**, **22**, and **24**) beamlines at the Advanced Photon Source at Argonne National Laboratory and processed with HKL2000 (Table 4.6).⁴² The structures were solved via molecular replacement in Molrep⁴³ using an in-house Mcl-1:Bim structure missing helix 237-257 as the search model. Iterative rounds of electron density fitting and refinement were completed using Coot³⁰ and Buster⁴⁴ respectively. The coordinates and geometric restraints for each inhibitor were created from smiles using Grade⁴⁴ with the qm+mogul option. The coordinates were validated with Molprobit.⁴⁵ Several additional inhibitor compounds acting as additives enabling crystal packing were also seen in **20** and **24** structures. In the case of **27**, the compound bound differently to the two protein chains with multiple chains in each binding site. In the Mcl-1:**20** structure, residues 171 and 197-202 are missing from the single protein chain in the asymmetric unit. In the Mcl-1:**27** crystal, residues 172-321 and residues 171-321, plus one residue of the N-terminal tag were fit into density for the A and B chains, respectively. For Mcl-1:**22**, residues 172-320 are present in protein chains A, B and D; chain C contains residues 171-321 plus one N-terminal residue of the tag. For Mcl-1:**24**, residues A (171-321), B (171-321) plus three residues of N-terminal tag, C (172-322) are present.

Table 4.6 Crystallography data collection and refinement statistics

Data Collection	Mcl-1:14	Mcl-1:17	Mcl-1:19	Mcl-1:21	Mcl-1:24
PDB ID	6U63	6U64	6U65	6U6F	6U67
SpaceGroup	P2 ₁ 2 ₁ 2 ₁	R32	P2 ₁ 2 ₁ 2 ₁	P6122	C222 ₁
Unit Cell a, b, c (Å)	68.980, 69.600, 110.340	111.68, 111.67, 72.34	69.712, 85.223, 109.753	68.454, 68.454, 363.651	67.514, 134.376, 70.794
Wavelength (Å)	0.97856	0.96295	0.97856	0.97856	0.9786
Resolution (Å) ¹	2.74 (2.74- 2.79)	2.55 (2.55- 2.59)	2.10 (2.10- 2.14)	2.90 (2.95- 2.90)	1.84 (1.84- 1.87)

Rmerge ²	0.095 (0.355)	0.069 (0.649)	0.064 (0.464)	0.120 (0.706)	0.054 (0.333)
$\langle I/\langle I \rangle \rangle^3$	10 (3)	20 (5)	10 (3)	29 (4)	10 (2)
Completeness (%) ⁴	99.3 (97.6)	99.6 (100)	100 (100)	99.9 (100)	99.8 (98.2)
Redundancy	5.3 (4.9)	20.5 (21.5)	7.4 (7.5)	18.0 (16.8)	7.2 (.6.0)
Refinement					
Resolution (Å)	2.75	2.55	2.1	2.90	1.84
R-Factor ⁵	0.2297	0.212	0.1874	0.2381	0.1910
Rfree ⁶	0.2616	0.251	0.2215	0.2793	0.2225
Protein atoms	4256	1081	4725	3494	2394
Water Molecules	24	10	188	52	180
Ligand	6	3	4	4	6
Unique Reflections	14204	5816	39167	12127	28248
R.m.s.d. ⁷					
Bonds (Å)	0.008	0.010	0.01	0.008	0.01
Angles (°)	0.90	1.04	0.90	0.89	0.88
Molecules/ASU	4	1	4	3	2
MolProbity Score ⁸	1.54	2.38	0.94	1.39	1.10
Clash Score ⁸	2.39	4.52	1.76	1.58	2.58
RSCC (%) ⁹	0.95/0.91/0.93/ 0.85/0.87/0.92	0.93/0.96/0.97	0.96/0.98/0.97/ 0.95	0.82/0.96/0.96/ /0.97	0.9/0.97/0.87/ 0.85/0.98/0.78
RSR (%) ⁹	0.18/0.20/0.18/ 0.31/0.23/0.18	0.21/0.2/0.11	0.13/0.10/0.10/ 0.12	0.29/0.19/0.20/ /0.18	0.14/0.09/0.19/ /0.16/0.07/0.17

¹Statistics for highest resolution bin of reflections in parentheses.

² $R_{\text{merge}} = \frac{\sum_h \sum_j |I_{hj} - \langle I_h \rangle|}{\sum_h \sum_j I_{hj}}$, where I_{hj} is the intensity of observation j of reflection h and $\langle I_h \rangle$ is the mean intensity for multiply recorded reflections.

³Intensity signal-to-noise ratio.

⁴Completeness of the unique diffraction data.

⁵R-factor = $\frac{\sum_h ||F_o| - |F_c||}{\sum_h |F_o|}$, where F_o and F_c are the observed and calculated structure factor amplitudes for reflection h .

⁶ R_{free} is calculated against a 5% random sampling of the reflections that were removed before structure refinement.

⁷Root mean square deviation of bond lengths and bond angles.

⁸Chen et al. (2010) MolProbity: all-atom structure validation for macromolecular crystallography. Acta Crystallographica D66:12-21.

⁹wwPDB Validation Server.

Bio-layer interferometry (BLI)

Mcl-1 and Bfl-1 proteins were biotinylated using the Thermo EZ-link Sulpho-NHS-LC-biotin biotinylation kit (CAT# 21435). Protein and biotin were mixed in a 1:1 molar ratio in PBS on ice for 2 hours, followed by dialysis in PBS buffer. BLI assays were performed on a ForteBio Octet Red96 instrument. Biotinylated anti-apoptotic proteins (10 µg/mL) were immobilized and saturated on Super Streptavidin Dip and Read Biosensors (ForteBio, #18-5065). All experiments were performed at 30 °C in the same buffer used for FP binding assays and were conducted in 96-well microplates (Greiner bio-one, #655209). Buffer was used for custom, baseline, and dissociation steps, while buffer containing serially diluted compounds with 5% DMSO was used for association. Association and dissociation cycles were fixed at 10 minutes each. Kinetic data was collected and processed with the Data Analysis software provided by ForteBio. All experiments were analyzed with referencing by subtraction of the DMSO and buffer-only wells. Plotting the response nm values of the binding sensorgrams with their respective compound concentration allowed for steady state analysis and was used to calculate K_d values.

Pulldown assay

Cell lysate from the M14 melanoma and 2LMP breast cancer cell lines was obtained from harvesting cells and lysing via sonication in CHAPS buffer [10 mM HEPES (pH 7.4), 2.5 mM EDTA, 150 mM NaCl, 1% (w/v) CHAPS] with protease inhibitor. Cell lysate (2 mg/mL for M14 and 1 mg/L for 2LMP) was pre-cleared with streptavidin-agarose beads and incubated on a tube rotator overnight at 4 °C with BL-

Bim (0.2 μM) or BL-Noxa (0.1 μM) and either DMSO, free Bim peptide, or small molecule inhibitors. Protein-peptide complexes were pulled down with streptavidin-agarose beads for 2 hrs at 4 °C. Beads were washed three times with CHAPS buffer and protein was eluted by boiling in 5X SDS loading dye. Samples were then run on a 4-20% Tris-Glycine gel and analyzed by western blot with Mcl-1 (Thermo Fisher # AHO0102), Bfl-1 (Cell Signaling #14093), Bcl-xL (Cell Signaling #2764), and Bcl-2 (Cell Signaling #15071) antibodies. The ThermoFisher iBright FL1000 imager was used to expose and quantify the western blot images.

E μ -Myc lymphoma cell lines

The retrovirally transduced lymphoma cells isolated from E μ -Myc transgenic mice were gifts from Ricky W. Johnstone at the University of Melbourne, Melbourne, Australia and were cultured as previously described.³⁵ The Mcl-1, Bfl-1, Bcl-2, and Bcl-xL E μ -Myc cells were seeded in 24-well plates at 0.5×10^6 cells/well. Cells were treated with compounds for 24 hrs then stained with violet LIVE/DEAD Fixable Dead Cell Stain Kit (Invitrogen, #L34964), according to manufacturers' protocol. The percentage of fluorescent positive cells was determined by flow cytometry and calculated using WinList 3.0; statistical analysis was performed using a two-tailed T-test, comparing to the corresponding DMSO controls

Molecular docking

Molecular docking calculations were performed using GOLD molecular docking tool.⁴⁶ The binding site was defined as a 8 Å cavity around the corresponding ligand in

the Mcl-1 binding site. Hydrogen atoms were added to the Mcl-1 protein using GOLD, with default settings of the amino acid protonation pattern. Side chains of amino acids were treated as rigid entities. Compounds were docked 10 times into the defined binding site by applying the following parameters of the GOLD genetic algorithm (GA) (population size = 100, selection pressure = 1.1, no. of operations = 100000, no. of islands = 5, niche size = 2, migrate = 10, mutate = 95, crossover = 95) and different scoring functions available in GOLD. The best agreement between the crystallized and docked pose was obtained using the ChemPLP scoring function present in GOLD. The docking calculation reproduced the experimental binding mode with the RMSD of 0.4 Å.

For the molecular docking of compounds **1**, **23**, and **24** into the Bfl-1 protein PDB structure 3MQP was used. The preformed alignment with the Mcl-1:**24** co-crystal structure yielded the initial Bfl-1: **24** complex and subsequent complex minimization are described in the Results section. Protein preparation, binding site definition and GOLD docking settings were taking analogously to the previous Mcl-1 docking calculations. Docking calculations were visualized using LigandScout software.⁴⁷

4.11 Contributions

Karson Kump performed all FP and BLI binding assays with associated SAR analysis, solubility experiments, and all biological assays (pulldown and cell treatments). Dr. Lei Miao originally synthesized compounds **1-22** and **27**; Dr. Mohan Pal synthesized compounds **23**, **25**, and **26**; Dr. Uttar Shrestha synthesized compound **24**; Dr. Nurul Ansari aided in the re-synthesis and characterization of several compounds. HSQC-NMR experiments using Mcl-1 were performed by Dr. Fardokht Abulwerdi and those

with Bcl-1 were done and analyzed by our collaborator Dr. May Khanna (University of Arizona) with help from Jacob Carlson. The expression and purification of the anti-apoptotic proteins and Mcl-1 co-crystallography with compounds **20** and **22** were performed at the Life Sciences Institute Center for Structural Biology by Krishnapriya Chinnaswamy and Dr. Jennifer Meagher under the supervision of Dr. Jeanne Stuckey. Dr. Yuting Yang solved the Mcl-1:**24** co-crystal structure. Molecular docking was done by Dr. Andrej Perdih (National Institute of Chemistry, Slovenia).

4.12 References

1. Ashkenazi A, Fairbrother WJ, Levenson JD, Souers AJ. From basic apoptosis discoveries to advanced selective BCL-2 family inhibitors. *Nat Rev Drug Discov.* 2017;16(4):273-284. doi:10.1038/nrd.2016.253
2. Roberts AW, Davids MS, Pagel JM, et al. Targeting BCL2 with Venetoclax in Relapsed Chronic Lymphocytic Leukemia. *N Engl J Med.* 2016;374(4):311-322. doi:10.1056/NEJMoa1513257
3. Tao Z-F, Hasvold L, Wang L, et al. Discovery of a Potent and Selective BCL-X_L Inhibitor with *in Vivo* Activity. *ACS Med Chem Lett.* 2014;5(10):1088-1093. doi:10.1021/ml5001867
4. Kotschy A, Szlavik Z, Murray J, et al. The MCL1 inhibitor S63845 is tolerable and effective in diverse cancer models. *Nature.* 2016;538(7626):477-482. doi:10.1038/nature19830
5. Caenepeel S, Brown SP, Belmontes B, et al. AMG 176, a Selective MCL1 Inhibitor, is Effective in Hematological Cancer Models Alone and in Combination with Established Therapies. *Cancer Discov.* 2018;8(12):CD-18-0387. doi:10.1158/2159-8290.CD-18-0387
6. Tron AE, Belmonte MA, Adam A, et al. Discovery of Mcl-1-specific inhibitor AZD5991 and preclinical activity in multiple myeloma and acute myeloid leukemia. *Nat Commun.* 2018;9(1):5341. doi:10.1038/s41467-018-07551-w
7. Vogler M. BCL2A1: the underdog in the BCL2 family. *Cell Death Differ.* 2012;19(1):67-74. doi:10.1038/cdd.2011.158

8. Hind CK, Carter MJ, Harris CL, Chan HTC, James S, Cragg MS. Role of the pro-survival molecule Bfl-1 in melanoma. *Int J Biochem Cell Biol.* 2015;59:94-102. doi:10.1016/j.biocel.2014.11.015
9. Akgul C. Mcl-1 is a potential therapeutic target in multiple types of cancer. *Cell Mol Life Sci.* 2009;66(8):1326-1336. doi:10.1007/s00018-008-8637-6
10. Simmons MJ, Fan G, Zong W-X, Degenhardt K, White E, Gélinas C. Bfl-1/A1 functions, similar to Mcl-1, as a selective tBid and Bak antagonist. *Oncogene.* 2008;27(10):1421-1428. doi:10.1038/sj.onc.1210771
11. Barile E, Marconi GD, De SK, et al. hBfl-1/hNOXA Interaction Studies Provide New Insights on the Role of Bfl-1 in Cancer Cell Resistance and for the Design of Novel Anticancer Agents. *ACS Chem Biol.* 2017;12(2):444-455. doi:10.1021/acscchembio.6b00962
12. Adams JM, Cory S. The Bcl-2 apoptotic switch in cancer development and therapy. *Oncogene.* 2007;26(9):1324-1337. doi:10.1038/sj.onc.1210220
13. Lanave C, Santamaria M, Saccone C. Comparative genomics: the evolutionary history of the Bcl-2 family. *Gene.* 2004;333:71-79. doi:10.1016/J.GENE.2004.02.017
14. Senft D, Berking C, Graf SA, Kammerbauer C, Ruzicka T, Besch R. Selective Induction of Cell Death in Melanoma Cell Lines through Targeting of Mcl-1 and A1. Sanchis D, ed. *PLoS One.* 2012;7(1):e30821. doi:10.1371/journal.pone.0030821
15. Esteve-Arenys A, Valero JG, Chamorro-Jorganes A, et al. The BET bromodomain inhibitor CPI203 overcomes resistance to ABT-199 (venetoclax) by downregulation of BFL-1/A1 in in vitro and in vivo models of MYC+/BCL2+ double hit lymphoma. *Oncogene.* 2018;37(14):1830-1844. doi:10.1038/s41388-017-0111-1
16. Yecies D, Carlson NE, Deng J, Letai A. Acquired resistance to ABT-737 in lymphoma cells that up-regulate MCL-1 and BFL-1. *Blood.* 2010;115(16):3304-3313. doi:10.1182/blood-2009-07-233304
17. Haq R, Yokoyama S, Hawryluk EB, et al. *BCL2A1* is a lineage-specific antiapoptotic melanoma oncogene that confers resistance to BRAF inhibition. *Proc Natl Acad Sci.* 2013;110(11):4321-4326. doi:10.1073/pnas.1205575110
18. Fofaria NM, Frederick DT, Sullivan RJ, Flaherty KT, Srivastava SK. Overexpression of Mcl-1 confers resistance to BRAFV600E inhibitors alone and in combination with MEK1/2 inhibitors in melanoma. *Oncotarget.* 2015;6(38):40535-40556. doi:10.18632/oncotarget.5755
19. Champa D, Russo MA, Liao X-H, Refetoff S, Ghossein RA, Di Cristofano A.

- Obatoclox overcomes resistance to cell death in aggressive thyroid carcinomas by countering Bcl2a1 and Mcl1 overexpression. *Endocr Relat Cancer*. 2014;21(5):755-767. doi:10.1530/ERC-14-0268
20. Du Y, Nikolovska-Coleska Z, Qui M, et al. A dual-readout F2 assay that combines fluorescence resonance energy transfer and fluorescence polarization for monitoring bimolecular interactions. *Assay Drug Dev Technol*. 2011;9(4):382-393. doi:10.1089/adt.2010.0292
 21. Mady ASA, Liao C, Bajwa N, et al. Discovery of Mcl-1 inhibitors from integrated high throughput and virtual screening. *Sci Rep*. 2018;8(1):10210. doi:10.1038/s41598-018-27899-9
 22. Petros AM, Swann SL, Song D, et al. Fragment-based discovery of potent inhibitors of the anti-apoptotic MCL-1 protein. *Bioorg Med Chem Lett*. 2014;24(6):1484-1488. doi:10.1016/J.BMCL.2014.02.010
 23. Abulwerdi FA, Liao C, Mady AS, et al. 3-Substituted-N-(4-hydroxynaphthalen-1-yl)arylsulfonamides as a novel class of selective Mcl-1 inhibitors: structure-based design, synthesis, SAR, and biological evaluation. *J Med Chem*. 2014;57(10):4111-4133. doi:10.1021/jm500010b
 24. Friberg A, Vigil D, Zhao B, et al. Discovery of Potent Myeloid Cell Leukemia 1 (Mcl-1) Inhibitors Using Fragment-Based Methods and Structure-Based Design. *J Med Chem*. 2013;56(1):15-30. doi:10.1021/jm301448p
 25. Bruncko M, Wang L, Sheppard GS, et al. Structure-Guided Design of a Series of MCL-1 Inhibitors with High Affinity and Selectivity. *J Med Chem*. 2015;58(5):2180-2194. doi:10.1021/jm501258m
 26. Tron AE, Belmonte MA, Adam A, et al. Discovery of Mcl-1-specific inhibitor AZD5991 and preclinical activity in multiple myeloma and acute myeloid leukemia. *Nat Commun*. 2018;9(1):5341. doi:10.1038/s41467-018-07551-w
 27. Aldeghi M, Malhotra S, Selwood DL, Chan AWE. Two- and Three-dimensional Rings in Drugs. *Chem Biol Drug Des*. 2014;83(4):450. doi:10.1111/CBDD.12260
 28. Meanwell NA. Improving Drug Candidates by Design: A Focus on Physicochemical Properties As a Means of Improving Compound Disposition and Safety. *Chem Res Toxicol*. 2011;24(9):1420-1456. doi:10.1021/tx200211v
 29. Belmar J, Fesik SW. Small molecule Mcl-1 inhibitors for the treatment of cancer. *Pharmacol Ther*. 2015;145:76-84. doi:10.1016/j.pharmthera.2014.08.003
 30. Emsley P, Cowtan K. *Coot*: model-building tools for molecular graphics. *Acta Crystallogr Sect D Biol Crystallogr*. 2004;60(12):2126-2132. doi:10.1107/S0907444904019158

31. Harvey EP, Seo H-S, Guerra RM, Bird GH, Dhe-Paganon S, Walensky LD. Crystal Structures of Anti-apoptotic BFL-1 and Its Complex with a Covalent Stapled Peptide Inhibitor. *Structure*. 2018;26(1):153-160.e4. doi:10.1016/j.str.2017.11.016
32. Herman MD, Nyman T, Welin M, et al. Completing the family portrait of the anti-apoptotic Bcl-2 proteins: crystal structure of human Bfl-1 in complex with Bim. *FEBS Lett*. 2008;582(25-26):3590-3594. doi:10.1016/j.febslet.2008.09.028
33. Czabotar PE, Lessene G, Strasser A, Adams JM. Control of apoptosis by the BCL-2 protein family: implications for physiology and therapy. *Nat Rev Mol Cell Biol*. 2014;15(1):49-63. doi:10.1038/nrm3722
34. Lee EF, Harris TJ, Tran S, et al. BCL-XL and MCL-1 are the key BCL-2 family proteins in melanoma cell survival. *Cell Death Dis*. 2019;10(5):342. doi:10.1038/s41419-019-1568-3
35. Whitecross KF, Alsop AE, Cluse LA, et al. Defining the target specificity of ABT-737 and synergistic antitumor activities in combination with histone deacetylase inhibitors. *Blood*. 2009;113(9):1982-1991. doi:10.1182/blood-2008-05-156851
36. Levenson JD, Zhang H, Chen J, et al. Potent and selective small-molecule MCL-1 inhibitors demonstrate on-target cancer cell killing activity as single agents and in combination with ABT-263 (navitoclax). *Cell Death Dis*. 2015;6(1):e1590. doi:10.1038/cddis.2014.561
37. Souers AJ, Levenson JD, Boghaert ER, et al. ABT-199, a potent and selective BCL-2 inhibitor, achieves antitumor activity while sparing platelets. *Nat Med*. 2013;19(2):202-208. doi:10.1038/nm.3048
38. Zhao B, Sensintaffar J, Bian Z, et al. Structure of a Myeloid cell leukemia-1 (Mcl-1) inhibitor bound to drug site 3 of Human Serum Albumin. *Bioorganic Med Chem*. 2017;25(12):3087-3092. doi:10.1016/j.bmc.2017.03.060
39. Delaglio F, Grzesiek S, Vuister GW, Zhu G, Pfeifer J, Bax A. NMRPipe: A multidimensional spectral processing system based on UNIX pipes. *J Biomol NMR*. 1995;6(3):277-293. doi:10.1007/BF00197809
40. Godoi PHC, Wilkie-Grantham RP, Hishiki A, et al. Orphan nuclear receptor NR4A1 binds a novel protein interaction site on anti-apoptotic B cell lymphoma gene 2 family proteins. *J Biol Chem*. 2016;291(27):14072-14084. doi:10.1074/jbc.M116.715235
41. Nikolovska-Coleska Z, Wang R, Fang X, et al. Development and optimization of a binding assay for the XIAP BIR3 domain using fluorescence polarization. *Anal Biochem*. 2004;332(2):261-273. doi:10.1016/j.ab.2004.05.055
42. Otwinowski Z, Minor W. Processing of X-ray diffraction data collected in oscillation

- mode. *Methods Enzymol.* 1997;276:307-326.
<http://www.ncbi.nlm.nih.gov/pubmed/27754618>. Accessed December 7, 2018.
43. Vagin A, Teplyakov A, IUCr. Molecular replacement with *MOLREP*. *Acta Crystallogr Sect D Biol Crystallogr.* 2010;66(1):22-25.
doi:10.1107/S0907444909042589
 44. Smart OS, Womack TO, Flensburg C, et al. Exploiting structure similarity in refinement: automated NCS and target-structure restraints in BUSTER. *Acta Crystallogr D Biol Crystallogr.* 2012;68(Pt 4):368-380.
doi:10.1107/S0907444911056058
 45. Chen VB, Arendall WB, Headd JJ, et al. *MolProbity*: all-atom structure validation for macromolecular crystallography. *Acta Crystallogr Sect D Biol Crystallogr.* 2010;66(1):12-21. doi:10.1107/S0907444909042073
 46. Jones G, Willett P, Glen RC, Leach AR, Taylor R. Development and validation of a genetic algorithm for flexible docking. *J Mol Biol.* 1997;267(3):727-748.
doi:10.1006/JMBI.1996.0897
 47. Wolber G, Langer T. LigandScout: 3-D Pharmacophores Derived from Protein-Bound Ligands and Their Use as Virtual Screening Filters. *J Chem Inf Model.* 2005;45(1):160-169. doi:10.1021/ci049885e

Chapter 5

Conclusions and Future Directions

5.1 Impact and translational relevance

The past decade has been an exciting time for oncology drug discovery, with the successes of immunotherapy,¹ strategic small molecule development strategies that have enabled targeting of previously undruggable oncogenic drivers,² the first FDA approved protein-protein interaction (PPI) inhibitor,³ and validation of proteolysis-targeting chimeras (PROTACS),^{4,5} to name a few. Along with novel therapeutic modalities, the ushering in of a personalized medicine era has brought a wave of diagnostics that help guide the use of new drugs to the right patient populations.⁶ These new therapeutics and diagnostics required intricate basic science research to make their way to patients and further necessitates disciplines like chemical biology to optimize and improve strategies to keep the ball rolling. With all the advanced chemical tools available, it is a great time to be a chemical biologist.

There has been a deluge of research advances in the field of apoptosis targeting for cancer therapy and with it has come a valuable quiver of chemical tools to continue advancing the field.^{7,8} In this body of work, we have taken advantage of a vast array of biological knowledge coupled with potent and selective chemical tools that allow for the dissecting of Bcl-2 family pro-survival dependence in cancer models. Driving these efforts has been the application of the functional BH3 profiling assay which enables to

pinpointing of anti-apoptotic dependence in cancers.⁹ We have been able to optimize this assay in a way that allows the fair comparison of data across a wide spectrum of cancers. We discovered novel survival dependence trends in lymphoma that segments B-cell and T-cell lymphoma subtypes by their innate preference to overexpress and display functional survival dependence on Bcl-2 or Mcl-1, respectively. Additionally, we evaluated pro-survival dependence in ovarian cancer for the first time and identified a novel approach to deploy Mcl-1 inhibitors as a therapeutic option in a personalized fashion. These novel functional elucidations will hopefully contribute to future clinical trial designs and improvement of clinical outcomes.

Our functional investigations and utilization of the BH3 mimetic tool kit highlighted the unmet need of targeting Bfl-1 with small molecules.¹⁰ We focused our medicinal chemistry efforts on the Mcl-1 and Bfl-1 proteins, as Bfl-1 is currently without a potent and biologically active small molecule inhibitor. Through structure-based design and structure activity relationship (SAR) studies we developed a first-in-class small molecule dual inhibitor of Mcl-1 and Bfl-1.¹¹ The most potent molecule in this series of 2,5-substituted benzoic acid inhibitors was compound **24**, which inhibited Mcl-1 and Bfl-1 with an equipotent binding constant of ~100 nM. Compound **24** selectively disrupted Mcl-1/Bfl-1 PPIs and killed Mcl-1/Bfl-1 dependent lymphoma cells, while leaving Bcl-2/Bcl-xL involved PPIs and dependent cells undisturbed. The structural and SAR data provided in these studies will hopefully contribute to the development of more potent Bfl-1 inhibitors that can be used to learn new biology and treat aggressive cancers.

5.2 Optimizing BH3 profiling for solid tumor patient samples

BH3 profiling has been successfully deployed in a variety of oncological indications and is typically used in two main formats, the plate based fluorometric and flow cytometry based protocols.¹² Testing hematologic cancer patient samples with high percentages of cancerous cells provides a near homogenous cell population that can be analyzed using the plate-based method, as we have done. However, samples with low tumor cell percentage and heterogeneous populations of cell types necessitates the use of the flow cytometry application of BH3 profiling, which is particularly important with solid tumors.¹³ BH3 profiling of solid tumor patient samples have been successfully performed with tissues from melanoma¹⁴ and thyroid cancer¹⁵, but require careful dissociation of tumors to a single cell suspension. Additional high throughput methods of analyzing solid tumor samples will be required to efficiently perform BH3 profiling on a clinical timeline to inform treatment decisions. The Letai lab has recently published a microscopy-based method that is performed with slides of freshly isolated solid tumor tissue and can effectively predict drug responses.¹⁶ Fluorescent microscopy and flow cytometry based BH3 profiling techniques provide new opportunities to explore the ability to predict efficacy of BH3 mimetics, as well as various chemo- and targeted therapies in the clinical setting.

5.3 Using BH3 profiling in clinical trials

Functional diagnostics are increasing in their importance to enhance precision medicine strategies, together with static genomics analysis. Our group and others have validated the translational applicability of the functional BH3 profiling assay to diagnose

the functional survival dependence in cancer cell lines and primary patient samples.^{12,17,18} As the number of clinical trials evaluating various BH3 mimetics grow, so does the need to focus on targeted patient populations. The already FDA approved Bcl-2 inhibitor venetoclax¹⁹ is currently being evaluated in numerous clinical trials for additional indications and in combination regimens, along with the additional Bcl-2 selective inhibitors S55746,²⁰ S65487, and APG-2575. Meanwhile, Bcl-2/Bcl-xL/Bcl-w inhibitors such as navitoclax²¹ and APG-1252 are still being evaluated clinically in a variety of cancers, especially in solid tumors. Also, in the clinical pipeline are five new selective Mcl-1 inhibitors AMG176,²² AMG397, AZD5991,²³ S64315/MIK665,²⁴ and ABBV-467 and an antibody conjugated Bcl-xL inhibitor, ABBV-155. The Mcl-1 inhibitor trials have faced a speedbump regarding cardiotoxicity, which was not unexpected due to previous studies showing the detrimental consequences of genetic ablation of Mcl-1 in cardiomyocytes, hopefully this can be overcome with creative dosing and drug delivery strategies.

With all the ongoing clinical action with BH3 mimetics, the companies involved in these trials including Abbvie, Amgen, AstraZeneca, Servier, Novartis, and Ascentage Pharma could benefit from clinical trial designs utilizing BH3 profiling for biomarker correlation and inclusion criteria. Initially, it would make sense to incorporate patient sample collection for BH3 profiling as part of the clinical trial protocols of these compounds, so that the predictive nature of BH3 profiling could be put to the test when compared to efficacy. When enough data has been collected and if there is a correlative cut off between certain levels of anti-apoptotic protein dependence and the efficacy of the BH3 mimetic for the respective target, it may serve as valuable criteria for clinical

trial inclusion. For example, patients enrolling in future clinical trials for Mcl-1 inhibitor treatment would need to have their tumor cells, which would already be collected as part of an initial screening process, subjected to BH3 profiling and demonstrate a certain level of sensitivity to the Mcl-1 selective peptide MS1 and low response to Bad/Hrk (Bcl-2/Bcl-xL targeting peptides) before starting treatment in the trial. This approach may be particularly useful in solid tumors due to known high survival dependence heterogeneity and smaller populations of tumors solely dependent on a single anti-apoptotic protein. Additionally, utilizing BH3 profiling to guide an umbrella clinical trial design²⁵ (Figure 5.1A) where patient's tumor cells all of a specific cancer are initially profiled for survival dependence before being assigned to treatment groups consisting of one of the selective BH3 mimetics (Bcl-2, Mcl-1, or Bcl-xL). This BH3 profiling screen could also work to orchestrate a basket clinical trial²⁵ (Figure 5.1B), where patients with a variety of cancer types are screened for Mcl-1 dependence, for example, before being treated with an Mcl-1 inhibitor, which would help increase patient sample size for enrollment. Furthermore, dynamic BH3 profiling has the advantage of being able to assess the efficacy of various targeted and chemo-therapies, not just BH3 mimetics. These opportunities are becoming realized with the many studies, including our own that are validating the utility of BH3 profiling to guide precision medicine strategies.²⁶⁻²⁸

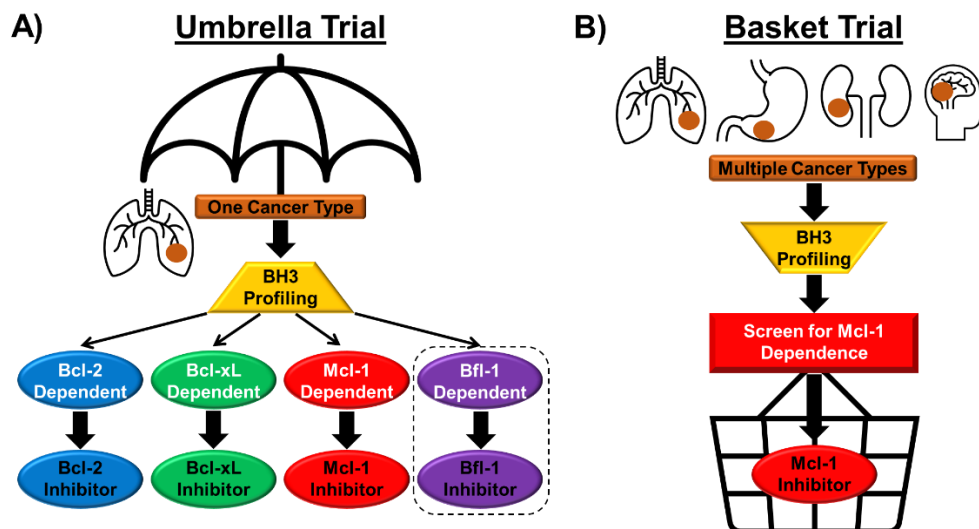


Figure 5.1 Future clinical trial designs for BH3 mimetics

A) Umbrella trial design that focuses on one cancer, screens for survival dependence and assigns patients to different BH3 mimetics. Bfl-1 segment highlighted due to there being no clinical stage Bfl-1 inhibitors to date. **B)** Basket trial design that screens multiple cancers for survival dependence of a particular anti-apoptotic protein (Mcl-1 as an example) and enrolls positive patients for treatment of the respective BH3 mimetic.

5.4 Further development of Mcl-1/Bfl-1 dual and Bfl-1 selective inhibitors

The dual Mcl-1/Bfl-1 inhibitors that we developed require stronger affinity in order to produce robust, on-target biological activity. It is well established that BH3 mimetics need to possess sub-nanomolar affinity for their targets in order to compete with the tight binding endogenous BH3-only proteins, as illustrated by all of the clinical stage compounds.²⁹ We provided a promising starting point through SAR and structural studies to continue our efforts of increasing potency for both Mcl-1 and Bfl-1. Having a potent Noxa-mimetic small molecule will be a therapeutic advantage in many cancers such as melanoma that display high dependence on both Mcl-1 and Bfl-1, but a selective Bfl-1 inhibitor would be particularly useful as a chemical tool.^{10,30–34} To this point all of our crystallography studies have come from Mcl-1 complex structures and a

key catalyst will be obtaining a co-crystal structure with one of our inhibitors and Bfl-1. This structural information would aid in diverging the SAR between Mcl-1 and Bfl-1 towards developing selective Bfl-1 inhibitors. Another key feature to exploit is the Cys residue (C55) in the BH3 binding pocket of Bfl-1 to develop covalent inhibitors, which has been done with peptides and one reported small molecule.^{35,36} Obtaining a selective Bfl-1 inhibitor would help complete the puzzle in drugging the Bcl-2 family anti-apoptotic proteins and provide a complete set of antagonists to target each protein. With the functional role of Bfl-1 being elucidated in melanoma and lymphoma and its emerging role as a resistance factor, it is becoming a promising therapeutic target that could benefit from selective inhibition.^{30,37}

5.5 Concluding remarks

If the next 10 years are exciting as the last, then there will be some exciting new developments in oncology drug discovery. The field of targeting the Bcl-2 family of proteins is just now gaining clinical traction after two decades of biological discoveries and small molecule development. The highly anticipated clinical trial data from the several Mcl-1 inhibitors will provide more opportunities for development and improvement. With the need for a Bfl-1 inhibitor still unmet, it is only a matter of time before a potent small molecule emerges that can complete the BH3 mimetic quiver. The hope is that functional assays like BH3 profiling will play a more prominent role together with genomics in guiding the right drugs to the right patients to enhance the application of precision medicine.

5.6 References

1. Larkin J, Chiarion-Sileni V, Gonzalez R, et al. Five-Year Survival with Combined Nivolumab and Ipilimumab in Advanced Melanoma. *N Engl J Med*. 2019;381(16):1535-1546. doi:10.1056/NEJMoa1910836
2. Canon J, Rex K, Saiki AY, et al. The clinical KRAS(G12C) inhibitor AMG 510 drives anti-tumour immunity. *Nature*. 2019;575(7781):217-223. doi:10.1038/s41586-019-1694-1
3. Roberts AW, Davids MS, Pagel JM, et al. Targeting BCL2 with Venetoclax in Relapsed Chronic Lymphocytic Leukemia. *N Engl J Med*. 2016;374(4):311-322. doi:10.1056/NEJMoa1513257
4. Gao H, Sun X, Rao Y. PROTAC Technology: Opportunities and Challenges. *ACS Med Chem Lett*. 2020;11(3):237-240. doi:10.1021/acsmchemlett.9b00597
5. Paiva SL, Crews CM. Targeted protein degradation: elements of PROTAC design. *Curr Opin Chem Biol*. 2019;50:111-119. doi:10.1016/j.cbpa.2019.02.022
6. Friedman AA, Letai A, Fisher DE, Flaherty KT. Precision medicine for cancer with next-generation functional diagnostics. *Nat Rev Cancer*. 2015;15(12):747-756. doi:10.1038/nrc4015
7. Delbridge ARD, Strasser A. The BCL-2 protein family, BH3-mimetics and cancer therapy. *Cell Death Differ*. 2015;22(7):1071-1080. doi:10.1038/cdd.2015.50
8. Suvarna V, Singh V, Murahari M. Current overview on the clinical update of Bcl-2 anti-apoptotic inhibitors for cancer therapy. *Eur J Pharmacol*. 2019;862:172655. doi:10.1016/j.ejphar.2019.172655
9. Del Gaizo Moore V, Letai A. BH3 profiling--measuring integrated function of the mitochondrial apoptotic pathway to predict cell fate decisions. *Cancer Lett*. 2013;332(2):202-205. doi:10.1016/j.canlet.2011.12.021
10. Vogler M. BCL2A1: the underdog in the BCL2 family. *Cell Death Differ*. 2012;19(1):67-74. doi:10.1038/cdd.2011.158
11. Kump KJ, Miao L, Mady ASA, et al. Discovery and Characterization of 2,5-Substituted Benzoic Acid Dual Inhibitors of the Anti-apoptotic Mcl-1 and Bfl-1 Proteins. *J Med Chem*. 2020;63(5):2489-2510. doi:10.1021/acs.jmedchem.9b01442
12. Ryan J, Letai A. BH3 profiling in whole cells by fluorimeter or FACS. *Methods*. 2013;61(2):156-164. doi:10.1016/j.ymeth.2013.04.006
13. Ryan J, Montero J, Rocco J, Letai A. IBH3: Simple, fixable BH3 profiling to determine apoptotic priming in primary tissue by flow cytometry. *Biol Chem*.

2016;397(7):671-678. doi:10.1515/hsz-2016-0107

14. Montero J, Gstalder C, Kim DJ, et al. Destabilization of NOXA mRNA as a common resistance mechanism to targeted therapies. *Nat Commun.* 2019;10(1). doi:10.1038/s41467-019-12477-y
15. Gunda V, Sarosiek KA, Brauner E, et al. Inhibition of MAPKinase pathway sensitizes thyroid cancer cells to ABT-737 induced apoptosis. *Cancer Lett.* 2017;395:1-10. doi:10.1016/j.canlet.2017.02.028
16. Bhola PD, Ahmed E, Guerriero JL, et al. High-throughput dynamic BH3 profiling may quickly and accurately predict effective therapies in solid tumors. *Sci Signal.* 2020;13(636). doi:10.1126/scisignal.aay1451
17. Chonghaile TN, Sarosiek KA, Vo TT, et al. Pretreatment mitochondrial priming correlates with clinical response to cytotoxic chemotherapy. *Science (80-).* 2011;334(6059):1129-1133. doi:10.1126/science.1206727
18. Deng J, Carlson N, Takeyama K, Dal Cin P, Shipp M, Letai A. BH3 Profiling Identifies Three Distinct Classes of Apoptotic Blocks to Predict Response to ABT-737 and Conventional Chemotherapeutic Agents. *Cancer Cell.* 2007;12(2):171-185. doi:10.1016/j.ccr.2007.07.001
19. Souers AJ, Levenson JD, Boghaert ER, et al. ABT-199, a potent and selective BCL-2 inhibitor, achieves antitumor activity while sparing platelets. *Nat Med.* 2013;19(2):202-208. doi:10.1038/nm.3048
20. Casara P, Davidson J, Claperon A, et al. S55746 is a novel orally active BCL-2 selective and potent inhibitor that impairs hematological tumor growth. *Oncotarget.* 2018;9(28):20075-20088. doi:10.18632/oncotarget.24744
21. Tse C, Shoemaker AR, Adickes J, et al. ABT-263: A Potent and Orally Bioavailable Bcl-2 Family Inhibitor. *Cancer Res.* 2008;68(9):3421-3428. doi:10.1158/0008-5472.CAN-07-5836
22. Caenepeel S, Brown SP, Belmontes B, et al. AMG 176, a Selective MCL1 Inhibitor, is Effective in Hematological Cancer Models Alone and in Combination with Established Therapies. *Cancer Discov.* 2018;8(12):CD-18-0387. doi:10.1158/2159-8290.CD-18-0387
23. Tron AE, Belmonte MA, Adam A, et al. Discovery of Mcl-1-specific inhibitor AZD5991 and preclinical activity in multiple myeloma and acute myeloid leukemia. *Nat Commun.* 2018;9(1):5341. doi:10.1038/s41467-018-07551-w
24. Kotschy A, Szlavik Z, Murray J, et al. The MCL1 inhibitor S63845 is tolerable and effective in diverse cancer models. *Nature.* 2016;538(7626):477-482. doi:10.1038/nature19830

25. Park JJH, Hsu G, Siden EG, Thorlund K, Mills EJ. An overview of precision oncology basket and umbrella trials for clinicians. *CA Cancer J Clin.* 2020;70(2):125-137. doi:10.3322/caac.21600
26. Pan R, Hogdal LJ, Benito JM, et al. Selective BCL-2 inhibition by ABT-199 causes on-target cell death in acute myeloid Leukemia. *Cancer Discov.* 2014;4(3):362-675. doi:10.1158/2159-8290.CD-13-0609
27. Konopleva M, Pollyea DA, Potluri J, et al. Efficacy and biological correlates of response in a phase II study of venetoclax monotherapy in patients with acute Myelogenous Leukemia. *Cancer Discov.* 2016;6(10):1106-1117. doi:10.1158/2159-8290.CD-16-0313
28. Koch R, Christie AL, Crombie JL, et al. Biomarker-driven strategy for MCL1 inhibition in T-cell lymphomas. *Blood.* 2019;133(6):566-575. doi:10.1182/blood-2018-07-865527
29. Belmar J, Fesik SW. Small molecule Mcl-1 inhibitors for the treatment of cancer. *Pharmacol Ther.* 2015;145:76-84. doi:10.1016/j.pharmthera.2014.08.003
30. Haq R, Yokoyama S, Hawryluk EB, et al. *BCL2A1* is a lineage-specific antiapoptotic melanoma oncogene that confers resistance to BRAF inhibition. *Proc Natl Acad Sci.* 2013;110(11):4321-4326. doi:10.1073/pnas.1205575110
31. Hind CK, Carter MJ, Harris CL, Chan HTC, James S, Cragg MS. Role of the pro-survival molecule Bfl-1 in melanoma. *Int J Biochem Cell Biol.* 2015;59:94-102. doi:10.1016/j.biocel.2014.11.015
32. Moujalled DM, Hanna DT, Hedyeh-Zadeh S, et al. Cotargeting BCL-2 and MCL-1 in high-risk B-ALL. *Blood Adv.* 2020;4(12):2762-2767. doi:10.1182/bloodadvances.2019001416
33. Senft D, Berking C, Graf SA, Kammerbauer C, Ruzicka T, Besch R. Selective Induction of Cell Death in Melanoma Cell Lines through Targeting of Mcl-1 and A1. Sanchis D, ed. *PLoS One.* 2012;7(1):e30821. doi:10.1371/journal.pone.0030821
34. Placzek WJ, Wei J, Kitada S, Zhai D, Reed JC, Pellecchia M. A survey of the anti-apoptotic Bcl-2 subfamily expression in cancer types provides a platform to predict the efficacy of Bcl-2 antagonists in cancer therapy. *Cell Death Dis.* 2010;1(5):e40. doi:10.1038/cddis.2010.18
35. Huhn AJ, Guerra RM, Harvey EP, Bird GH, Walensky LD. Selective Covalent Targeting of Anti-Apoptotic BFL-1 by Cysteine-Reactive Stapled Peptide Inhibitors. *Cell Chem Biol.* 2016;23(9):1123-1134. doi:10.1016/j.chembiol.2016.07.022
36. Harvey EP, Seo H-S, Guerra RM, Bird GH, Dhe-Paganon S, Walensky LD.

Crystal Structures of Anti-apoptotic BFL-1 and Its Complex with a Covalent Stapled Peptide Inhibitor. *Structure*. 2018;26(1):153-160.e4. doi:10.1016/j.str.2017.11.016

37. Esteve-Arenys A, Valero JG, Chamorro-Jorganes A, et al. The BET bromodomain inhibitor CPI203 overcomes resistance to ABT-199 (venetoclax) by downregulation of BFL-1/A1 in in vitro and in vivo models of MYC+/BCL2+ double hit lymphoma. *Oncogene*. 2018;37(14):1830-1844. doi:10.1038/s41388-017-0111-1